System-Modeling and System-Analysis, G Propst, USW Graz, 2020

final update of this page: June 9

contents:

Tellus (1983), *35B*, 284–289

Biological homeostasis of the global environment: the parable of Daisyworld

By ANDREW J. WATSON, *Marine Biological Association, The Laboratory, Citadel Hill, Plymouth PL1 2PB, England and* JAMES E. LOVELOCK, *Coombe Mill, St. Giles on the Heath, Launceston, Cornwall PL15 9RY, England*

(Manuscript received October 20, 1982; in final form February 14, 1983)

ABSTRACT

The biota have effected profound changes on the environment of the surface of the earth. At the same time, that environment has imposed constraints on the biota, so that life and the environment may be considered as two parts of a coupled system. Unfortunately, the system is too complex and too little known for us to model it adequately. To investigate the properties which this close-coupling might confer on the system, we chose to develop a model of an imaginary planet having a very simple biosphere. It consisted of just two species of daisy of different colours and was first described by Lovelock (1982). The growth rate of the daisies depends on only one environmental variable, temperature, which the daisies in turn modify because they absorb different amounts of radiation. Regardless of the details of the interaction, the effect of the daisies is to stabilize the temperature. The result arises because of the peaked shape of the growth-temperature curve and is independent of the mechanics by which the biota are assumed to modify the temperature. We sketch out the elements of a biological feedback system which might help regulate the temperature of the earth.

1. Introduction

On earth, modification of the environment by living things is apparent on any scale that one cares to look at, up to and including the global scale. In turn, geophysical and geochemical constraints have shaped the evolution of life and continue to dictate what type of life, and how much of it, can colonize the available space. One can think of the biota and their environment as two elements of a closely-coupled system: perturbations of one will affect the other and this may in turn feed back on the original change. The feedback may tend either to enhance or to diminish the initial perturbation, depending on whether its sign is positive or negative.

If we wish to explore the properties which this close-coupling may confer on the system, we at once come upon a substantial problem: the earth's biota and environment are vastly complex and there is hardly a single aspect of their interaction which can as yet be described with any confidence by a mathematical equation. For this reason we have chosen to study an artificial world, having a very simple biota which is specifically designed to display the characteristic in which we are interested—namely, close-coupling of the biota and the global environment. By simplifying our biosphere enormously we can describe it in terms of a few equations borrowed directly from population ecology theory. But let the reader be warned in advance: we are not trying to model the Earth, but rather a fictional world which displays clearly a property which we believe is important for the Earth.

2. The equations for Daisyworld

Daisyworld is a cloudless planet with a negligible atmospheric greenhouse on which the only plants are two species of daisy of different colours. One species is dark—ground covered by it reflects less light then bare ground—while the other is light and reflects more than the bare ground. To emphasize

Daisyworld

Georg Engel, Seminar Quantitative Systemwissenschaften, SS 2011

1 The model

On Daisyworld, the temperature is regulated by life, governed by the interplay between growth of plants, the albedo and the temperature on the planet. All that exists on the flat planet is incident solar radiation, two species of daisies (white and black), albedo and the temperature. Daisyworld is determined by the following system of equations:

$$\frac{d}{dt}\alpha_{b,w} = (x\beta_{b,w} - \gamma)\alpha_{b,w} \quad (1)$$

$$x = p - \alpha_b - \alpha_w \quad (2)$$

$$\beta_{b,w} = 1 - 0.003265(22.5 - T_{b,w})^2 \quad (3)$$

$$\sigma(T_{eff} + 273.15)^4 = SL(1 - A) \quad (4)$$

$$A = \alpha_g A_g + \alpha_b A_b + \alpha_w A_w \quad (5)$$

$$(T_{b,w} + 273.15)^4 = q(A - A_{b,w}) + (T_{eff} + 273.15)^4 \quad (6)$$

Eqs. 1 are two ordinary diff. eqs. governing the development of the areas covered by daisies (α_b, α_w). Eq. 2 gives the remaining uncovered fertile ground. Eqs. 3 ensure that the growth rates $\beta_{b,w}$ are peaked curves with a maximum at $T = 22.5°\mathrm{C}$ and zero for $T < 5°\mathrm{C}$ and $T > 40°\mathrm{C}$. Eq. 4 determines the effective global temperature T_{eff} of Daisyworld from the incident solar radiation L and the Stefan-Boltzmann law. Eq. 5 gives the effective global albedo A (where $\alpha_g = 1 - \alpha_b - \alpha_w$ is the bare ground). Eqs. 6 describe how the local temperatures $T_{b,w}$ are allowed to deviate from the global temperature T_{eff}, controlled by the difference of the local albedos $A_{b,w}$ to the global albedo A.

The parameters are: $A_w = 0.75$ albedo white daisies, $A_b = 0.25$ albedo black daisies, $A_g = 0.5$ albedo bare ground, $\gamma = 0.3$ daisy death rate, $S = 9.17 * 10^5$ flux constant [ergs/cm^2/s], $L = 0.6 - 1.7$ incident solar radiation, $\sigma = 5.67 * 10^{-5}$ Stefan-Boltzmann constant, $p - 1$ proportion of fertile ground, $q = 0.06S/\sigma$ effective isolation of heat. The total area of the planet is set to unity.

We briefly summarize the feedback mechanism: The daisy areas enter A through Eq. 5, which determines T_{eff} by Eq. 4. Using T_{eff}, the local temperatures $T_{b,w}$ are calculated with Eqs. 6, which regulate $\beta_{b,w}$ via Eqs. 3. Finally, $\beta_{b,w}$ enter the diff. eqs. 1 to determine the change of the daisy areas.

There are four different fixed points of the daisy areas (α_b, α_w): $(0,0), (\alpha_b^*, 0), (0, \alpha_w^*)$ and (α_b^*, α_w^*). The non-trivial steady state solutions $\alpha_{b,w}^* \neq 0$ have to fulfill $x^*\beta_{b,w}^* = \gamma$. To investigate the stability of the fixed points, we look at the eigenvalues of the Jacobi matrix

$$\frac{\partial}{\partial\alpha_i}\dot{\alpha}_j = [(p - \alpha_b - \alpha_w)\beta_j - \gamma]\,\delta_{ij} - \beta_j\alpha_j \cdot \quad (7)$$

$\times (p - \alpha_b - \alpha_w)\frac{\partial}{\partial\alpha_i}\beta_j \cdot \alpha_j$

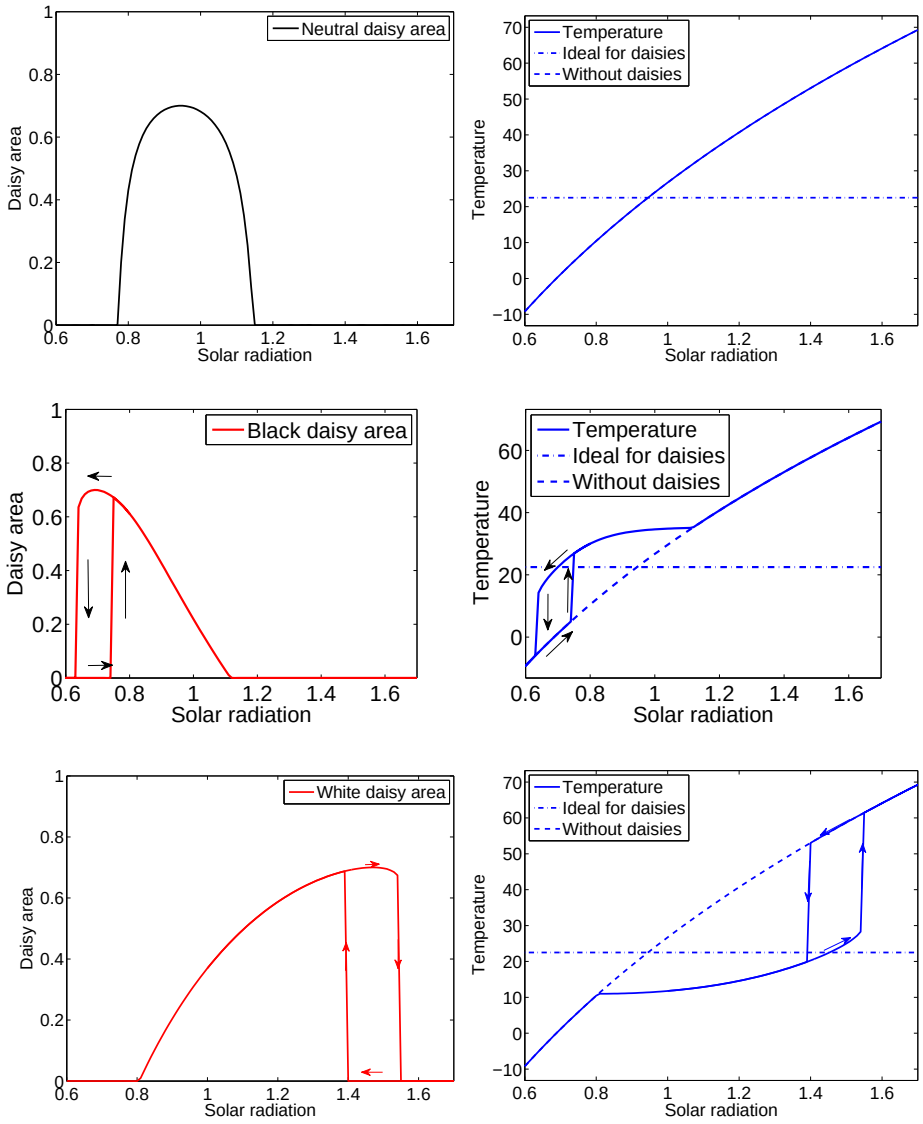

Figure 6: Daisyworld with one species of daisies only. Left hand side: area of daisies depending on the solar radiation, right hand side: global temperature versus the solar radiation shown. From top to bottom we show results for only neutral daisies (which have the same albedo as the bare ground), only black daisies and only white daisies. Note the hysteresis loops.

neutral daisies, which have an albedo of $A_n = 0.5$, the same as bare ground, shown in Figure 6. The local temperature equals the global temperature, which is therefore not influenced by the growth of the daisies. Next we look at only

2 Results and conclusion

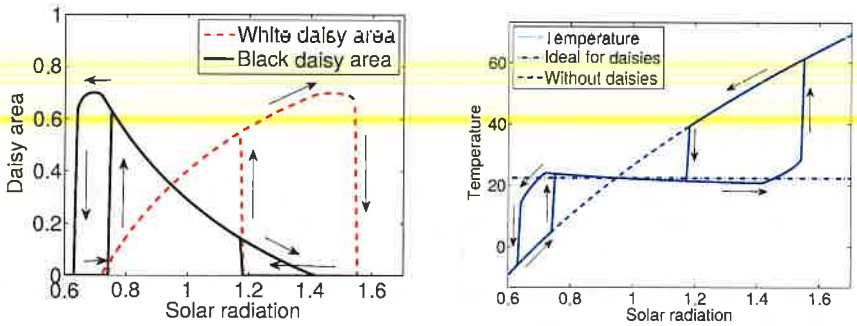

The figure shows steady state solutions for various solar radiations. Black daisies favour less radiation while the white ones favour more. In the region of the doubly non-trivial fixed point (α_b, α_w), the global temperature is very flat and close to the ideal temperature over a broad range of solar radiation ("homeostasis"). It even decreases with increasing radiation. Note also that the hysteresis loops are fairly large, which means broad regions of bistability.

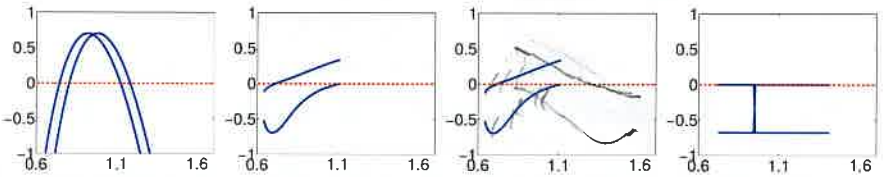

Here, eigenvalues of the Jacobi matrix are shown for the four fixed points $(0,0), (\alpha_b^*, 0), (0, \alpha_w^*), (\alpha_b^*, \alpha_w^*)$, from left to right, vs. the solar radiation. Note that there is a region where (0,0) is repulsive, i.e. where life cannot die out. The fixed point (α_b^*, α_w^*) seems not to become repulsive, it is rather abandoned by the system if one of the corresponding areas α_b^* or α_w^* would become negative. Then there is a continuous crossover to $(\alpha_b^*, 0)$ or $(0, \alpha_w^*)$.

The system shows two principles at work: *Survival of the fittest* and *homeostasis by symbioses*. This means that both competition and cooperation are crucial mechanisms in the system. The chosen parameters determine which of them is stronger and thus which fixed point is chosen. Furthermore, regardless of the particular albedos, *the system always shows greater stability with life than without them*. This is because life favours a small region of temperature (see Eq. 3). Even if life drives the temperature in a direction which is less favorable, the resulting reduction of life will limit the effect of life on the environment and finally lead to a steady state. Since it is a univeral property of life to favor certain environmental conditions, this stabilization mechanism is expected to apply to any arbitrary environmental property, not only temperature.

Some references are:

"Biological homeostastis of the global environment: the parable of Daisyworld", *A.J. Watson and J.E. Lovelock*, Tellus(1983),*35B*,284-289;

"Daisyworld: A review" *A.J. Wood, G.J. Ackland, J.G. Dyke and H.T.P. Williams*, Reviews of Geophysics(2008), *46*, RG1001/2008

Dieter M. Imboden • Stefan Pfenninger

Introduction to Systems Analysis

Mathematically Modeling Natural Systems

Cartoons by Nikolas Stürchler

Springer

Dieter M. Imboden
Department of Environmental Systems Science
ETH Zurich
Zurich
Switzerland

Stefan Pfenninger
International Institute for Applied Systems Analysis (IIASA)
Laxenburg
Austria

ISBN 978-3-642-43050-3 ISBN 978-3-642-30639-6 (eBook)
DOI 10.1007/978-3-642-30639-6
Springer Heidelberg New York Dordrecht London

Example 5.12: The global carbon cycle

Figure 5.12 shows the global carbon cycle in highly simplified form as a box diagram. Carbon is stored in three geochemical reservoirs: the atmosphere, the ocean surface and the deep sea. It is stored predominantly in the form of carbon dioxide (CO_2) as well as carbonate ($CO_3^=$ or HCO_3^-). Of course, carbon is continuously exchanged between these reservoirs. The fourth important reservoir is terrestrial biomass. Ocean biomass is so small that we can neglect it. The size of the four boxes and the width of the arrows roughly represent the system's pre-industrial steady state. By far the largest reservoir is the deep sea, while the atmosphere is the smallest. The fact that carbon exchange between the deep sea and the other reservoirs is small will be important for the model.
With the onset of rapid industrialization in the mid-nineteenth century, the combustion of fossil fuels (initially mostly coal, then also oil and gas) led to an increase of atmospheric CO_2 concentration. The pre-industrial CO_2 concentration was around 280 ppmv.[a] The value in the atmosphere box in Fig. 5.12 represents this concentration. Figure 5.13 shows the rapid increase of atmospheric CO_2 concentration during the past 150 years. By now, of course, the CO_2 concentration has surpassed 390 ppmv and the carbon cycle is no longer in an equilibrium.

[a] The unit ppmv is a non-dimensional concentration measure. It means *parts per million per volume*, that is, 1 ppmv means that a 10^{-6} volume portion of the air consists of CO_2.

We want to construct a dynamic model from the pre-industrial steady state (Fig. 5.12). Then, we will treat the disturbance of the system through fossil fuel combustion as a singularity in time, i.e., we will introduce the total amount of 300×10^{15} g C into the atmosphere at time $t = 0$ in one fell swoop. This represents roughly the amount of carbon introduced to the atmosphere by the burning of fossil fuels between 1,850 and 2,000, not taking into account additional sources of carbon such as emissions from land-use change and deforestation.
We want to answer three questions with our model:

1. How does the carbon inventory $M_i(t)$ develop over time in the four boxes?
2. Where will the additional carbon be stored in the long term?
3. How long will it take for the system to reach an equilibrium again, if no further (anthropogenic or natural) disturbances occur?

How do we get from the static image in Fig. 5.12 to a dynamic model? At this point we have to make an assumption about how the fluxes $F_{i,j}$

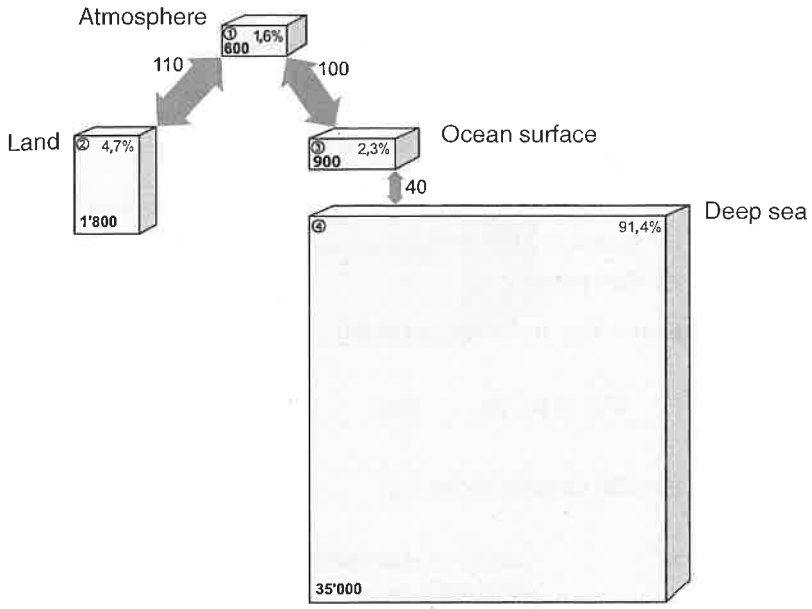

Fig. 5.12: *Simplified global carbon model with the most important exchange fluxes. The numbers in the boxes give the yearly carbon stock (unit is $10^{15}\,g\,C$), the numbers next to the arrows give the fluxes (unit $10^{15}\,g\,C\,a^{-1}$), the percent values give the relative proportion of the entire carbon stock that the box holds. The situation represents roughly the pre-industrial steady state (numbers are simplified from Moore et al. 1994)*

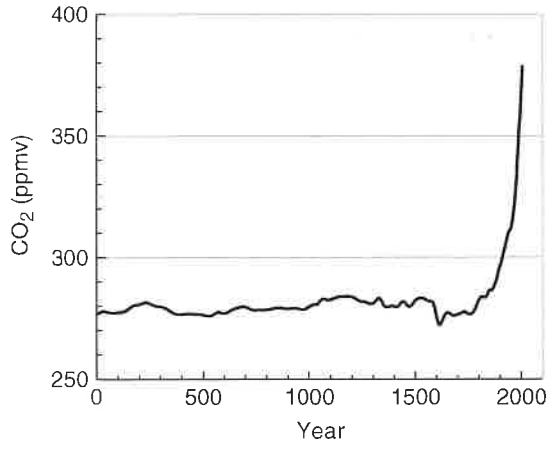

Fig. 5.13: *Atmospheric concentrations of CO_2 over the last 2,000 years (Source: Forster et al. (2007))*

between the boxes react to changes of substance mass in the reservoirs. We define them such that the first index (i) denominates the receiving box and the second index (j) the originating box (see Table 5.3). Since we want to construct a linear model, the simplest way is to describe the fluxes $F_{i,j}$ as linear functions of the content M_j of the originating box. To do so, we will first look at the two boxes *atmosphere* and *land* (Fig. 5.14).

Table 5.3: *Exchange rates and dynamic equations of the global linear carbon model. Labeling of fluxes and rates: first index = number of the destination box, second index = number of the originating box*

M_i	$[10^{15}\,\mathrm{g\,C}]$	Reservoir size of the box i
$F_{i,j}$	$[10^{15}\,\mathrm{g\,C\,year^{-1}}]$	Flux from box j into box i
$k_{i,j}$	$[\mathrm{year^{-1}}]$	linear flux rate for the transport from box j into box i

Calculation of the rates:

Because we assume $F_{i,j}$ to be proportional to the originating reservoir j, we get:

$$F_{i,j} = k_{i,j} M_j \qquad \text{thus} \qquad k_{i,j} = \frac{F_{i,j}}{M_j}$$

Values of the specific transfer rates $k_{i,j}$:

$k_{1,2} = 0.061\ \mathrm{a^{-1}}$	(Land → atmosphere)
$k_{2,1} = 0.183\ \mathrm{a^{-1}}$	(Atmosphere → land)
$k_{1,3} = 0.111\ \mathrm{a^{-1}}$	(Ocean surface → atmosphere)
$k_{3,1} = 0.167\ \mathrm{a^{-1}}$	(Atmosphere → ocean surface)
$k_{3,4} = 1.14 \times 10^{-3}\ \mathrm{a^{-1}}$	(Deep sea → ocean surface)
$k_{4,3} = 0.044\ \mathrm{a^{-1}}$	(Ocean surface → deep sea)

The dynamic mass balance equations for the reservoirs are:

$$\begin{aligned}
\frac{\mathrm{d}M_1}{\mathrm{d}t} &= -(k_{2,1} + k_{3,1})M_1 + k_{1,2}M_2 + k_{1,3}M_3 \\
\frac{\mathrm{d}M_2}{\mathrm{d}t} &= k_{2,1}M_1 - k_{1,2}M_2 \\
\frac{\mathrm{d}M_3}{\mathrm{d}t} &= k_{3,1}M_1 - (k_{1,3} + k_{4,3})M_3 + k_{3,4}M_4 \\
\frac{\mathrm{d}M_4}{\mathrm{d}t} &= k_{4,3}M_3 - k_{3,4}M_4
\end{aligned}$$

We calculate the specific exchange rates $k_{i,j}$ between land and atmosphere as follows:

$$k_{1,2} = \frac{F_{1,2}}{M_2} = \frac{110 \times 10^{15}\,\mathrm{g\ a^{-1}}}{1,800 \times 10^{15}\,\mathrm{g}} = 0.061\ \mathrm{a^{-1}}$$

$$k_{2,1} = \frac{F_{2,1}}{M_1} = \frac{110 \times 10^{15}\,\mathrm{g\ a^{-1}}}{600 \times 10^{15}\,\mathrm{g}} = 0.183\ \mathrm{a^{-1}}$$

Table 5.3 shows the calculations for the transfer rates and the transport equations of the entire model. The smallest rates are, as we already noted, the ones between the ocean surface and the deep sea.

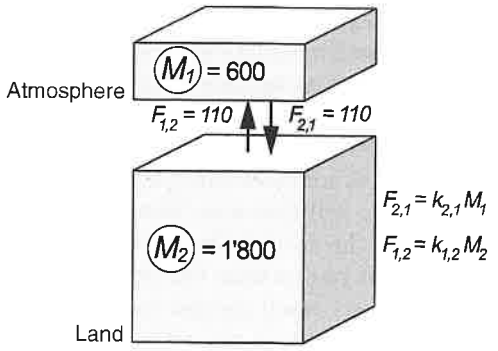

Fig. 5.14: *From the description of the steady state we can calculate exchange rates for a linear dynamic model by assuming that the flux between two boxes is a linear function of mass in the originating box (Excerpt from Fig. 5.12)*

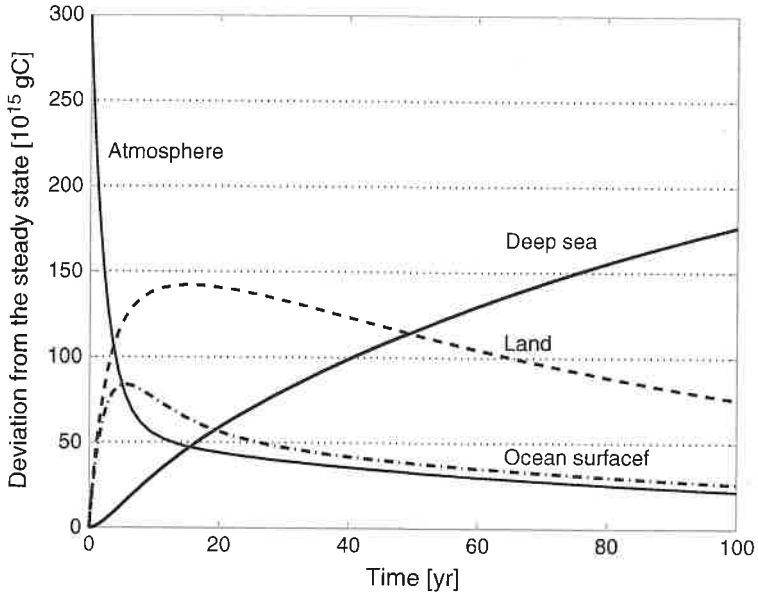

Fig. 5.15: *Numerical solution of the linear carbon model. Starting from the sudden addition of* 300×10^{15} *g C to the atmosphere, the figure shows the deviation of the four carbon reservoirs from their pre-industrial steady state as a function of elapsed time. Note that after 50 years, the system is still far from a new steady state. For any point in time the sum of all curves is equal to the added mass of* 300×10^{15} *g C*

How can this simple model be used to answer the three questions posed above? The dynamic development of the four carbon reservoirs $M_i(t)$ can be calculated analytically or with the aid of a computer program. In the first case, each variable $M_i(t)$ is described by a constant and four time-dependent exponential functions (see Eq. 5.83). The initial values of $M_i (i = 2, 3, 4)$ are those in Fig. 5.12, while the atmospheric reservoir (M_1) is increased by the anthropogenic input of 300×10^{15} to 900×10^{15} g C.

Figure 5.15 shows the result of a numerical simulation of the model's development through time. As expected, the biggest reservoir, M_4 (the deep sea), reacts most slowly. That is because it's only coupled to the other reservoirs by a fairly small (relative to the reservoir size) mass flux.

The second question, regarding the new steady state, can easily be answered from Table 5.3 without solving the system of equations. Because we are dealing with a linear homogeneous model, the relative sizes of the M_i at

steady state remain unchanged, i.e. as given by the pre-industrial values of Fig. 5.12. In other words: Each box absorbs an amount of the additional carbon (300×10^{15} g C) in proportion to its original size. Even though the deep sea reacts slowly, it will—always according to our simple model—eventually contain 91.4 % of the additional carbon. Overall, the 300×10^{15} g C only make up 0.8 % of the sum of all reservoirs ($38'300 \times 10^{15}$ g C). In the new steady state, the reservoirs will therefore have grown by less than 1 % of their original size. In fact, the carbon drama of modern society is not primarily one of total mass but results from the unfavorable fact that by burning fossil fuels we load a fairly small carbon reservoir which is dynamically "far away" from the largest reservoir, the deep sea.[10]

Finally, to predict how long it will take for the new equilibrium to be reached (thereby answering our last question), we need to calculate the eigenvalues of the coefficient matrix $\mathbf{P}$:

$$\mathbf{P} = \begin{pmatrix} -0.35 & 0.061 & 0.111 & 0 \\ 0.183 & -0.061 & 0 & 0 \\ 0.167 & 0 & -0.155 & 0.00114 \\ 0 & 0 & 0.044 & -0.00114 \end{pmatrix} \tag{5.84}$$

Because $\mathbf{P}$ is constructed from the steady-state solution of a *homogeneous* system of equations, the matrix must be singular with one eigenvalue of zero. The result of a numerical eigenvalue calculation confirms this prediction.
We get:

$$\begin{aligned} \lambda_1 &= -0.443\,\text{year}^{-1} \\ \lambda_2 &= -0.114\,\text{year}^{-1} \\ \lambda_3 &= -0.00971\,\text{year}^{-1} \\ \lambda_4 &= 0 \end{aligned}$$

Thus, we can estimate the adjustment time with Eq. (5.16):

$$\tau_{5\,\%} \approx \frac{3}{\min\left(|\lambda_i| \neq 0\right)} = \frac{3}{0.00971\ \text{year}^{-1}} \approx 310\ \text{year} \tag{5.85}$$

Of course, this carbon model is not very realistic. First, we treated the anthropogenic disturbance as a single input event. Figure 5.13 however shows that an exponentially growing input function comes much closer to reality. A second simplification is the assumption that all fluxes are linear functions of the reservoir sizes.

Nevertheless, the model illustrates important properties of the carbon cycle that are confirmed by more complex models. As mentioned above, the anthropogenic disturbance, although relatively small compared to the natural fluxes, has a large impact on the atmosphere for two reasons: the

[10] Of course, this leaves aside the increasing acidity of our oceans as a result of their atmospheric carbon uptake, a process which has severe effects of its own.

disturbance is directed at the smallest reservoir, and that reservoir is positioned "far" from the main reservoir—the deep sea. Experienced systems thinkers will be able to make qualitative statements like this just from looking at Fig. 5.12 and the sizes of the different mass transfer rates $k_{i,j}$.

Dieter M. Imboden
Sabine Koch

Systemanalyse

Einführung in die mathematische Modellierung natürlicher Systeme

mit 84 Abbildungen und 8 Tabellen
Cartoons von Nikolas Stürchler

Springer

geschieht. Das Verhalten von mehrdimensionalen Modellen kann dann wie bei den zweidimensionalen Modellen anhand der Eigenwerte analysiert werden. Sind alle Eigenwerte reell und negativ, so sind die Koeffizienten $a_{i,0}$ identisch mit den entsprechenden Stationärzuständen $\mathcal{V}_i^\infty$ des Systems.

Es ist in den wenigsten Fällen sinnvoll, sehr große lineare Modelle zu konstruieren. Wenn schon ein Sachverhalt nach einem komplizierteren Modell verlangt, dann kommt man meistens nicht um gewisse nichtlineare Komponenten herum. Aus diesem Grund wollen wir uns hier mit einem einzigen Beispiel begnügen; ein weiteres findet sich in der Aufgabe 5.3.

Der Kohlenstoff-Kreislauf ist einer der wichtigsten geochemischen Kreisläufe unserer Umwelt. Wir wollen hier versuchen, ihn stark vereinfachend mit einem linearen mehrdimensionalen Modell zu beschreiben.

Beispiel 5.12 (Der globale Kohlenstoff-Kreislauf)
Abbildung 5.12 zeigt in sehr vereinfachter Form den globalen Kohlenstoff-Kreislauf als Boxschema. Kohlenstoff wird in den geochemischen Reservoirs Atmosphäre, Ozeanoberfläche und Tiefsee vor allem in Form von Kohlendioxid (CO_2) bzw. von Karbonat ($CO_3^=$ oder HCO_3^-) gespeichert und zwischen den Reservoirs ausgetauscht. Ein viertes wichtiges Kohlenstoff-Reservoir ist die Land-Biomasse. Die Biomasse im Meer ist hingegen so klein, dass man sie vernachlässigen kann. Die Größe der vier Boxen und die Pfeildicke der Flüsse entspricht in etwa dem vorindustriellen Stationärzustand des Systems. Das weitaus größte Reservoir stellt die Tiefsee dar, das kleinste die Atmosphäre. Wichtig wird die Tatsache sein, dass der Kohlenstoff-Austausch zwischen der Tiefsee und den anderen Reservoirs klein ist.
Mit Beginn der starken Industrialisierung Mitte des neunzehnten Jahrhunderts führte die Verbrennung von fossilem Kohlenstoff, anfangs Kohle dann hauptsächlich Erdöl und Erdgas, zu einem Anstieg der CO_2-Konzentration in der Atmosphäre. Die vorindustrielle CO_2-Konzentration betrug 280 ppmv[a]. Der Wert in der Atmosphären-Boxe in Abbildung 5.12 entspricht dieser Konzentration. Abbildung 5.13 zeigt den rasanten Anstieg der atmosphärischen CO_2-Konzentration während der letzten 150 Jahre. Die CO_2-Konzentration in der Atmosphäre hat mittlerweile den Wert 360 ppmv überschritten. Der Kohlenstoff-Kreislauf ist nicht mehr im Gleichgewicht.

[a]Die Einheit ppmv ist eine dimensionslose Konzentrationsangabe. Sie bedeutet *parts per million* auf das Volumen bezogen. Die Konzentrationsangabe 1 ppmv bedeutet also, dass 10^{-6} Volumenanteile in der Luft aus CO_2 bestehen.

Wir wollen versuchen, aus dem vorindustriellen Stationärzustand (Abb. 5.12) ein dynamisches Modell zu konstruieren. Dabei behandeln wir die Störung des Systems durch die Verbrennung der fossilen Brennstoffe als zeitliche Singularität, d.h. wir führen die totale Menge von 300×10^{15} g C auf einen Schlag zur Zeit $t = 0$ in die Atmosphäre ein.

Das Modell soll für die Beantwortung der folgenden drei Fragen dienen:

1. Wie verläuft das Kohlenstoffinventar $M_i(t)$ in den vier Boxen?
2. Wo wird langfristig der zusätzliche Kohlenstoff zu finden sein?
3. Wie lange dauert es, bis das System wieder im Gleichgewicht ist, falls keine weitere (anthropogene oder natürliche) Störung auftritt?

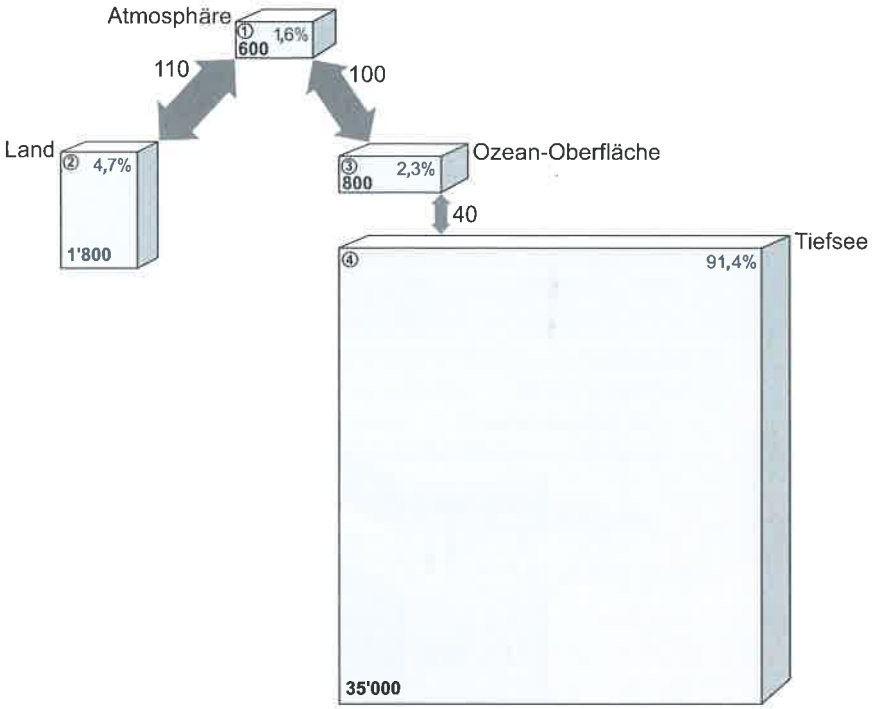

Abb. 5.12: *Vereinfachtes globales Kohlenstoff-Modell mit den wichtigsten Austauschflüssen. Die Zahlen in den Boxen geben das Kohlenstoffinventar an (Einheiten $10^{15} g\,C$), die Zahlen bei den Pfeilen die jährlichen Flüsse (Einheiten $10^{15} g\,C\,a^{-1}$), die Prozentzahlen den relativen Anteil der Box am gesamten Kohlenstoffinventar des Modells. Die Situation entspricht etwa dem vorindustriellen Stationärzustand. (Zahlen vereinfacht nach Moore et al. (1994)).*

Wie kommen wir nun von dem statischen Bild in Abbildung 5.12 zu einem dynamischen Modell? An diesem Punkt müssen wir eine Annahme darüber treffen, wie die Flüsse $F_{i,j}$ zwischen den Boxen auf die Veränderungen der Stoffmenge in den Reservoirs reagieren. In der gewählten Schreibweise für die Flüsse bezieht sich der erste Index (i) auf die empfangende Box, der zweite Index (j) auf die Ursprungs-Box. Da wir ein lineares Modell konstruieren wollen, besteht die einfachste Möglichkeit darin, die Flüsse $F_{i,j}$ als lineare Funktionen des Inhaltes M_j der Ursprungs-Box zu beschreiben. Schauen wir uns dazu zuerst die beiden Boxen „Atmosphäre" und „Land" an (Abb. 5.14):

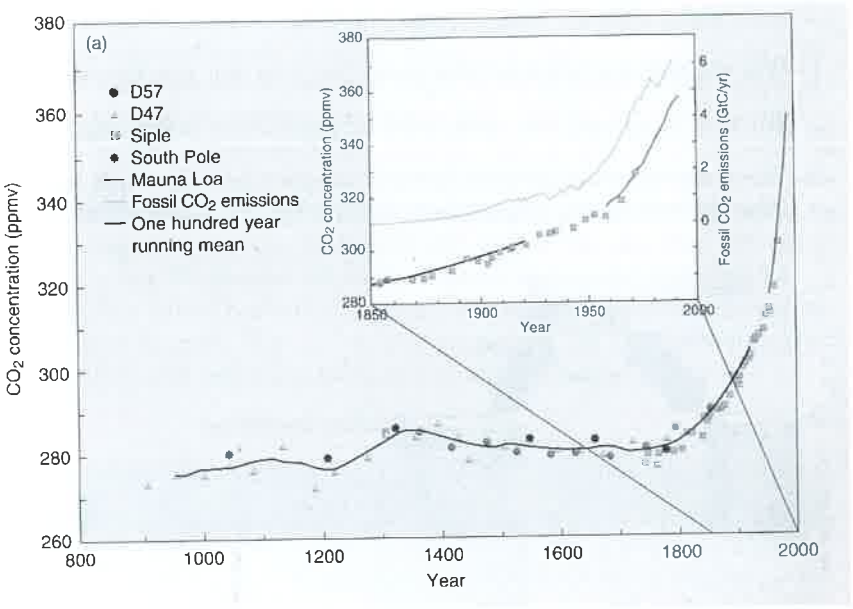

Abb. 5.13: *Die CO_2-Konzentration in der Atmosphäre während der letzten 1000 Jahre. Die Daten vor 1958 wurden aus Eisbohrkernen in der Antarktis (D57, D47, Siple und South Pole) rekonstruiert. Ab 1958 handelt es sich um eine direkte Messreihe der CO_2-Konzentration in der Atmosphäre einer Messstation am Mauna Loa (Hawaii). Quelle: Intergovernmental Panel on Climate Change (IPCC 1995 u. 2001)*

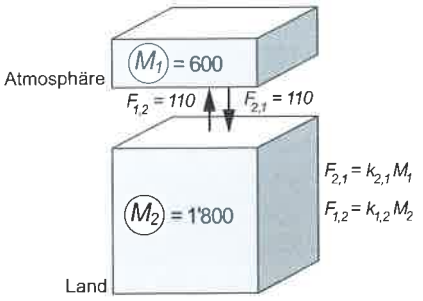

Abb. 5.14: *Aus der Darstellung des Stationärzustandes können die Austauschraten für ein lineares dynamisches Modell berechnet werden, indem wir annehmen, dass der Fluss zwischen zwei Boxen eine lineare Funktion der Masse in der Ausgangsbox ist. (Ausschnitt aus Abb. 5.12)*

Wir erhalten also für die spezifischen Austauschraten $k_{i,j}$ zwischen Land und Atmosphäre:

$$k_{1,2} = \frac{F_{1,2}}{M_2} = \frac{110 \times 10^{15}\text{g a}^{-1}}{1800 \times 10^{15}\text{g}} = 0.061\ \text{a}^{-1}$$

$$k_{2,1} = \frac{F_{2,1}}{M_1} = \frac{110 \times 10^{15}\text{g a}^{-1}}{600 \times 10^{15}\text{g}} = 0.183\ \text{a}^{-1}$$

In Tabelle 5.3 sind die Berechnung der Transferraten und die Transportgleichungen des gesamten Modells zusammengestellt. Die kleinsten Raten sind, wie bereits festgestellt, diejenigen zwischen der Meeresoberfläche und der Tiefsee.

Tabelle 5.3: *Die Austauschraten und die dynamischen Gleichungen des globalen linearen Kohlenstoff-Modells. Bezeichnungen der Flüsse und Raten: erster Index = Nummer der Endbox, zweiter Index = Nummer der Ausgangsbox.*

M_i	$[10^{15}\ \mathrm{g\,C}]$	Reservoirgröße der Box i
$F_{i,j}$	$[10^{15}\ \mathrm{g\,C\,a^{-1}}]$	Flux von Box j in Box i
$k_{i,j}$	$[\mathrm{a}^{-1}]$	lineare Fluxrate für den Transport von der Box j in die Box i

Berechnung der Raten:
Da angenommen wird, $F_{i,j}$ sei proportional zum Ursprungsreservoir j, ergibt sich:

$$F_{i,j} = k_{i,j} M_j \qquad \text{also} \qquad k_{i,j} = \frac{F_{i,j}}{M_j}$$

Werte der spezifischen Transferraten $k_{i,j}$:

$k_{1,2} = 0.061\ \mathrm{a}^{-1}$	(Land → Atmosphäre)
$k_{2,1} = 0.183\ \mathrm{a}^{-1}$	(Atmosphäre → Land)
$k_{1,3} = 0.111\ \mathrm{a}^{-1}$	(Meeresoberfläche → Atmosphäre) $= 0,125$
$k_{3,1} = 0.167\ \mathrm{a}^{-1}$	(Atmosphäre → Meer/Oberfläche)
$k_{3,4} = 1.14 \times 10^{-3}\ \mathrm{a}^{-1}$	(Tiefsee → Meeresoberfläche)
$k_{4,3} = 0.044\ \mathrm{a}^{-1}$	(Meeresoberfläche → Tiefsee) $= 0,05$

die angegebenen k_{13}, k_{43} entsprechen $M_3 = 900$

Damit ergibt sich für die Transportgleichungen:

$$\begin{aligned}
\frac{\mathrm{d}M_1}{\mathrm{d}t} &= -(k_{2,1} + k_{3,1})M_1 + k_{1,2}M_2 + k_{1,3}M_3 \\
\frac{\mathrm{d}M_2}{\mathrm{d}t} &= k_{2,1}M_1 - k_{1,2}M_2 \\
\frac{\mathrm{d}M_3}{\mathrm{d}t} &= k_{3,1}M_1 - (k_{1,3} + k_{4,3})M_3 + k_{3,4}M_4 \\
\frac{\mathrm{d}M_4}{\mathrm{d}t} &= k_{4,3}M_3 - k_{3,4}M_4
\end{aligned}$$

Wie können wir mit diesem Modell die drei gestellten Fragen beantworten? Die dynamische Entwicklung der vier Kohlenstoff-Reservoirs $M_i(t)$ berechnet man entweder analytisch oder numerisch mit Hilfe eines der zahlreichen Computerprogramme. Im ersten Fall werden die Variablen $M_i(t)$ durch die Summe einer Konstante und vier zeitabhängigen Exponentialfunktionen dargestellt (vgl. Gl. 5.83). Die Anfangswerte entsprechen für $M_i(i = 2, 3, 4)$ denjenigen in der Abbildung 5.12; das atmosphärische Reservoir M_1 wird um den „anthropogenen" Betrag von 300×10^{15} g C auf insgesamt 900×10^{15} g C erhöht.

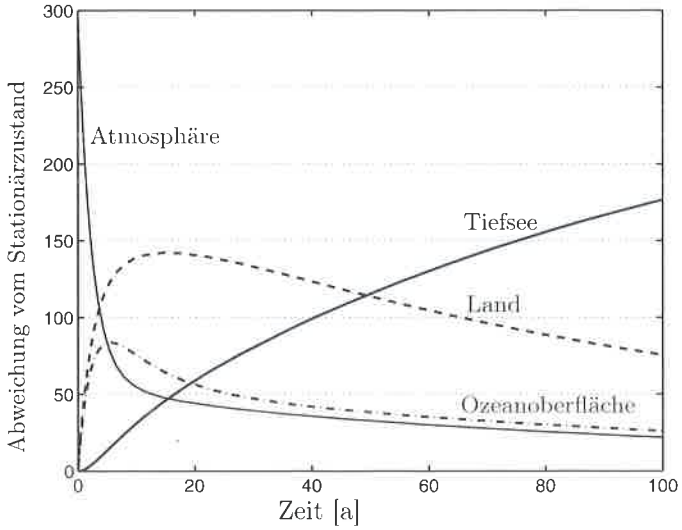

Abb. 5.15: *Numerische Modellierung des Kohlenstoff-Kreislaufs: Auf der y-Achse ist die Abweichung vom Anfangszustand im Gleichgewicht dargestellt. Die Summe aller Kurven ergibt zu jeder Zeit wieder die zusätzliche Kohlenstoffmasse von* 300×10^{15} *g C.*

Abbildung 5.15 zeigt als Resultat einer numerischen Simulation die zeitliche Entwicklung der vier Reservoirinhalte M_i. Nicht überraschend reagiert das größte Reservoir M_4 (Tiefsee) am langsamsten, da es nur schlecht an die anderen Kohlenstoff-Reservoire gekoppelt ist.

Die zweite Frage nach dem neuen Stationärzustand lässt sich leicht und ohne Lösung des Gleichungssystems von Tabelle 5.3 beantworten. Da es sich um ein lineares homogenes Modell handelt, müssen im neuen Stationärzustand die relativen Größenverhältnisse der M_i untereinander wieder den ursprünglichen Wert haben. Mit anderen Worten: Jede Box übernimmt den zu seiner ursprünglichen Größe proportionalen Anteil des Zusatz-Kohlenstoffs von 300×10^{15} g C. Auch wenn die Tiefsee nur langsam reagiert, so wird — immer gemäß des einfachen Modells — 91.4% des zusätzlichen Kohlenstoffes dereinst dort enden. Insgesamt machen die 300×10^{15} g C nur 0.8% der Summe aller Reservoire aus ($38'300 \times 10^{15}$ g C); um diesen kleinen Bruchteil werden die Reservoirs im neuen Stationärzustand größer sein.

Schließlich zur letzten Frage: Um vorherzusagen wie lange es dauert, bis der neue Gleichgewichtszustand erreicht wird, müssen wir die Eigenwerte der Koeffizientenmatrix $\mathbf{P}$ berechnen:

$$\mathbf{P} = \begin{pmatrix} -0.35 & 0.061 & 0.111 & 0 \\ 0.183 & -0.061 & 0 & 0 \\ 0.167 & 0 & -0.155 & 0.00114 \\ 0 & 0 & 0.044 & -0.00114 \end{pmatrix} \tag{5.84}$$

Da $\mathbf{P}$ aus der stationären Lösung eines homogenen linearen Gleichungssystems konstruiert worden ist, muss die Matrix singulär sein und einen

Eigenwert null haben. Das Resultat einer numerischen Eigenwertberechnung bestätigt diese Voraussage. Wir erhalten:

$$\begin{aligned} \lambda_1 &= -0.443\ \mathrm{a}^{-1} \\ \lambda_2 &= -0.114\ \mathrm{a}^{-1} \\ \lambda_3 &= -0.00971\ \mathrm{a}^{-1} \\ \lambda_4 &= 0 \end{aligned}$$

Damit können wir die Anpassungszeit mit Gleichung (5.16) abschätzen:

$$\tau_{5\%} \approx \frac{3}{\min\left(\{\lambda_i | \neq 0\}\right)} = \frac{3}{0.00971\ \mathrm{a}^{-1}} \approx 310\ \mathrm{a} \tag{5.85}$$

Natürlich ist dieses Kohlenstoff-Modell nicht sehr realistisch. Erstens haben wir die anthropogene Störung als zeitliche Singularität behandelt. Abbildung 5.13 zeigt aber, dass eine exponentiell wachsende Input-Funktion der Wirklichkeit näher käme. Eine zweite Vereinfachung besteht in der Annahme, die Flüsse seien lineare Funktionen der Reservoir-Massen.

Dennoch illustriert das Modell wichtige Eigenschaften des Kohlenstoff-Kreislaufs, die auch komplexere Modelle und vor allem Beobachtungen bestätigen. Die an sich im Vergleich zu den natürlichen Flüssen kleine anthropogene Störung hat nur deswegen (vorübergehend) eine große Wirkung in der Atmosphäre, weil die Störung auf das kleinste Reservoir einwirkt und dieses systemmäßig weit weg vom Hauptreservoir Tiefsee positioniert ist. Geübte Systemanalytiker und -analytikerinnen sollten in der Lage sein, ohne explizite Rechnung nur schon aus der Betrachtung von Abbildung 5.12 qualitative Aussagen dieser Art machen zu können.

Introduction to the Modeling and Analysis of Complex Systems

Hiroki Sayama

ISBN:
978-1-942341-06-2 (deluxe color edition)
978-1-942341-08-6 (print edition)
978-1-942341-09-3 (ebook)

This publication was made possible by a SUNY Innovative Instruction Technology Grant (IITG). IITG is a competitive grants program open to SUNY faculty and support staff across all disciplines. IITG encourages development of innovations that meet the Power of SUNY's transformative vision.

Published by Open SUNY Textbooks, Milne Library
State University of New York at Geneseo
Geneseo, NY 14454

Chapter 8

Bifurcations

8.1 What Are Bifurcations?

One of the important questions you can answer by mathematically analyzing a dynamical system is how the system's long-term behavior depends on its parameters. Most of the time, you can assume that a slight change in parameter values causes only a slight quantitative change in the system's behavior too, with the essential structure of the system's phase space unchanged. However, sometimes you may witness that a slight change in parameter values causes a drastic, qualitative change in the system's behavior, with the structure of its phase space topologically altered. This is called a *bifurcation*, and the parameter values at which a bifurcation occurs are called the *critical thresholds*.

Bifurcation is a qualitative, topological change of a system's phase space that occurs when some parameters are slightly varied across their critical thresholds.

Bifurcations play important roles in many real-world systems as a switching mechanism. Examples include excitation of neurons, pattern formation in morphogenesis (this will be discussed later), catastrophic transition of ecosystem states, and binary information storage in computer memory, to name a few.

There are two categories of bifurcations. One is called a *local bifurcation*, which can be characterized by a change in the stability of equilibrium points. It is called local because it can be detected and analyzed only by using localized information around the equilibrium point. The other category is called a *global bifurcation*, which occurs when non-local features of the phase space, such as limit cycles (to be discussed later), collide with equilibrium points in a phase space. This type of bifurcation can't be characterized just by using localized information around the equilibrium point. In this textbook, we focus only on

the local bifurcations, as they can be easily analyzed using the concepts of linear stability that we discussed in the previous chapters.

Local bifurcations occur when the stability of an equilibrium point changes between stable and unstable. Mathematically, this condition can be written down as follows:

> Local bifurcations occur when the eigenvalues λ_i of the Jacobian matrix at an equilibrium point satisfy the following:
>
> **For discrete-time models:** $|\lambda_i| = 1$ for some i, while $|\lambda_i| < 1$ for the rest.
>
> **For continuous-time models:** $\mathrm{Re}(\lambda_i) = 0$ for some i, while $\mathrm{Re}(\lambda_i) < 0$ for the rest.

These conditions describe a critical situation when the equilibrium point is about to change its stability. We can formulate these conditions in equations and then solve them in terms of the parameters, in order to obtain their critical thresholds. Let's see how this analysis can be done through some examples below.

8.2 Bifurcations in 1-D Continuous-Time Models

For bifurcation analysis, continuous-time models are actually simpler than discrete-time models (we will discuss the reasons for this later). So let's begin with the simplest example, a continuous-time, first-order, autonomous dynamical system with just one variable:

$$\frac{dx}{dt} = F(x) \tag{8.1}$$

In this case, the Jacobian matrix is a 1×1 matrix whose eigenvalue is its content itself (because it is a scalar), which is given by dF/dx. Since this is a continuous-time model, the critical condition at which a bifurcation occurs in this system is given by

$$\mathrm{Re}\left(\frac{dF}{dx}\right)\bigg|_{x=x_{\mathrm{eq}}} = \frac{dF}{dx}\bigg|_{x=x_{\mathrm{eq}}} = 0. \tag{8.2}$$

Let's work on the following example:

$$\frac{dx}{dt} = r - x^2 \tag{8.3}$$

The first thing we need to do is to find the equilibrium points, which is easy in this case. Letting $dx/dt = 0$ immediately gives

$$x_{\mathrm{eq}} = \pm\sqrt{r}, \tag{8.4}$$

which means that equilibrium points exist only for non-negative r. The critical condition when a bifurcation occurs is given as follows:

$$\frac{dF}{dx} = -2x \tag{8.5}$$

$$\left.\frac{dF}{dx}\right|_{x=x_{\text{eq}}} = \pm 2\sqrt{r} = 0 \tag{8.6}$$

$$r = 0 \tag{8.7}$$

Therefore, now we know a bifurcation occurs when $r = 0$. Moreover, by plugging each solution of Eq. (8.4) into $dF/dx = -2x$, we know that one equilibrium point is stable while the other is unstable. These results are summarized in Table 8.1.

Table 8.1: Summary of bifurcation analysis of $dx/dt = r - x^2$.

Equilibrium point	$r < 0$	$0 < r$
$x_{\text{eq}} = \sqrt{r}$	doesn't exist	stable
$x_{\text{eq}} = -\sqrt{r}$	doesn't exist	unstable

There is a more visual way to illustrate the results. It is called a *bifurcation diagram*. This works only for systems with one variable and one parameter, but it is still conceptually helpful in understanding the nature of bifurcations. A bifurcation diagram can be drawn by using the parameter being varied as the horizontal axis, while using the location(s) of the equilibrium point(s) of the system as the vertical axis. Then you draw how each equilibrium point depends on the parameter, using different colors and/or line styles to indicate the stability of the point. Here is an example of how to draw a bifurcation diagram in Python:

Code 8.1: bifurcation-diagram.py

```
from pylab import *

def xeq1(r):
    return sqrt(r)

def xeq2(r):
    return -sqrt(r)

domain = linspace(0, 10)
plot(domain, xeq1(domain), 'b-', linewidth = 3)
```

```
plot(domain, xeq2(domain), 'r--', linewidth = 3)
plot([0], [0], 'go')
axis([-10, 10, -5, 5])
xlabel('r')
ylabel('x_eq')

show()
```

The result is shown in Fig. 8.1, where the blue solid curve indicates a stable equilibrium point $x_{\text{eq}} = \sqrt{r}$, and the red dashed curve indicates an unstable equilibrium point $x_{\text{eq}} = -\sqrt{r}$, with the green circle in the middle showing a neutral equilibrium point. This type of bifurcation is called a *saddle-node bifurcation*, in which a pair of equilibrium points appear (or collide and annihilate, depending on which way you vary r).

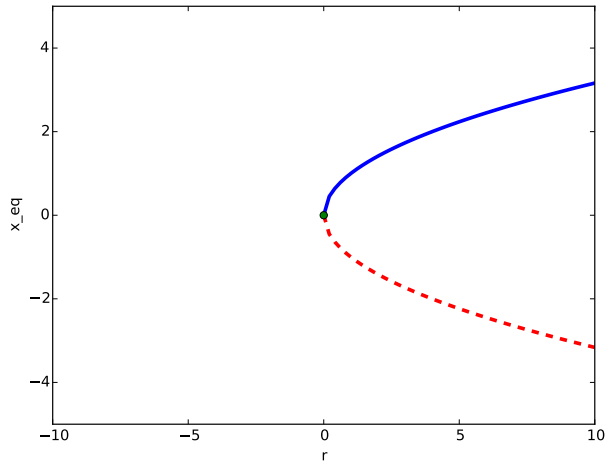

Figure 8.1: Visual output of Code 8.1, showing a bifurcation diagram of a saddle-node bifurcation, obtained from Eq (8.3).

Each vertical slice of the bifurcation diagram for a particular parameter value depicts a phase space of the dynamical system we are studying. For example, for $r = 5$ in the diagram above, there are two equilibrium points, one stable (blue/solid) and the other unstable (red/dashed). You can visualize flows of the system's state by adding a downward arrow above the stable equilibrium point, an upward arrow from the unstable one to the stable one, and then another downward arrow below the unstable one. In this way, it is

clear that the system's state is converging to the stable equilibrium point while it is repelling from the unstable one. If you do the same for several different values of r, you obtain Fig. 8.2, which shows how to interpret this diagram.

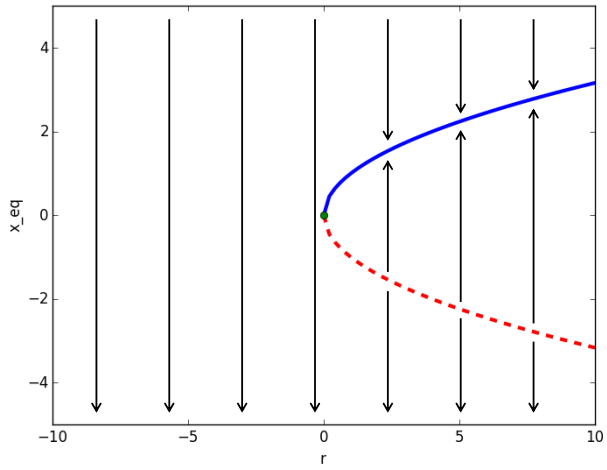

Figure 8.2: How to interpret a bifurcation diagram. Each vertical slice of the diagram depicts a phase space of the system for a particular parameter value.

There are other types of bifurcations. A *transcritical bifurcation* is a bifurcation where one equilibrium point "passes through" another, exchanging their stabilities. For example:

$$\frac{dx}{dt} = rx - x^2 \tag{8.8}$$

This dynamical system always has the following two equilibrium points

$$x_{\text{eq}} = 0, r, \tag{8.9}$$

with the exception that they collide when $r = 0$, which is when they swap their stabilities. Its bifurcation diagram is shown in Fig. 8.3.

Another one is a *pitchfork bifurcation*, where an equilibrium point splits into three. Two of these (the outermost two) have the same stability as the original equilibrium point, while the one between them has a stability opposite to the original one's stability. There are two types of pitchfork bifurcations. A *supercritical pitchfork bifurcation* makes a stable

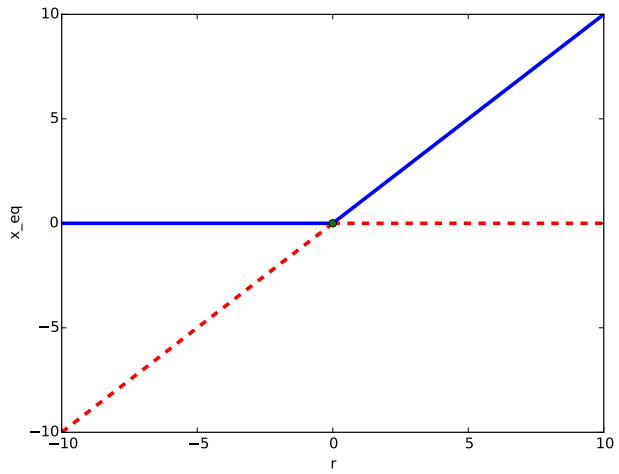

Figure 8.3: Bifurcation diagram of a transcritical bifurcation, obtained from Eq (8.8).

equilibrium point split into three, two stable and one unstable. For example:

$$\frac{dx}{dt} = rx - x^3 \tag{8.10}$$

This dynamical system has the following three equilibrium points

$$x_{\text{eq}} = 0, \pm\sqrt{r}, \tag{8.11}$$

but the last two exist only for $r \geq 0$. You can show that $x_{\text{eq}} = 0$ is stable for $r < 0$ and unstable for $r > 0$, while $x_{\text{eq}} = \pm\sqrt{r}$ are always stable if they exist. Its bifurcation diagram is shown in Fig. 8.4.

In the meantime, a *subcritical pitchfork bifurcation* makes an unstable equilibrium point split into three, two unstable and one stable. For example:

$$\frac{dx}{dt} = rx + x^3 \tag{8.12}$$

This dynamical system has the following three equilibrium points

$$x_{\text{eq}} = 0, \pm\sqrt{-r}, \tag{8.13}$$

but the last two exist only for $r \leq 0$. Its bifurcation diagram is shown in Fig. 8.5.

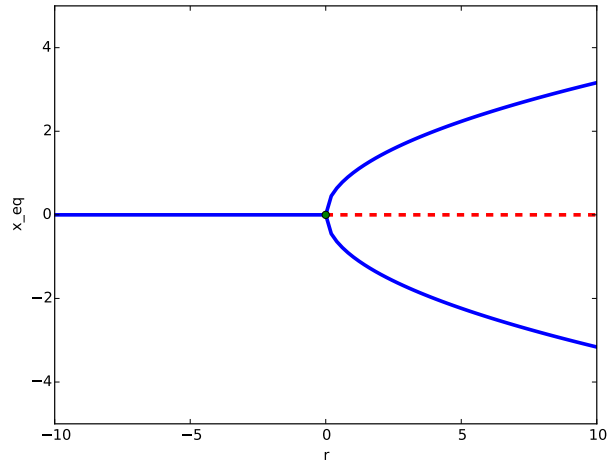

Figure 8.4: Bifurcation diagram of a supercritical pitchfork bifurcation, obtained from Eq (8.10).

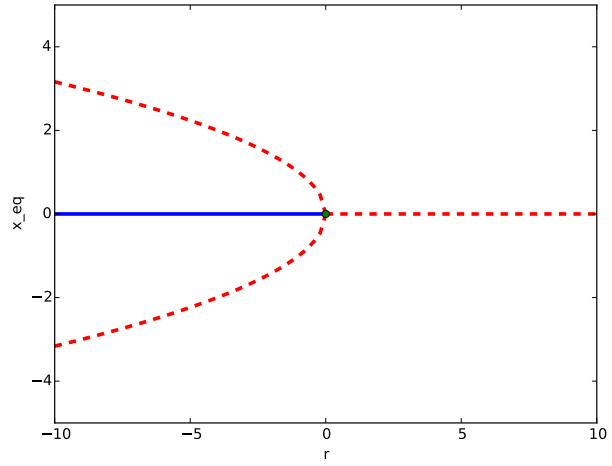

Figure 8.5: Bifurcation diagram of a subcritical pitchfork bifurcation, obtained from Eq (8.10).

These bifurcations can arise in combined forms too. For example:

$$\frac{dx}{dt} = r + x - x^3 \tag{8.14}$$

This dynamical system has three equilibrium points, which are rather complicated to calculate in a straightforward way. However, if we solve $dx/dt = 0$ *in terms of* r, we can easily obtain

$$r = -x + x^3, \tag{8.15}$$

which is sufficient for drawing the bifurcation diagram. We can also know the stability of each equilibrium point by calculating

$$\mathrm{Re}\left(\frac{dF}{dx}\right)\Big|_{x=x_{\mathrm{eq}}} = 1 - 3x^2, \tag{8.16}$$

i.e., when $x^2 > 1/3$, the equilibrium points are stable, otherwise they are unstable. The bifurcation diagram of this system is shown in Fig. 8.6.

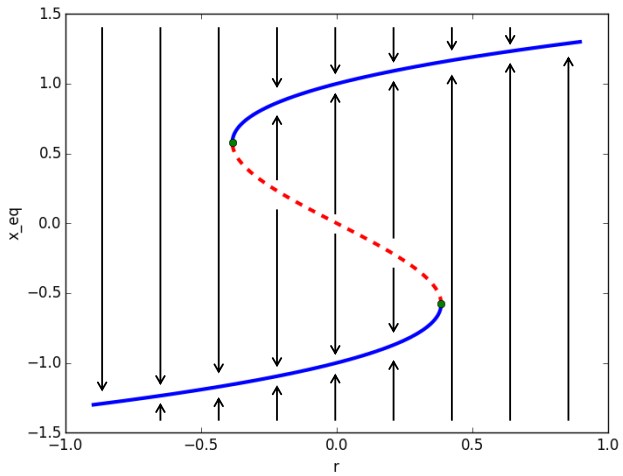

Figure 8.6: Bifurcation diagram showing hysteresis, obtained from Eq (8.14). Arrows are added to help with interpretation.

This diagram is a combination of two saddle-node bifurcations, showing that this system has *hysteresis* as its dynamical property. Hysteresis is the dependence of a system's

output (asymptotic state in this case) not only on the input (parameter r in this case) but also on its history. To understand what this means, imagine that you are slowly changing r from -1 upward. Initially, the system's state stays at the stable equilibrium at the bottom of the diagram, which continues until you reach a critical threshold at $r \approx 0.4$. As soon as you cross this threshold, the system's state suddenly jumps up to another stable equilibrium point at the top of the diagram. Such a sudden jump in the system's state is often called a *catastrophe*. You get upset, and try to bring the system's state back to where it was, by reducing r. However, counter to your expectation, the system's state remains high even after you reduce r below 0.4. This is hysteresis; the system's asymptotic state depends not just on r, but also on where its state was in the immediate past. In other words, the system's state works as a memory of its history. In order to bring the system's state back down to the original value, you have to spend extra effort to reduce r all the way below another critical threshold, $r \approx -0.4$.

Such hysteresis could be useful; every bit (binary digit) of computer memory has this kind of bifurcation dynamics, which is why we can store information in it. But in other contexts, hysteresis could be devastating—if an ecosystem's state has this property (many studies indicate it does), it takes a huge amount of effort and resources to revert a deserted ecosystem back to a habitat with vegetation, for example.

Exercise 8.1 Conduct a bifurcation analysis of the following dynamical system with parameter r:

$$\frac{dx}{dt} = rx(x+1) - x \tag{8.17}$$

Find the critical threshold of r at which a bifurcation occurs. Draw a bifurcation diagram and determine what kind of bifurcation it is.

Exercise 8.2 Assume that two companies, A and B, are competing against each other for the market share in a local region. Let x and y be the market share of A and B, respectively. Assuming that there are no other third-party competitors, $x + y = 1$ (100%), and therefore this system can be understood as a one-variable system. The growth/decay of A's market share can thus be modeled as

$$\frac{dx}{dt} = ax(1-x)(x-y), \tag{8.18}$$

where x is the current market share of A, $1 - x$ is the size of the available potential customer base, and $x - y$ is the relative competitive edge of A, which can be

rewritten as $x - (1 - x) = 2x - 1$. Obtain equilibrium points of this system and their stabilities.

Then make an additional assumption that this regional market is connected to and influenced by a much larger global market, where company A's market share is somehow kept at p (whose change is very slow so we can consider it constant):

$$\frac{dx}{dt} = ax(1 - x)(x - y) + r(p - x) \tag{8.19}$$

Here r is the strength of influence from the global to the local market. Determine a critical condition regarding r and p at which a bifurcation occurs in this system. Draw its bifurcation diagram over varying r with $a = 1$ and $p = 0.5$, and determine what kind of bifurcation it is.

Finally, using the results of the bifurcation analysis, discuss what kind of marketing strategy you would take if you were a director of a marketing department of a company that is currently overwhelmed by its competitor in the local market. How can you "flip" the market?

8.3 Hopf Bifurcations in 2-D Continuous-Time Models

For dynamical systems with two or more variables, the dominant eigenvalues of the Jacobian matrix at an equilibrium point could be complex conjugates. If such an equilibrium point, showing an oscillatory behavior around it, switches its stability, the resulting bifurcation is called a *Hopf bifurcation.* A Hopf bifurcation typically causes the appearance (or disappearance) of a *limit cycle* around the equilibrium point. A limit cycle is a cyclic, closed trajectory in the phase space that is defined as an asymptotic limit of other oscillatory trajectories nearby. You can check whether the bifurcation is Hopf or not by looking at the imaginary components of the dominant eigenvalues whose real parts are at a critical value (zero); if there are non-zero imaginary components, it must be a Hopf bifurcation.

Here is an example, a dynamical model of a nonlinear oscillator, called the *van der Pol oscillator*:

$$\frac{d^2x}{dt^2} + r(x^2 - 1)\frac{dx}{dt} + x = 0 \tag{8.20}$$

This is a second-order differential equation, so we should introduce an additional variable

$y = dx/dt$ to make it into a 2-D first-order system, as follows:

$$\frac{dx}{dt} = y \tag{8.21}$$

$$\frac{dy}{dt} = -r(x^2 - 1)y - x \tag{8.22}$$

From these, we can easily show that the origin, $(x, y) = (0, 0)$, is the only equilibrium point of this system. The Jacobian matrix of this system at the origin is given as follows:

$$\left(\begin{array}{cc} 0 & 1 \\ -2rxy - 1 & -r(x^2 - 1) \end{array} \right) \Big|_{(x,y)=(0,0)} = \left(\begin{array}{cc} 0 & 1 \\ -1 & r \end{array} \right) \tag{8.23}$$

The eigenvalues of this matrix can be calculated as follows:

$$\left| \begin{array}{cc} 0 - \lambda & 1 \\ -1 & r - \lambda \end{array} \right| = 0 \tag{8.24}$$

$$-\lambda(r - \lambda) + 1 = \lambda^2 - r\lambda + 1 = 0 \tag{8.25}$$

$$\lambda = \frac{r \pm \sqrt{r^2 - 4}}{2} \tag{8.26}$$

The critical condition for a bifurcation to occur is

$$\mathrm{Re}(\lambda) = 0, \tag{8.27}$$

whose left hand side can be further detailed as

$$\mathrm{Re}(\lambda) = \begin{cases} \dfrac{r \pm \sqrt{r^2 - 4}}{2} & \text{if } r^2 \geq 4, \text{ or} \\ \dfrac{r}{2} & \text{if } r^2 < 4. \end{cases} \tag{8.28}$$

The first case can't be zero, so the only critical condition for a bifurcation to occur is the second case, i.e.

$$r = 0, \text{ when } \mathrm{Re}(\lambda) = 0 \text{ and } \mathrm{Im}(\lambda) = \pm i. \tag{8.29}$$

This is a Hopf bifurcation because the eigenvalues have non-zero imaginary parts when the stability change occurs. We can confirm this analytical prediction by numerical simulations of the model with systematically varied r, as follows:

Code 8.2: van-del-pol-Hopf-bifurcation.py

```
from pylab import *
```

```
Dt = 0.01

def initialize():
    global x, xresult, y, yresult
    x = y = 0.1
    xresult = [x]
    yresult = [y]

def observe():
    global x, xresult, y, yresult
    xresult.append(x)
    yresult.append(y)

def update():
    global x, xresult, y, yresult
    nextx = x + y * Dt
    nexty = y + (-r * (x**2 - 1) * y - x) * Dt
    x, y = nextx, nexty

def plot_phase_space():
    initialize()
    for t in xrange(10000):
        update()
        observe()
    plot(xresult, yresult)
    axis('image')
    axis([-3, 3, -3, 3])
    title('r = ' + str(r))

rs = [-1, -0.1, 0, .1, 1]
for i in xrange(len(rs)):
    subplot(1, len(rs), i + 1)
    r = rs[i]
    plot_phase_space()

show()
```

Figure 8.7 shows the results where a clear transition from a stable spiral focus (for $r < 0$) to an unstable spiral focus surrounded by a limit cycle (for $r > 0$) is observed.

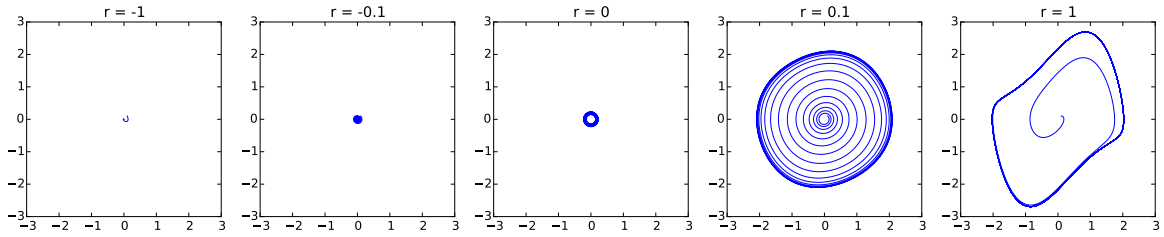

Figure 8.7: Visual output of Code 8.2.

Exercise 8.3 **FitzHugh-Nagumo model** The FitzHugh-Nagumo model [30, 31] is a simplified model of neuronal dynamics that can demonstrate both *excited* and *resting* behaviors of neurons. In a normal setting, this system's state converges and stays at a stable equilibrium point (resting), but when perturbed, the system's state moves through a large cyclic trajectory in the phase space before coming back to the resting state, which is observed as a big pulse when plotted over time (excitation). Moreover, under certain conditions, this system can show a nonlinear oscillatory behavior that continuously produces a sequence of pulses. The behavioral shift between convergence to the resting state and generation of a sequence of pulses occurs as a Hopf bifurcation, where the external current is used as a control parameter. Here are the model equations:

$$\frac{dx}{dt} = c\left(x - \frac{x^3}{3} + y + z\right) \tag{8.30}$$

$$\frac{dy}{dt} = -\frac{x - a + by}{c} \tag{8.31}$$

z is the key parameter that represents the external current applied to the neuron. Other parameters are typically constrained as follows:

$$1 - \frac{2}{3}b < a < 1 \tag{8.32}$$

$$0 < b < 1 \tag{8.33}$$

$$b < c^2 \tag{8.34}$$

With $a = 0.7$, $b = 0.8$, and $c = 3$, do the following:

- Numerically obtain the equilibrium point of this model for several values of z, ranging between -2 and 0. There is only one real equilibrium point in this system.
- Apply the result obtained above to the Jacobian matrix of the model, and numerically evaluate the stability of that equilibrium point for each value of z.
- Estimate the critical thresholds of z at which a Hopf bifurcation occurs. There are two such critical thresholds.
- Draw a series of its phase spaces with values of z varied from 0 to -2 to confirm your analytical prediction.

8.4 Bifurcations in Discrete-Time Models

The bifurcations discussed above (saddle-node, transcritical, pitchfork, Hopf) are also possible in discrete-time dynamical systems with one variable:

$$x_t = F(x_{t-1}) \tag{8.35}$$

The Jacobian matrix of this system is, again, a 1×1 matrix whose eigenvalue is its content itself, which is given by dF/dx. Since this is a discrete-time model, the critical condition at which a bifurcation occurs is given by

$$\left| \frac{dF}{dx} \right|_{x=x_{\mathrm{eq}}} = 1. \tag{8.36}$$

Let's work on the following example:

$$x_t = x_{t-1} + r - x_{t-1}^2 \tag{8.37}$$

This is a discrete-time analog of Eq. (8.3). Therefore, it has the same set of equilibrium points:

$$x_{\mathrm{eq}} = \pm\sqrt{r} \tag{8.38}$$

Next, we calculate dF/dx as follows:

$$\frac{dF}{dx} = (r + x - x^2)' = 1 - 2x \tag{8.39}$$

$$\left| \frac{dF}{dx} \right|_{x=\pm\sqrt{r}} = |1 \pm 2\sqrt{r}| \tag{8.40}$$

To find out which value of r makes this 1, we consider the following four scenarios:

- $1 + 2\sqrt{r} = 1 \quad \Rightarrow \quad r = 0$
- $1 - 2\sqrt{r} = 1 \quad \Rightarrow \quad r = 0$
- $1 + 2\sqrt{r} = -1 \quad \Rightarrow$ (no real solution)
- $1 - 2\sqrt{r} = -1 \quad \Rightarrow \quad r = 1$

As you see, $r = 0$ appears as a critical threshold again, at which a saddle-node bifurcation occurs. But now we see another critical threshold, $r = 1$, also showing up, which was not there in its continuous-time version. This is why I said before that continuous-time models are simpler than discrete-time models for bifurcation analysis; *discrete-time models can show a new form of bifurcation that wasn't possible in their continuous-time counterparts.* To learn more about this, we can study the stability of the two equilibrium points by checking whether $|dF/dx|$ is greater or less than 1 at each point. The result is summarized in Table 8.2.

Table 8.2: Summary of bifurcation analysis of $x_t = x_{t-1} + r - x_{t-1}^2$.

Equilibrium point	$r < 0$	$0 < r < 1$	$1 < r$
$x_{\text{eq}} = \sqrt{r}$	doesn't exist	stable	unstable
$x_{\text{eq}} = -\sqrt{r}$	doesn't exist	unstable	unstable

The result shown in the table is pretty much the same as before up to $r = 1$, but when $r > 1$, *both equilibrium points become unstable.* This must mean that the system is not allowed to converge toward either of them. Then what is going to happen to the system in this parameter range? We can let the system show its actual behavior by numerical simulations. Here is an example:

Code 8.3: period-doubling-bifurcation.py

```
from pylab import *

def initialize():
    global x, result
    x = 0.1
    result = [x]

def observe():
```

```
    global x, result
    result.append(x)

def update():
    global x, result
    x = x + r - x**2

def plot_phase_space():
    initialize()
    for t in xrange(30):
        update()
        observe()
    plot(result)
    ylim(0, 2)
    title('r = ' + str(r))

rs = [0.1, 0.5, 1.0, 1.1, 1.5, 1.6]
for i in xrange(len(rs)):
    subplot(2, 3, i + 1)
    r = rs[i]
    plot_phase_space()

show()
```

The results are shown in Fig. 8.8, visualizing actual trajectories of the system's state over time for several values of r. The cobweb plot version is also shown in Fig. 8.9 (the code is not shown here; try implementing the code yourself!).

There are some new behaviors that were not seen in continuous-time versions of the same model. For example, at $r = 0.5$, there was a signature of "overshooting" right before the system state converged to a stable equilibrium point. But more importantly, at $r = 1$, the system began to fail to converge to a single stable point, and for $r > 1$, it started oscillating between two distinct states. This is called a *period-doubling bifurcation.* It is a bifurcation that typically occurs in discrete-time systems (but it is also possible in continuous-time systems of higher dimensions), where the system loses stability of a period T trajectory and begins to move in another trajectory with period $2T$. The bifurcation observed for $r = 1$ was a transition from an equilibrium point (which is a periodic trajectory with period $T = 1$, i.e., the system takes the same state value in each time step)

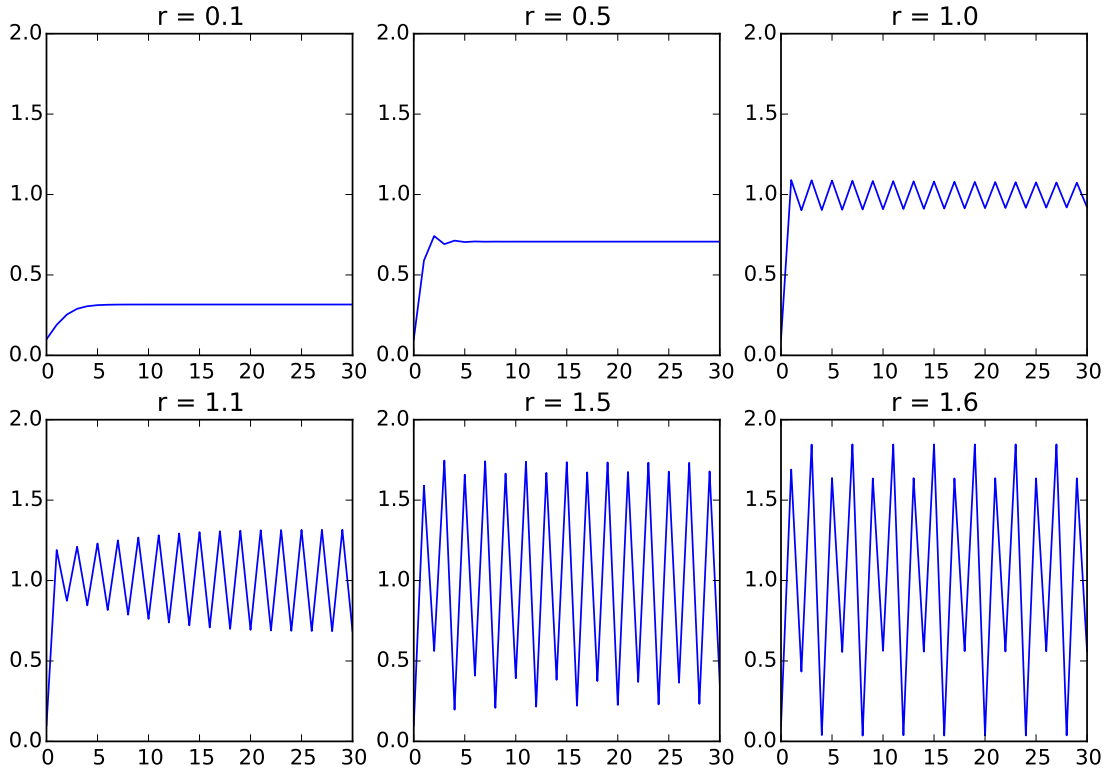

Figure 8.8: Visual output of Code 8.3.

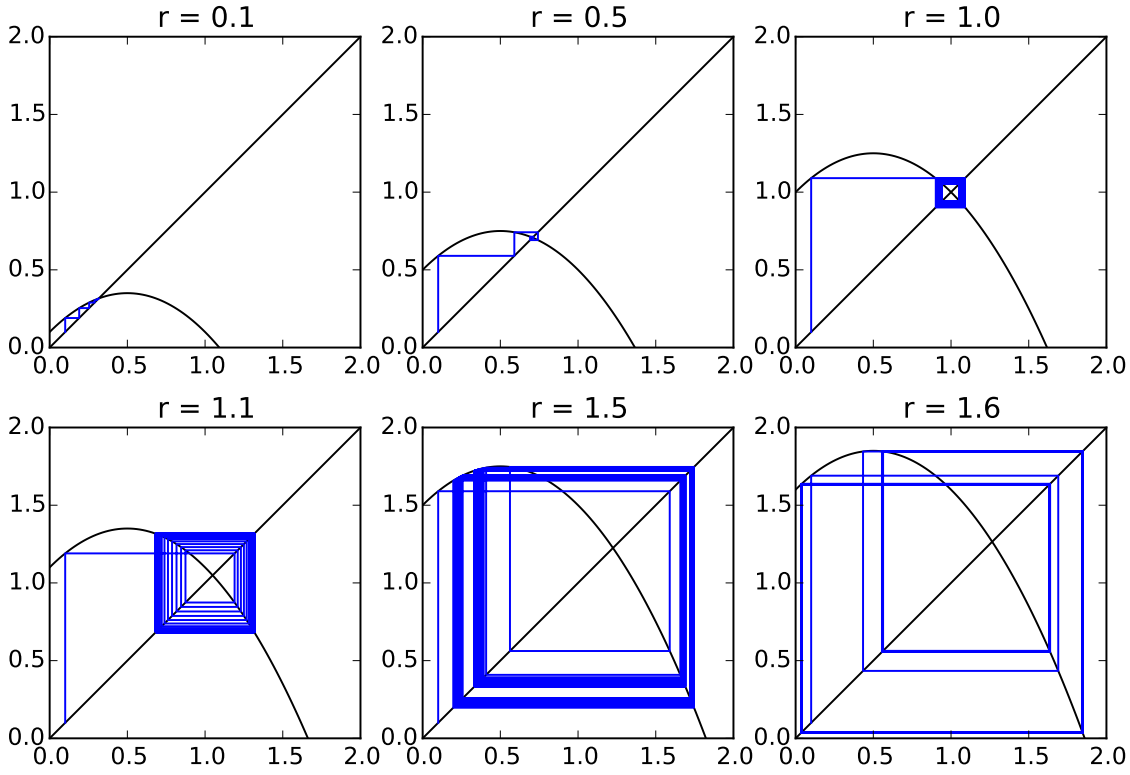

Figure 8.9: Cobweb plot version of Fig. 8.8.

to a trajectory with period $2T = 2$. Interestingly, the period-doubling bifurcations happen in a cascade if you keep increasing r. In this particular case, another period-doubling bifurcation was observed at $r = 1.5$, where the period-2 trajectory lost its stability and the system moved to a period-4 trajectory. This continues as you continue to increase r.

The first period-doubling bifurcation from period-1 to period-2 trajectories can still be characterized as the loss of stability of an equilibrium point, but the dominant eigenvalue destabilizing the equilibrium point must be *negative* in order to induce the flipping behavior. This can be mathematically written as follows:

> A first period-doubling bifurcation from period-1 to period-2 trajectories occurs in a discrete-time model when the eigenvalues λ_i of the Jacobian matrix at an equilibrium point satisfy the following:
>
> $\lambda_i = -1$ for some i, while $|\lambda_i| < 1$ for the rest.

In the example above, $dF/dx|_{x_{\rm eq}=\sqrt{r}} = -1$ when $r = 1$, which triggers the first period-doubling bifurcation.

Exercise 8.4 Consider the following discrete-time dynamical system:

$$x_t = (1-a)x_{t-1} + ax_{t-1}^3 \tag{8.41}$$

This equation has $x_{\rm eq} = 0$ as an equilibrium point. Obtain the value of a at which this equilibrium point undergoes a first period-doubling bifurcation.

Once the system begins to show period-doubling bifurcations, its asymptotic states are no longer captured by the locations of analytically obtained equilibrium points, as drawn in bifurcation diagrams (e.g., Figs. 8.1, 8.3, etc.). However, there is still a way to visualize bifurcation diagrams numerically by simulating the behavior of the system explicitly and then collecting the actual states the system visits for a certain period of time. Then we can plot their distributions in a diagram. The data points should be collected after a sufficiently long initial transient time has passed in each simulation, so that the system's trajectory is already showing its "final" behavior. Here is a sample code showing how to draw such a bifurcation diagram numerically:

Code 8.4: bifurcation-diagram-numerical.py

```
from pylab import *
```

```
def initialize():
    global x, result
    x = 0.1
    result = []

def observe():
    global x, result
    result.append(x)

def update():
    global x, result
    x = x + r - x**2

def plot_asymptotic_states():
    initialize()
    for t in xrange(100): # first 100 steps are discarded
        update()
    for t in xrange(100): # second 100 steps are collected
        update()
        observe()
    plot([r] * 100, result, 'b.', alpha = 0.3)

for r in arange(0, 2, 0.01):
    plot_asymptotic_states()

xlabel('r')
ylabel('x')
show()
```

In this code, `r` is gradually varied from 0 to 2 at intervals of 0.01. For each value of `r`, the model (Eq. (8.37)) is simulated for 200 steps, and only the second half of the state values are recorded in `result`. Once the simulation is finished, the states stored in `result` are plotted at a particular value of `r` in the plot (note that the expression `[r] * 100` in Python produces a list of one hundred `r`'s). The `alpha` option is used to make the markers transparent so that the densities of markers are also visible.

The result is shown in Fig. 8.10. This bifurcation diagram still shows how the system's state depends on the parameter, but what is plotted here are no longer analytically ob-

tained equilibrium points but numerically sampled sets of asymptotic states, i.e., where the system is likely to be after a sufficiently long period of time. If the system is converging to a stable equilibrium point, you see one curve in this diagram too. Unstable equilibrium points never show up because they are never realized in numerical simulations. Once the system undergoes period-doubling bifurcations, the states in a periodic trajectory are all sampled during the sampling period, so they all appear in this diagram. The period-doubling bifurcations are visually seen as the branching points of those curves.

But what are those noisy, crowded, random-looking parts at $r > 1.7$? *That is chaos,* the hallmark of nonlinear dynamics. We will discuss what is going on there in the next chapter.

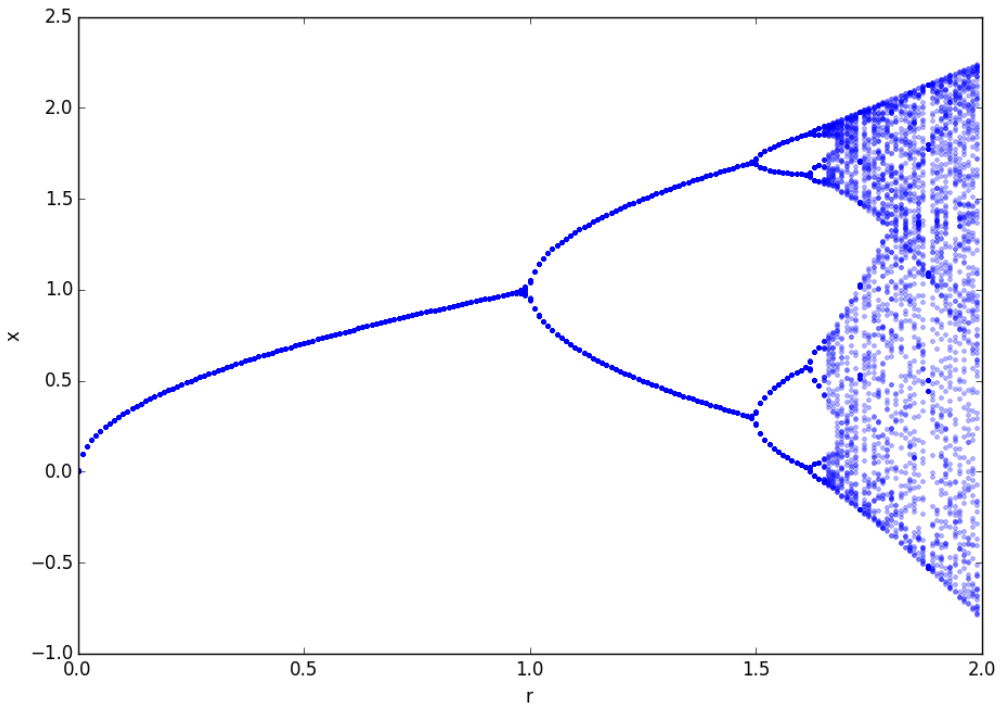

Figure 8.10: Visual output of Code 8.4, showing the numerically constructed bifurcation diagram of Eq. (8.37).

Exercise 8.5 **Logistic map** Period-doubling bifurcations and chaos are not just for abstract, contrived mathematical equations, but they can occur in various models of real-world biological, ecological, social, and engineering phenomena. The simplest possible example would be the *logistic map* we introduced in Section 5.5:

$$x_t = rx_{t-1}(1 - x_{t-1}) \tag{8.42}$$

This is a mathematical model of population dynamics, where x_t represents the population of a species that reproduce in discrete (non-overlapping) generations. This model was used by British/Australian mathematical ecologist Robert May in his influential 1976 Nature paper [32] to illustrate how a very simple mathematical model could produce astonishingly complex behaviors.

- Conduct a bifurcation analysis of this model to find the critical thresholds of r at which bifurcations occur.
- Study the stability of each equilibrium point in each parameter range and summarize the results in a table.
- Simulate the model with several selected values of r to confirm the results of analysis.
- Draw a bifurcation diagram of this model for $0 < r < 4$.

Exercise 8.6 **Stability analysis of periodic trajectories** The stability of a period-2 trajectory of a discrete-time model $x_t = F(x_{t-1})$ can be studied by the stability analysis of another model made of a composite function of F:

$$y_\tau = G(y_{\tau-1}) = F(F(y_{\tau-1})) \tag{8.43}$$

This is because the period-2 trajectory in F corresponds to one of the equilibrium points of $G(\circ) = F(F(\circ))$. If such an equilibrium point of G is being destabilized so that $dG/dx \approx -1$, it means that the period-2 trajectory in question is losing the stability, and thus another period-doubling bifurcation into a period-4 trajectory is about to occur. Using this technique, analytically obtain the critical threshold of r in Eq. (8.37) at which the second period-doubling bifurcation occurs (from period 2 to period 4). Then, draw cobweb plots of $y_\tau = G(y_{\tau-1})$ for several values of r near the critical threshold to see what is happening there.

Chapter 9

Chaos

9.1 Chaos in Discrete-Time Models

Figure 8.10 showed a cascade of period-doubling bifurcations, with the intervals between consecutive bifurcation thresholds getting shorter and shorter geometrically as r increased. This cascade of period doubling eventually leads to the divergence of the period to infinity at $r \approx 1.7$ in this case, which indicates the onset of *chaos*. In this mysterious parameter regime, the system loses any finite-length periodicity, and its behavior looks essentially random. Figure 9.1 shows an example of such chaotic behavior of Eq. (8.37) with $r = 1.8$.

So what is chaos anyway? It can be described in a number of different ways, as follows:

Chaos—

- is a long-term behavior of a nonlinear dynamical system that never falls in any static or periodic trajectories.
- looks like a random fluctuation, but still occurs in completely deterministic, simple dynamical systems.
- exhibits sensitivity to initial conditions.
- occurs when the period of the trajectory of the system's state diverges to infinity.
- occurs when no periodic trajectories are stable.

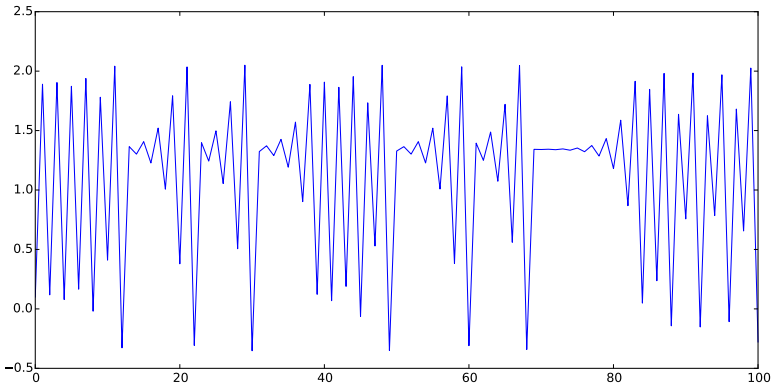

Figure 9.1: Example of chaotic behavior, generated using Eq. (8.37) with $r = 1.8$ and the initial condition $x_0 = 0.1$.

- is a prevalent phenomenon that can be found everywhere in nature, as well as in social and engineered environments.

The sensitivity of chaotic systems to initial conditions is particularly well known under the moniker of the *"butterfly effect,"* which is a metaphorical illustration of the chaotic nature of the weather system in which "a flap of a butterfly's wings in Brazil could set off a tornado in Texas." The meaning of this expression is that, in a chaotic system, a small perturbation could eventually cause very large-scale difference in the long run. Figure 9.2 shows two simulation runs of Eq. (8.37) with $r = 1.8$ and two slightly different initial conditions, $x_0 = 0.1$ and $x_0 = 0.100001$. The two simulations are fairly similar for the first several steps, because the system is fully deterministic (this is why weather forecasts for just a few days work pretty well). But the "flap of the butterfly's wings" (the 0.000001 difference) grows eventually so big that it separates the long-term fates of the two simulation runs. Such extreme sensitivity of chaotic systems makes it practically impossible for us to predict exactly their long-term behaviors (this is why there are no two-month weather forecasts[1]).

[1] But this doesn't necessarily mean we can't predict climate change over longer time scales. What is not possible with a chaotic system is the prediction of the *exact* long-term behavior, e.g., when, where, and how much it will rain over the next 12 months. It *is* possible, though, to model and predict long-term changes of a system's statistical properties, e.g., the average temperature of the global climate, because it can be described well in a much simpler, non-chaotic model. We shouldn't use chaos as an excuse to avoid making

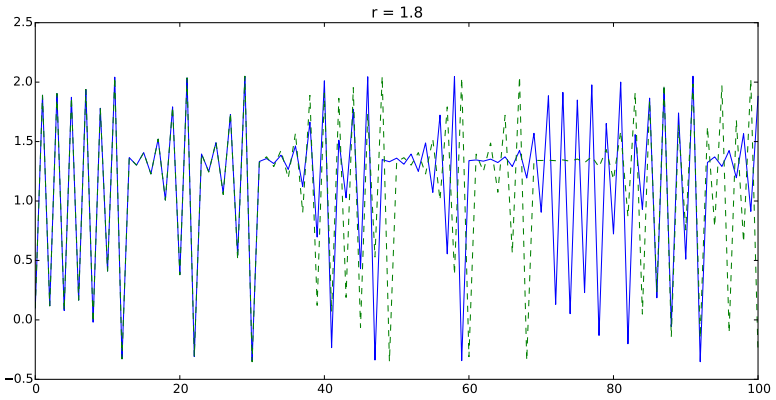

Figure 9.2: Example of the "butterfly effect," the extreme sensitivity of chaotic systems to initial conditions. The two curves show time series generated using Eq. (8.37) with $r = 1.8$; one with $x_0 = 0.1$ and the other with $x_0 = 0.100001$.

Exercise 9.1 There are many simple mathematical models that exhibit chaotic behavior. Try simulating each of the following dynamical systems (shown in Fig. 9.3). If needed, explore and find the parameter values with which the system shows chaotic behaviors.

- Logistic map: $x_t = rx_{t-1}(1 - x_{t-1})$
- Cubic map: $x_t = x_{t-1}^3 - rx_{t-1}$
- Sinusoid map: $x_t = r \sin x_{t-1}$
- Saw map: $x_t =$ fractional part of $2x_{t-1}$

Note: The saw map may not show chaos if simulated on a computer, but it *will* show chaos if it is manually simulated on a cobweb plot. This issue will be discussed later.

predictions for our future!

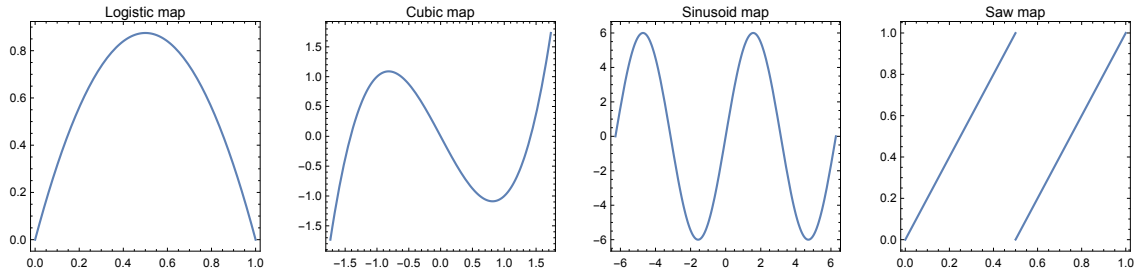

Figure 9.3: Simple maps that show chaotic behavior (for Exercise 9.1).

9.2 Characteristics of Chaos

It is helpful to realize that there are two dynamical processes always going on in any kind of chaotic systems: *stretching and folding* [33]. Any chaotic system has a dynamical mechanism to *stretch*, and then *fold*, its phase space, like kneading pastry dough (Fig. 9.4). Imagine that you are keeping track of the location of a specific grain of flour in the dough while a pastry chef kneads the dough for a long period of time. Stretching the dough magnifies the tiny differences in position at microscopic scales to a larger, visible one, while folding the dough always keeps its extension within a finite, confined size. Note that folding is the primary source of nonlinearity that makes long-term predictions so hard—if the chef were simply stretching the dough all the time (which would look more like making ramen), you would still have a pretty good idea about where your favorite grain of flour would be after the stretching was completed.

This stretching-and-folding view allows us to make another interpretation of chaos:

> Chaos can be understood as a dynamical process in which microscopic information hidden in the details of a system's state is dug out and expanded to a macroscopically visible scale (*stretching*), while the macroscopic information visible in the current system's state is continuously discarded (*folding*).

This kind of information flow-based explanation of chaos is quite helpful in understanding the essence of chaos from a multiscale perspective. This is particularly clear when you consider the saw map discussed in the previous exercise:

$$x_t = \text{fractional part of } 2x_{t-1} \tag{9.1}$$

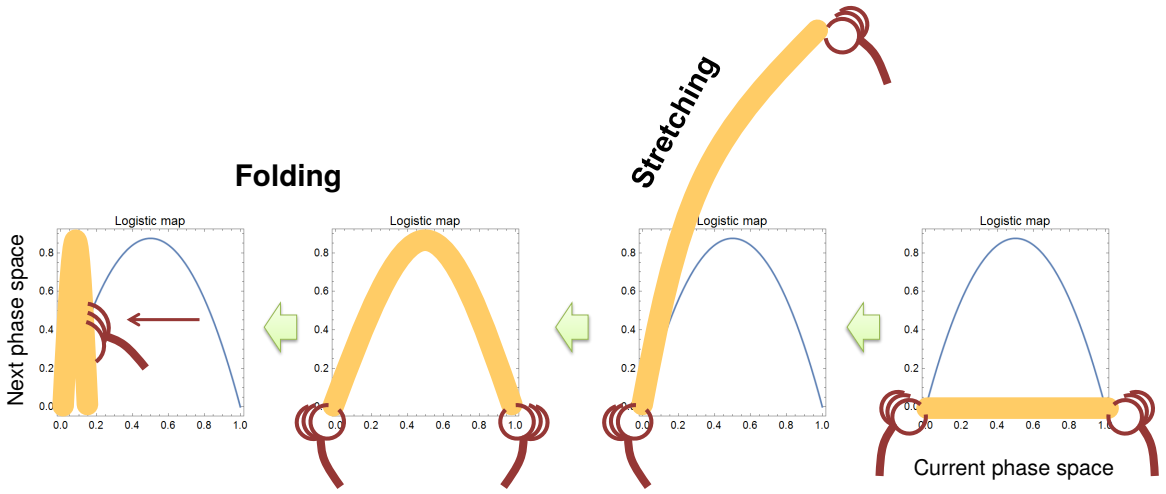

Figure 9.4: Schematic illustration of stretching and folding taking place in a chaotic iterative map. The current phase space (right) is first stretched (middle right) and then folded (middle left, left) to generate the next phase space in each iteration.

If you know binary notations of real numbers, it should be obvious that this iterative map is simply shifting the bit string in x always to the left, while forgetting the bits that came before the decimal point. And yet, such a simple arithmetic operation can still create chaos, if the initial condition is an irrational number (Fig. 9.5)! This is because an irrational number contains an infinite length of digits, and chaos continuously digs them out to produce a fluctuating behavior at a visible scale.

> *Exercise 9.2* The saw map can also show chaos even from a rational initial condition, if its behavior is manually simulated by hand on a cobweb plot. Explain why.

9.3 Lyapunov Exponent

Finally, I would like to introduce one useful analytical metric that can help characterize chaos. It is called the *Lyapunov exponent,* which measures how quickly an infinitesimally

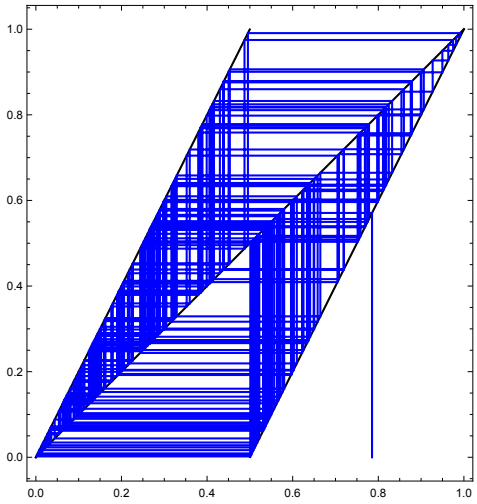

Figure 9.5: Cobweb plot of the saw map with $\pi/4$ as the initial condition.

small distance between two initially close states grows over time:

$$\left|F^t(x_0+\varepsilon) - F^t(x_0)\right| \approx \varepsilon e^{\lambda t} \tag{9.2}$$

The left hand side is the distance between two initially close states after t steps, and the right hand side is the assumption that the distance grows exponentially over time. The exponent λ measured for a long period of time (ideally $t \to \infty$) is the Lyapunov exponent. If $\lambda > 0$, small distances grow indefinitely over time, which means the stretching mechanism is in effect. Or if $\lambda < 0$, small distances don't grow indefinitely, i.e., the system settles down into a periodic trajectory eventually. Note that the Lyapunov exponent characterizes only stretching, but as we discussed before, stretching is not the only mechanism of chaos. You should keep in mind that the folding mechanism is not captured in this Lyapunov exponent.

We can do a little bit of mathematical derivation to transform Eq. (9.2) into a more

easily computable form:

$$e^{\lambda t} \approx \frac{\left|F^t(x_0+\varepsilon) - F^t(x_0)\right|}{\varepsilon} \tag{9.3}$$

$$\lambda = \lim_{t\to\infty,\,\varepsilon\to 0} \frac{1}{t}\log\left|\frac{F^t(x_0+\varepsilon) - F^t(x_0)}{\varepsilon}\right| \tag{9.4}$$

$$= \lim_{t\to\infty} \frac{1}{t}\log\left|\frac{dF^t}{dx}\Big|_{x=x_0}\right| \tag{9.5}$$

(applying the chain rule of differentiation...)

$$= \lim_{t\to\infty} \frac{1}{t}\log\left|\frac{dF}{dx}\Big|_{x=F^{t-1}(x_0)=x_{t-1}} \cdot \frac{dF}{dx}\Big|_{x=F^{t-2}(x_0)=x_{t-2}} \cdots \frac{dF}{dx}\Big|_{x=x_0}\right| \tag{9.6}$$

$$= \lim_{t\to\infty} \frac{1}{t}\sum_{i=0}^{t-1}\log\left|\frac{dF}{dx}\Big|_{x=x_i}\right| \tag{9.7}$$

The final result is quite simple—the Lyapunov exponent is a time average of $\log|dF/dx|$ at every state the system visits over the course of the simulation. This is very easy to compute numerically. Here is an example of computing the Lyapunov exponent of Eq. 8.37 over varying r:

Code 9.1: Lyapunov-exponent.py

```
from pylab import *

def initialize():
    global x, result
    x = 0.1
    result = [logdFdx(x)]

def observe():
    global x, result
    result.append(logdFdx(x))

def update():
    global x, result
    x = x + r - x**2

def logdFdx(x):
```

```
    return log(abs(1 - 2*x))

def lyapunov_exponent():
    initialize()
    for t in xrange(100):
        update()
        observe()
    return mean(result)

rvalues = arange(0, 2, 0.01)
lambdas = [lyapunov_exponent() for r in rvalues]
plot(rvalues, lambdas)
plot([0, 2], [0, 0])

xlabel('r')
ylabel('Lyapunov exponent')
show()
```

Figure 9.6 shows the result. By comparing this figure with the bifurcation diagram (Fig. 8.10), you will notice that the parameter range where the Lyapunov exponent takes positive values nicely matches the range where the system shows chaotic behavior. Also, whenever a bifurcation occurs (e.g., $r = 1$, 1.5, etc.), the Lyapunov exponent touches the $\lambda = 0$ line, indicating the criticality of those parameter values. Finally, there are several locations in the plot where the Lyapunov exponent diverges to negative infinity (they may not look so, but they are indeed going infinitely deep). Such values occur when the system converges to an extremely stable equilibrium point with $dF^t/dx|_{x=x_0} \approx 0$ for certain t. Since the definition of the Lyapunov exponent contains logarithms of this derivative, if it becomes zero, the exponent diverges to negative infinity as well.

Exercise 9.3 Plot the Lyapunov exponent of the logistic map (Eq. (8.42)) for $0 < r < 4$, and compare the result with its bifurcation diagram.

Exercise 9.4 Plot the bifurcation diagram and the Lyapunov exponent of the following discrete-time dynamical system for $r > 0$:

$$x_t = \cos^2(r x_{t-1}) \tag{9.8}$$

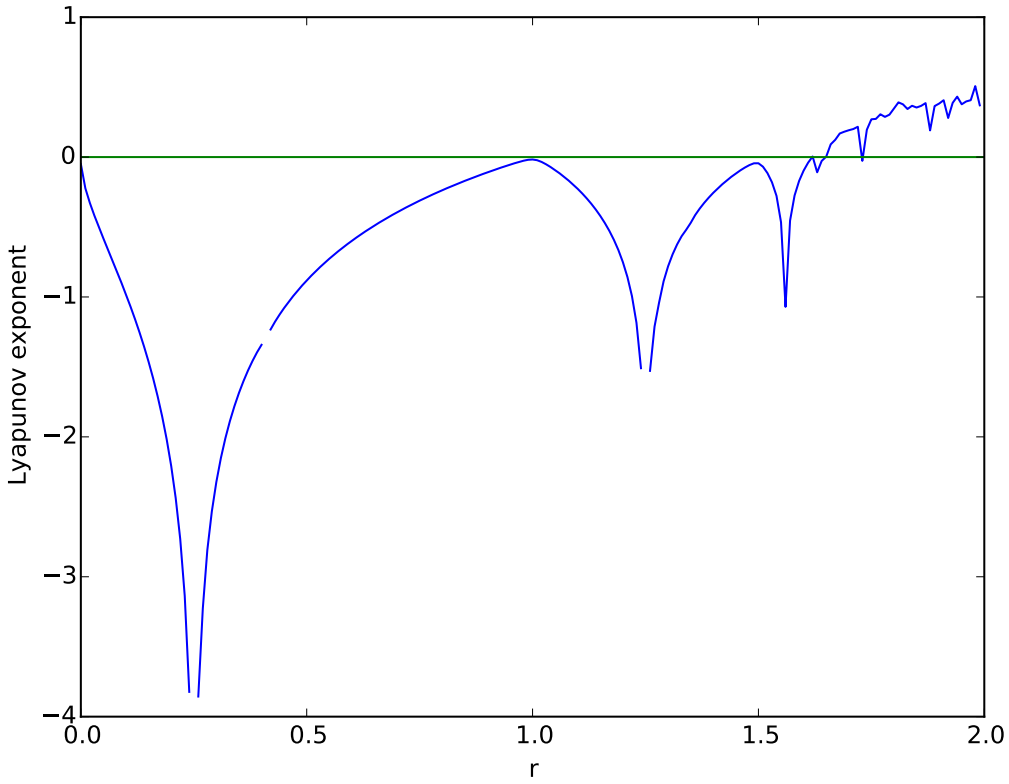

Figure 9.6: Visual output of Code 9.1, showing the Lyapunov exponent of Eq. (8.37) over varying r. Compare this with Fig. 8.10.

Then explain in words how its dynamics change over r.

9.4 Chaos in Continuous-Time Models

As we reviewed above, chaos is really easy to show in discrete-time models. But the discovery of chaos was originally made with continuous-time dynamical systems, i.e., differential equations. Edward Lorenz, an American mathematician and meteorologist, and one of the founders of chaos theory, accidentally found chaotic behavior in the following model (called the *Lorenz equations*) that he developed to study the dynamics of atmospheric convection in the early 1960s [5]:

$$\frac{dx}{dt} = s(y - x) \tag{9.9}$$

$$\frac{dy}{dt} = rx - y - xz \tag{9.10}$$

$$\frac{dz}{dt} = xy - bz \tag{9.11}$$

Here s, r, and b are positive parameters.This model is known to be one of the first that can show chaos in continuous time. Let's simulate this model with $s = 10$, $r = 30$, and $b = 3$, for example:

Code 9.2: Lorenz-equations.py

```
from pylab import *
from mpl_toolkits.mplot3d import Axes3D

s = 10.
r = 30.
b = 3.
Dt = 0.01

def initialize():
    global x, xresult, y, yresult, z, zresult, t, timesteps
    x = y = z = 1.
    xresult = [x]
    yresult = [y]
    zresult = [z]
```

```
    t = 0.
    timesteps = [t]

def observe():
    global x, xresult, y, yresult, z, zresult, t, timesteps
    xresult.append(x)
    yresult.append(y)
    zresult.append(z)
    timesteps.append(t)

def update():
    global x, xresult, y, yresult, z, zresult, t, timesteps
    nextx = x + (s * (y - x)) * Dt
    nexty = y + (r * x - y - x * z) * Dt
    nextz = z + (x * y - b * z) * Dt
    x, y, z = nextx, nexty, nextz
    t = t + Dt

initialize()
while t < 30.:
    update()
    observe()

subplot(3, 1, 1)
plot(timesteps, xresult)
xlabel('t')
ylabel('x')

subplot(3, 1, 2)
plot(timesteps, yresult)
xlabel('t')
ylabel('y')

subplot(3, 1, 3)
plot(timesteps, zresult)
xlabel('t')
ylabel('z')
```

```
figure()
ax = gca(projection='3d')
ax.plot(xresult, yresult, zresult, 'b')

show()
```

This code produces two outputs: one is the time series plots of x, y, and z (Fig. 9.7), and the other is the trajectory of the system's state in a 3-D phase space (Fig. 9.8). As you can see in Fig. 9.7, the behavior of the system is highly unpredictable, but there is definitely some regularity in it too. x and y tend to stay on either the positive or negative side, while showing some oscillations with growing amplitudes. When the oscillation becomes too big, they are thrown to the other side. This continues indefinitely, with occasional switching of sides at unpredictable moments. In the meantime, z remains positive all the time, with similar oscillatory patterns.

Plotting these three variables together in a 3-D phase space reveals what is called the *Lorenz attractor* (Fig. 9.8). It is probably the best-known example of *strange attractors*, i.e., attractors that appear in phase spaces of chaotic systems.

Just like any other attractors, strange attractors are sets of states to which nearby trajectories are attracted. But what makes them really "strange" is that, even if they look like a bulky object, their *"volume"* is zero relative to that of the phase space, and thus they have a *fractal dimension*, i.e., a dimension of an object that is not integer-valued. For example, the Lorenz attractor's fractal dimension is known to be about 2.06, i.e., it is pretty close to a 2-D object but not quite. In fact, any chaotic system has a strange attractor with fractal dimension in its phase space. For example, if you carefully look at the intricate patterns in the chaotic regime of Fig. 8.10, you will see fractal patterns there too.

Exercise 9.5 Draw trajectories of the states of the Lorenz equations in a 3-D phase space for several different values of r while other parameters are kept constant. See how the dynamics of the Lorenz equations change as you vary r.

Exercise 9.6 Obtain the equilibrium points of the Lorenz equations as a function of r, while keeping $s = 10$ and $b = 3$. Then conduct a bifurcation analysis on each equilibrium point to find the critical thresholds of r at which a bifurcation occurs.

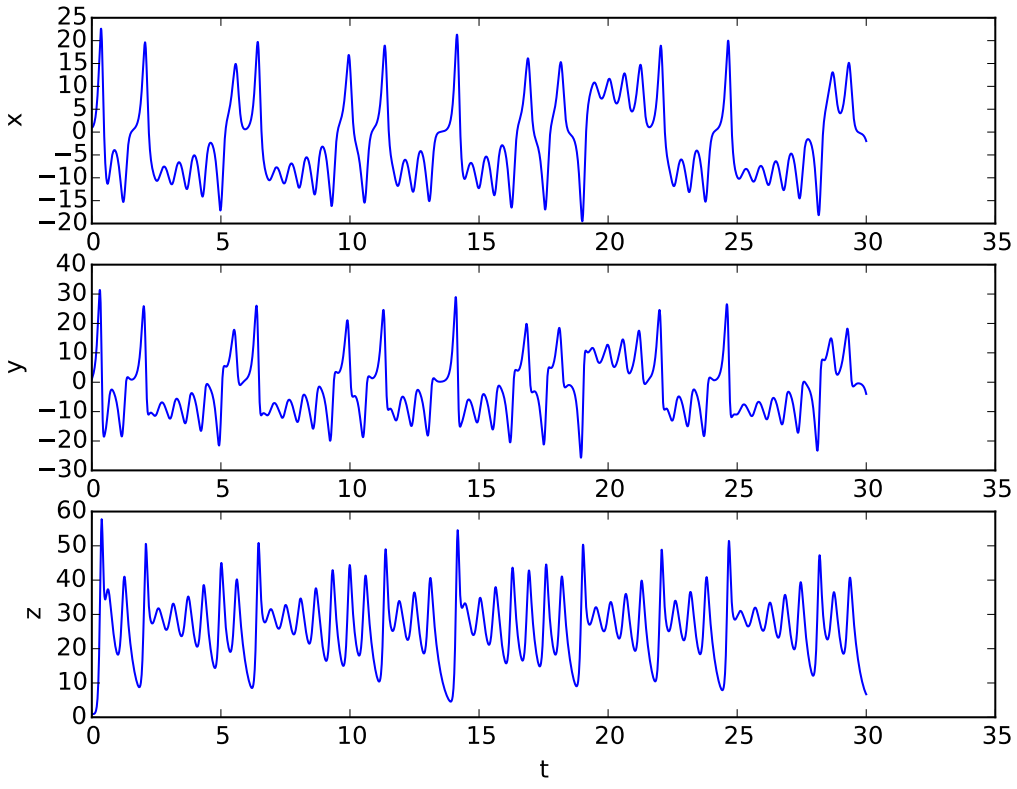

Figure 9.7: Visual output of Code 9.2 (1): Time series plots of x, y, and z.

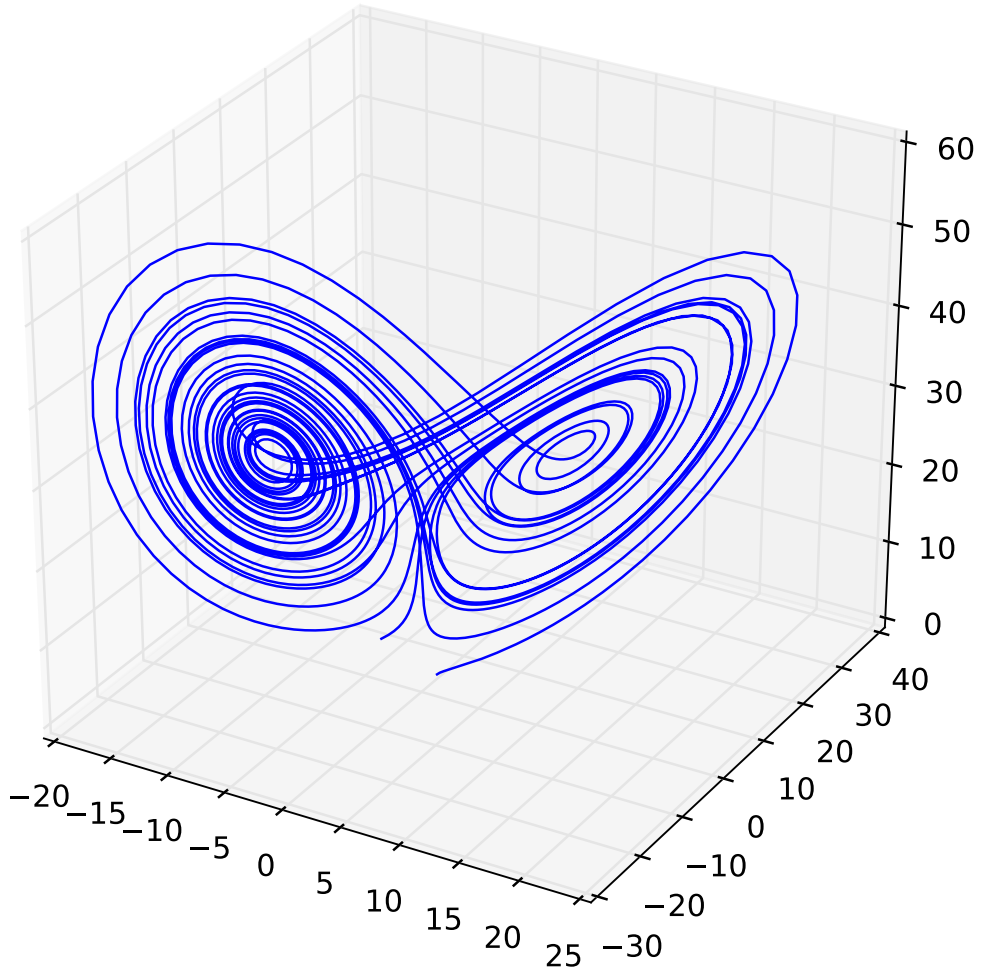

Figure 9.8: Visual output of Code 9.2 (2): Trajectory of the state of the Lorenz equations in a 3-D phase space.

> Compare your result with numerical simulation results obtained in the previous exercise.

By the way, I said before that any chaotic system has two dynamical processes: stretching and folding. Where do these processes occur in the Lorenz attractor? It is not so straightforward to fully understand its structure, but the stretching occurs where the trajectory is circling within one of the two "wings" of the attractor. The spirals seen on those wings are unstable ones going outward, so the distance between initially close states are expanded as they circle around the spiral focus. In the meantime, the folding occurs at the center of the attractor, where two "sheets" of trajectories meet. Those two sheets actually never cross each other, but they keep themselves separated from each other, forming a "wafer sandwich" made of two thin layers, whose right half goes on to circle in the right wing while the left half goes on to the left wing. In this way, the "dough" is split into two, each of which is stretched, and then the two stretched doughs are stacked on top of each other to form a new dough that is made of two layers again. As this process continues, the final result, the Lorenz attractor, acquires infinitely many, recursively formed layers in it, which give it the name of a "strange" attractor with a fractal dimension.

> *Exercise 9.7* Plot the Lorenz attractor in several different perspectives (the easiest choice would be to project it onto the x-y, y-z, and x-z planes) and observe its structure. Interpret its shape and the flows of trajectories from a stretching-and-folding viewpoint.

I would like to bring up one more important mathematical fact before we close this chapter:

In order for continuous-time dynamical systems to be chaotic, the dimensions of the system's phase space must be at least 3-D. In contrast, discrete-time dynamical systems can be chaotic regardless of their dimensions.

The Lorenz equations involved three variables, so it was an example of continuous-time chaotic systems with minimal dimensionality.

This fact is derived from the *Poincaré-Bendixson theorem* in mathematics, which states that no strange attractor can arise in continuous 2-D phase space. An intuitive explanation of this is that, in a 2-D phase space, every existing trajectory works as a "wall" that you

can't cross, which imposes limitations on where you can go in the future. In such an increasingly constraining environment, it is not possible to maintain continuously exploring dynamics for an indefinitely long period of time.

Exercise 9.8 Gather a pen and a piece of blank paper. Start drawing a continuous curve on the paper that represents the trajectory of a hypothetical dynamical system in a 2-D phase space. The shape of the curve you draw can be arbitrary, but with the following limitations:

- You can't let the pen go off the paper. The curve must be drawn in one continuous stroke.
- The curve can't merge into or cross itself.
- You can't draw curves flowing in opposing directions within a very tiny area (this violates the assumption of phase space continuity).

Keep drawing the curve as long as you can, and see what happens. Discuss the implications of the result for dynamical systems. Then consider what would happen if you drew the curve in a 3-D space instead of 2-D.

Exercise 9.9 Let z_i denote the value of the i-th peak of $z(t)$ produced by the Lorenz equations. Obtain time series data $\{z_1, z_2, z_3, \ldots\}$ from numerical simulation results. Plot z_t against z_{t-1}, like in a cobweb plot, and see what kind of structure you find there. Do this visualization for various values of r, while keeping $s = 10$ and $b = 3$, and compare the results with the results of the bifurcation analysis obtained in Exercise 9.6.

As reviewed through this and previous chapters, bifurcations and chaos are the most distinctive characteristics of nonlinear systems. They can produce unexpected system behaviors that are often counter-intuitive to our everyday understanding of nature. But once you realize the possibility of such system behaviors and you know how and when they can occur, your view of the world becomes a more informed, enriched one. After all, bifurcations and chaos are playing important roles in our physical, biological, ecological, and technological environments (as well as inside our bodies and brains). They should thus deserve our appreciation.

This chapter concludes our journey through systems with a small number of variables. We will shift gears and finally go into the realm of complex systems that are made of a

large number of variables in the next chapter.

Systemmodellierung, Karl-Franzens-Universität Graz, SS 2015
Georg Propst, following a script by G.Desch

1 Differential Equations with distributed states

In the courses Systemwissenschaften 1 & 2 we considered dynamic models (discrete or continuous in time) describing the state of the model as vectors that consist – at any time t – of state components that are real numbers. In these models, each state component is a real-valued function of time – either discrete instants of time $t_k, k \in \mathbb{N}$, or of continuous time $t \in [t_0, t_1) \subset \mathbb{R}$.

Examples for real-valued state components:

- the concentrations $c_D(t)$ and $c_{NO}(t)$ in the donor- NO-reaction model
- the size of the subpopulations $R(t)$ and $B(t)$ in the predator-prey model

In these models, at a given time t, the state components do NOT vary in space, which might be a simplification or idealization.

For some systems such a simplification may be reasonable and useful, in other models the spatial variation of the model components might be essential – depending on the purpose of the mathematical model.

To emphasize the fact, that the statevector of a differential equation model is in $\mathbb{R}^n$ one calls such differential equations **ordinary** (ODE).

This is in contrast to **partial differential equations** (PDE) where the state components at any time t are functions of a space variable, which is often denoted by x. In the present course, we are going to study PDEs.

Examples of systems that are described by space-dependet state components:

- static extended bodies (string, beam, plate, membrane, elastic body: elliptic PDEs)
- dynamic extended bodies (same examples, but moving) (hyperbolic PDEs)
- diffusion, heat conduction (parabolic PDEs)
- electro-dynamics (Maxwell equation)
- fluid flow: liquid (incompressible), gas (compressible) (nonlinear hyperbolic PDEs)
- nonlinear reaction/diffusion equations
- space dependent dynamic ecosystems
- etc.

Cellular automata are time-discrete models that are discrete in space too, as the cells are regions in space, that vary their states at discrete time steps. Typically, the rules of a CA are local in the sense, that the evolution in a cell is influenced only by its neighborhood. The same is typically true for PDEs, which leads to derivatives in space. But the CA models are discrete both in space and time, whereas the PDE models are continuous both in space and time.

In the literature the term "Distributed Parameter Systems" is used for PDEs, which is misleading: although a PDE model may have spatially distributed parameters, another PDE may contain no parameters at all, or only parameters that are not space dependent. But a PDE always includes space dependent states, so we should rather say "Distributed State Systems".

There are intermediate models, that are continuous in time and discrete in space, see the cell ODE model below. The combination discrete in time and continuous in space is also possible (but not considered in this lecture).

1.1 Contamination of a river

Here we give a suggestive description of a system which will be modelled in various variants. This serves as an introduction to the modelling techniques for spatially varying dynamic systems.

Example 1.1. *An organic pollutant is injected into a river for a short period of time, eg by an accident in a factory*

the pollutant is advected (ie carried with) by the flow of water

diffusion and dispersion also contribute to the distribution of the pollutant

the pollutant is reduced by oxygen, but this in turn reduces the concentration of oxygen in the water, which is dangerous for the live species in the river

at the same time, by gas exchange, oxygen enters from the air above the water into the water

Problem: Find models of varying complexity, to understand the processes and try to predict the concentrations of pollutant and oxygen in the river, when the time-span and rate of injection of the pollutant are known. In particular, when and where does the minimal oxygen concentration occur ? This is the moment and location of minimal water quality. We expect that this will take place shortly after the pollution is turned off and downstream of the injection, when the oxidation and the refreshment by air exchange balance each other.

The state of the system consists of the concentrations of pollutant and oxygen, their spatial distribution along a region of the river downstream of the injection. These concentration will vary in time and space.
The following factors determine the structure of the system:

- *Sources:* The factory is modelled as a point source which is turned on and off. In addition we can easily handle pollutant coming from upstream of the factory or from distributed sources along the river (eg from agriculture).
- *Advection:* This is transport due to the flow of water, in the region of the river, that is considered (downstream of the factory).

- *Diffusion and Dispersion:* This is due to random movements of molecules and droplets. The details are not modelled but the overall effect is that the spatial variations in the concentrations are levelled out.
- *Chemical Reactions:* Everywhere in the water a chemical reaction between pollutant and diluted oxygen takes place. It diminishes the pollutant and the oxygen. The reaction product is not modelled, as it is harmless.
- *Absorption:* Through the surface of the water, oxygen is exchanged with the air. The rate (and direction) of gas exchange depends on the difference (and its sign) of the partial oxygen pressure inside and above the water.
- *Not considered* are (for example) water influx other than from upstream the factory, percolation and evaporation of water, time variation of the influx of water, sedimentation of the pollutant and so on.

1.2 Modeling with cells

The idea here is to divide the river into cells. This can be done arbitrarily, or according to considerations of (nonuniform) resolution. For each cell, and for each of the two reactants pollutant and oxygen, a dynamic mass balance is set up. We make the simplifying assumption, that the reactant-concentrations have the same value for every cross section of the river perpendicular to the flow direction, so that spatial variations in the concentrations only occur in the direction of the flow. Furthermore, at first we neglect effects due to dispersion and diffusion. The resulting model will not a PDE but a system of ODEs.

Thus, we divide the region of the river into cells that are numerated by indices $i = 1, 2, 3, \ldots, N$ (see Figure 1.1). We work with the simplification, that in each cell both the pollutant and the oxygen are uniformly distributed, so that their concentrations in each cell can be represented by two real numbers. The smaller the cells are, the better this simplification approximates the reality (and the larger is the number of state variables).

The concentrations of pollutant in the cells $1, 2, \ldots, N$ at time t are denoted by $L_1(t), L_2(t), \cdots, L_N(t)$ and the oxygen concentrations by $C_1(t), C_2(t), \cdots, C_N(t)$. These $2N$ real numbers are the state components of the model at time t. It is convenient to measure the amount of pollutant not in kmol pollutant but in oxygen equivalents, which is the amount of oxygen that is needed to completely oxidate the considered amount of pollutant. The parameters to characterize the geometry of the cells are the volumes of water $V_1, \cdots, V_N$ contained in the cells, and the upper surfaces of areas $a_1, \cdots, a_N$ separating the water and the air above it. The cells recieve $S_1(t), \cdots, S_N(t)$ amount of pollutant per unit of time through sources at the banks of the river. $S_1(t)$ incudes the pollutant that comes from the factory. From upstream of the factory $L_0(t)$ and $C_0(t)$ amount of pollutant and oxygen enter cell 1. All these numbers and functions are assumed to be known. Also, the amount of water that enters cell 1 per unit of time is assumed to be a given constant

Figure 1.1: Contamination of a river: cells

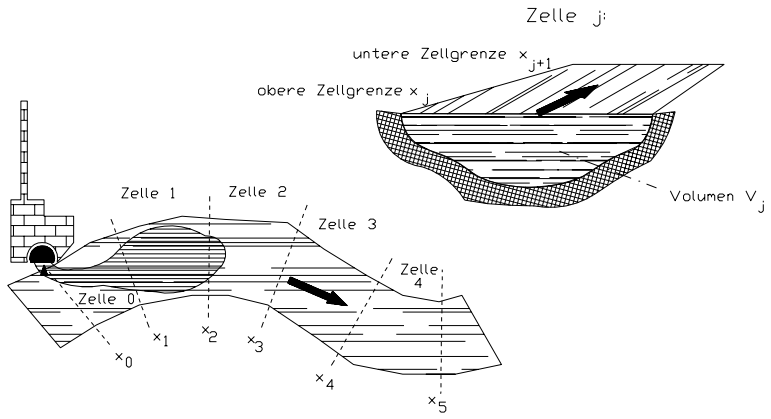

denoted by F. As the water is incompressible, the flow through every cross section of the river is given by the constant F. When the cross section varies, then the velocity of the water has to vary accordingly: at narrow parts of the river the water is relatively fast, at wide parts it is relatively slow. A varying cross section can be taken into account in the cell model, by choosing appropriate cell volumes V_i (see below).

Now we consider a single cell, the cell with index i, and we derive a dynamic mass balance for this cell. At time t there is the mass $V_i L_i(t)$ pollutant and $V_i C_i(t)$ oxygen in cell i (because mass is concentration times volume).

Modeling the Advection: Upstream of cell i is cell $i-1$ with the concentration of pollutant $L_{i-1}(t)$. Per second F m^3 water from cell $i-1$ enter into cell i. Per second this brings $FL_{i-1}(t)$ kmol pollutant and $FC_{i-1}(t)$ kmol into the cell i. Of the water in cell i (with pollutant concentration $L_i(t)$) per unit of time leave F m^3 water and take pollutant out of the cell. This diminishes the amount of pollutant by $FL_i(t)$ kmol per second. Analogously for oxygen, $FC_i(t)$ kmol per second leave cell i. Together the mass balance is:

$$\begin{aligned} \text{variation of pollutant by advection:} \quad & FL_{i-1}(t) - FL_i(t), \\ \text{variation of oxygen by advection:} \quad & FC_{i-1}(t) - FC_i(t). \end{aligned}$$

Note that the indices of $L_0(t)$ und $C_0(t)$ for the given concentrations in the water that enters cell 1 are chosen such that the same balances hold for cell 1.

Modeling the Oxidation: For simplicity we choose the simplest possible model, a reaction of first order (if necessary, the submodel for the oxidation can be elaborated later without changing the other parts of the river model). The rate of reaction in a reaction of first order is proportional to the product of the concentrations of the reactants. But we make the even more simplifying assumption, that despite of the decrease of oxygen, the reaction rate only depends on the pollutant concentration, as if - for the reaction - the oxygen concentration were constant. Thereby we get a linear model that is easier to analyze. Let k_S denote the reaction rate. Per second and per kmol diluted pollutant (in oxygen

equivalents) k_S kmol pollutant is oxidated. And this uses up the same amount of oxygen. In principle k_S depends on the temperature, but we assume that the temperature is constant throughout the river and therefore is not present in our model. Since cell i contains $V_i L_i(t)$ pollutant, the balance is:

$$\begin{aligned} \text{decrease of pollutant by oxidation:} &\quad -k_S V_i L_i(t), \\ \text{decrease of oxygen by oxidation:} &\quad -k_S V_i L_i(t). \end{aligned}$$

Modeling the absorption of oxygen from the air: We use the realistic assumption, that the partial pressure of oxygen in the air is constant. Following Henry's law, corresponding to this partial pressure in air there is a saturation concentration c_S of diluted oxygen in the water which defines the equilibrium where no oxygen is exchanged through the surface. When the equilibrium is perturbed, i.e. when $C_i(t) \neq c_S$, then, per m^2 suface and per second, the amount of $k_O(c_S - C_i(t))$ kmol oxygen will pass through the surface. If $C_i(t)$ is larger than the saturation concentration c_S, then this term is negative and oxygen will escape the water; otherwise oxygen from the air is desolved in the water. In principle the Henry constant $k_O > 0$ depends on the temperature, which is not modeled here. The cell i has an effective surface area of a_i square meters. We say "effective" to take into account natural or engineered enhancement of gas exchange by waterfalls, rapids, etc.. Thus we get

$$\text{variation of oxygen by gas exchange with air:} \quad k_O a_i (c_S - C_i(t)).$$

Modeling the pollutant sources: Cell 1 and maybe others recieve $S_i(t)$ kmol pollutant (in oxygen equivalents) per second, which are given input functions

$$\text{increase of pollutant from sources:} \quad S_i(t).$$

Suming up the balances of all processes, we get the rate of variation (increase if the sum is positive, decrease if the sum is negative) for the pollutant and the oxygen, respectively, in cell i. Recall that the mass of pollutant and oxygen in cell i is $V_i L_i(t)$ and $V_i C_i(t)$, respectively. This yields the dynamic mass balances:

$$\begin{aligned} \frac{d}{dt}(V_i L_i(t)) &= F L_{i-1}(t) - F L_i(t) - k_S V_i L_i(t) + S_i(t), \\ \frac{d}{dt}(V_i C_i(t)) &= F C_{i-1}(t) - F C_i(t) - k_S V_i L_i(t) + k_O a_i (c_S - C_i(t)). \end{aligned}$$

Division by the constant V_i yields the concentration balance of cell i:

$$\begin{aligned} \frac{d}{dt} L_i(t) &= -(\frac{F}{V_i} + k_S) L_i(t) + \frac{F}{V_i} L_{i-1}(t) + \frac{S_i(t)}{V_i}, \\ \frac{d}{dt} C_i(t) &= -\frac{F + k_O a_i}{V_i} C_i(t) - k_S L_i(t) + \frac{F}{V_i} C_{i-1}(t) + \frac{k_O a_i c_S}{V_i}. \end{aligned}$$

These equations are valid in each of the cells $i = 1, \cdots, N$. With 10 cells we get a system of 20 coupled ordinary differential equations; the coupling of the cells consists of the

Table 1.1: One dimensional cell model for example 1.1

state components and parameters

variable	units	meaning
t	sec	time
N	1	number of cells
$L_i(t)$	kmol/m^3	concentration of pollutant in cell i
$C_i(t)$	kmol/m^3	concentration of oxygen in cell i
$L_0(t)$	kmol/m^3	concentration of pollutant upstream of cell 1
$C_0(t)$	kmol/m^3	concentration of oxygen upstream of cell 1
$S_i(t)$	kmol/sec	input pollutant into cell i (oxygen equivalents)
V_i	m^3	volume water in cell i
a_i	m^2	area of water-air interface in cell i
F	m^3/sec	flow (constant)
k_S	1/sec	reaction rate oxidation
k_O	m/sec	rate of gas exchange water-air
c_S	kmol/m^3	saturation concentration O_2

model equations

$$\frac{d}{dt}L_i(t) = -(\frac{F}{V_i} + k_S)L_i(t) + \frac{F}{V_i}L_{i-1}(t) + \frac{S_i(t)}{V_i},$$
$$\frac{d}{dt}C_i(t) = -\frac{F + k_O a_i}{V_i}C_i(t) - k_S L_i(t) + \frac{F}{V_i}C_{i-1}(t) + \frac{k_O a_i c_S}{V_i}.$$

The two ODEs hold for each cell number $i = 1 \cdots N$.

$i-1$-terms in the ith equation, the coupling of L_i and C_i within cell i is caused by the L_i term in the C_i equation.

As always with dynamic models that describe the evolution of the system when time goes on, we need initial values of all state components $L_i(t_0), C_i(t_0), i = 1, \ldots, N$ at the initial time t_0. Furthermore, all input functions $L_0(t), C_0(t), S_i(t), i = 1, \ldots, N$ must be given for a time intervall $[t_0, t_1]$. Given all this and the parameters $V_i, a_i, F, k_S, k_O, c_S > 0$ there exists a unique solution of the model, which consists of $2N$ functions $L_i(t), C_i(t)$ that satisfy the ODEs on $[t_0, t_1]$.

It is not difficult to implement the model using numerics software on a computer. It is reasonable to keep the parameters and the inputs easily modifyable, so that numerical experiments can be carried out by running simulations (=computations of concrete examples) and their graphical presentation as in Figure 1.2. In this particular example $N = 12$ and we started at time $t_0 = 0$ with initial state
$L_i(0) = 0, C_i(0) = c_S = 6.44 \times 10^{-4}, i = 1, \ldots, 12$ (not shown in Figure 1.2). We set $L_0(t) = 0, C_0(t) = c_s$ for the simulation interval $t \in [0, 3600]$. All sources $S_i(t)$ are zero except for cell 1: we choose $S_1(t) = 5 \cdot 10^{-3}$ for $t \in [0, 360]$ (injection from the factory) and $S_1(t) = 0$ for $t \in (360, 3600]$. For Figure 1.2 we have choosen identical V_i, a_i but this could

Figure 1.2: Simulation results with 12 cells at the times t=900, 1800, 2700, 3600. * = pollutant concentration, o = oxygen concentration. The values in the cells are graphically connected by straight lines, for ease of finding them

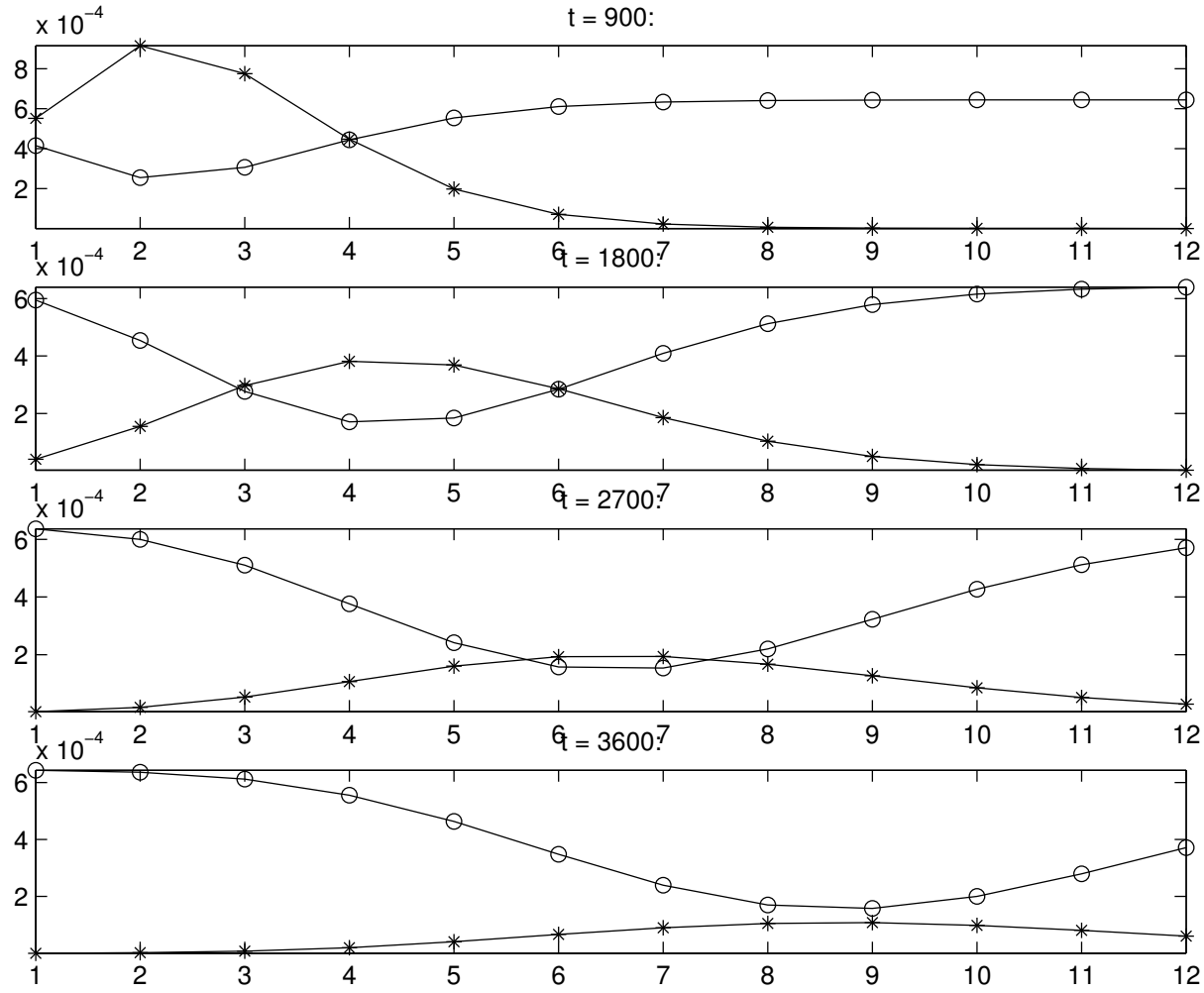

easily be chosen differently. (When writing a simulation code, it is often wise not to give up flexibility too early. On the other hand, keeping maximal flexiblity increases the danger of programing errors.)

Observe how the maximum of the pollutant concentration wanders downstream with (here constant) velocity $v = 2$ meters per second. At the same time, pollutant as well as oxygen is reduced by the reaction, everywhere and in particular near the wandering maximum. The minimal oxygen concentration occurs at time 2700 in cell 7 and is about $1.55 \cdot 10^{-4}$. This is the model's answer to the question raised in the problem setup, but it strongly depends on the model parameters, of course. After stopping the pollutant injection into cell 1, the oxygen recovers in the upper cells due to fresh water, decreasing pollutant concentration, and absorption of oxygen from the air (which is not really identifiable in the graphics). After sufficiently long time (not shown) the initial conditions will get more and more restored, namely

$$\lim_{t\to\infty} L_i(t) = 0 \text{ and } \lim_{t\to\infty} C_i(t) = c_S, \quad i = 1, \ldots, 12$$

Figure 1.3: Three-dimensional cell modell

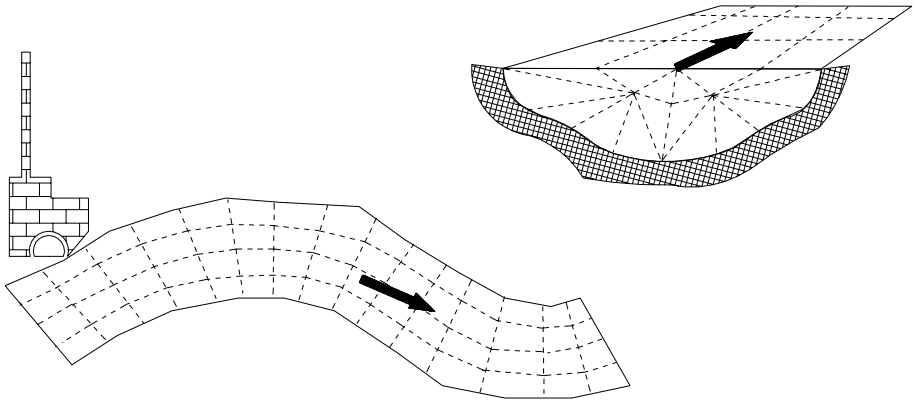

The speed of the wandering maximum of L_i which graphically is about 2-3 cells per plot is v =2 m/s as required by F and the cross section of the river (chosen to be 60 m^3/s and 30 m^2).
However, note that the graphics indicate pretty smooth spatial distribution of the concentrations. For example, at $t = 900$ the pollutant conentration in cell 7 is definitely positive, although the transport of pollutant by the flow should reach at most $x = 900v = 1800$ which is at cell 3. This error is due to approximation by coupled ODEs which mathematically induces immediate influence of a cell on all cells downstream of it. The smoothing by coupling of ODEs also reduces the maxima of L_i and increases the minima of C_i. This model deficiency will be remedied by the PDE advection model.

The choice $N = 12$ is arbitrary and can be changed with the strikes of a few keys, eg. 'appending a zero' as programers say, when they switch to $N = 120$. Then a system of 240 ODEs is solved numerically, which is possible within short computation times.

Figure 1.3 shows a possibility, to divide the river into cells when the simplifying assumption is droped, that the concentrations are uniform across each cross section. To set up such a three-dimensional model along the lines discussed above, one needs to know the flow from and to each cell to its neighbor cells, which is sort of impossible. Furthermore, the size of the model, i.e. the number of unknowns is much larger than in the one-dimensional version. In three dimensions, when the side length of the cells is halved, their number increases by the factor eight (in one dimension it doubles) when the same region is to be covered.
If a three-dimensional model of flow is necessary, it should be set up by basic principles from hydrodynamics, which renders a PDE model. For simulations, the PDE model must be discretized, which also leads to a large number of unknowns.

1.3 Partial derivatives

To prepare for modeling with partial derivatives, we shortly recall, what they are.

Definition 1.2. *Let w be a realvalued function of two real variables t and x. The partial derivative with respect to x of w at the point (t, x) is given by*

$$\frac{\partial}{\partial x} w(t,x) = \lim_{h \to 0} \frac{w(t, x+h) - w(t,x)}{h}.$$

That means that one of the variables (here t) is held fixed; these gives a function $w(t, \cdot)$ of *one* variable (here x) the derivative of which is defined as usual and is called the partial derivative of w wrt x (wrt means 'with respect to'). When we build the partial derivative wrt x at all points (t, x) in a continuum, we get a value for all such points which are used to define a new function of t and x. It is called the partial derivative of w wrt to x and it is denoted by $\frac{\partial}{\partial x} w$ or by $\partial_x w$ or by w_x.
When we interchange the role of t and x, that is the variable x is held fixed and the derivative of $w(\cdot, x)$ wrt to t at the point (t, x) is defined by

$$\frac{\partial}{\partial t} w(t,x) = \lim_{k \to 0} \frac{w(t+k, x) - w(t,x)}{k},$$

then we get the partial derivative of w with respect to t, denoted by $w_t(t, x)$ or by w_t if $w_t(t, x)$ exists on a t-interval.
If the new functions can again be differentiated, we get partial derivatives of second order, namely $w_{xx}, w_{xt}, w_{tx}, w_{tt}$. The Theorem of Schwarz asserts: when the derivatives of second order are continuous functions, then $w_{xt} = w_{tx}$, that is: the derivative wrt t of w_x equals the derivative wrt x of w_t.
Exercise. Compute the partial derivatives of $f(x, y) = 3x^4y^2 + x^2 + 5y$ up to order 2.

1.4 Advection and reaction in one dimension

At any time t, the cell model has concentrations that are step functions in space that are discontinuous at the cell interfaces. (In Figure 1.2 the lines connecting the values in the cells are just graphical artefacts.) But discontinuous concentrations in the river are not realistic. What happens, when we make the cells smaller and smaller ? In the limit we will get partial derivatives and a PDE model with continuous concentrations. The PDE model will be more elegant and in a sense simpler than the many cells model. Mathematically, it can be difficult to analyze a PDE model on paper or numerically. But setting up and understanding a PDE model often is not difficult, can be done by non-mathematicians and can give insights into the structure and the working of the system.

We still assume, that throughout a cross section perpendicular to the direction of the flow the concentrations are constant. Thereby we can reduce the three-dimensional spatial complexity to a one-dimensional model. Thus, we introduce just one spatial coordinate: let x denote the distance of the factory and a cross section downstream in the river. Thus, the

factory is located at $x = 0$ and the place at $x = 76$ is located 76 meters downstream the factory. We will consider a region of the river of length l, thus our space coordinate will be between 0 and l, $x \in [0, l]$, a continuous interval of real numbers.

For every instant of time t let $L(t, x)$ and $C(t, x)$ denote the concentrations at the cross section with space coordinate x. Thereby we introduce functions L and C of the two variables t, x. The units of $L(t, x)$ and $C(t, x)$ are kmol/m^3 (in oxygen equivalents for L), as before. For every instant t, the state components of the model will be the functions $L(t, \cdot)$ and $C(t, \cdot)$, which are realvalued functions on $[0, l]$.

The idea to derive the model is, to consider a small cell in the river, namely the region between the coordinates x and $x + \Delta x$; Δx is a length which we imagine to be very small and - at first - positive. For this little cell we set up a dynamic mass balance and then watch what happens when we let Δx go to zero. (Note that Δx denotes one real number, Δ alone was not defined).

Geometry und hydrodynamics of the river We denote the area of the cross section of the river at x by $A(x)$. The velocity of the water in the middle of the cross section is faster than close to the banks or near the ground. To simplfy, we work with one velocity $u(x)$ at x which can be thought of as the average over the cross section. Then the volume of water that flows through the cross section at x is $A(x)u(x)$ cubic meter per second. We assume that A and u do not depend on time, meaning that during the time span of interest, the river always carries the same amount of water. For the absorption we need the interface water/air. We introduce the effective width $b(x)$ of the river at x. Then the surface of the water in a litte cell of length Δx at x is approximated by $b(x)\Delta x$. The effective width $b(x)$ has the dimension of a length and depends on the real width of the river at x as well as on the roughness of the interface (see above).

Amount of pollutant and of oxygen in the cell: As Δx is very short, the cross section A along a cell between x and Δx is well approximated by $A(x)$. (We also could choose any other position between x and $x + \Delta x$, when $\Delta x \to 0$ this position will converge to x.) Therefore, our little cell contains $A(x)\Delta x$ volume of water. Therein we have concentrations $C(t, x)$ of oxygen and $L(t, x)$ of pollutant. Thus

$$\begin{aligned} \text{amount of pollutant in the cell:} &\quad L(t, x)A(x)\Delta x, \\ \text{amount of oxygen in the cell:} &\quad C(t, x)A(x)\Delta x. \end{aligned}$$

Modeling the advection: From upstream per second enter $A(x)u(x)$ m^3 water through the cross section at x. This water has the concentrations $L(t, x)$ and $C(t, x)$. Therefore, per second enter $A(x)u(x)L(t, x)$ kmol pollutant (in oxygen equivalents) and $A(x)u(x)C(t, x)$ kmol oxygen. At the other end of the cell, at $x + \Delta x$, $A(x + \Delta x)u(x + \Delta x)L(t, x + \Delta x)$

kmol pollutant and $A(x+\Delta x)u(x+\Delta x)C(t,x+\Delta x)$ kmol oxygen leave the cell, per second. This yields the balance

$$\begin{aligned}&\text{balance of pollutant by advection:}\\&A(x)u(x)L(t,x) - A(x+\Delta x)u(x+\Delta x)L(t,x+\Delta x),\\&\text{balance of oxygen by advection:}\\&A(x)u(x)C(t,x) - A(x+\Delta x)u(x+\Delta x)C(t,x+\Delta x).\end{aligned}$$

Modeling distributed sources: We assume that at $x \in (0,l)$ per second $s(t,x)$ pollutant enters the river from the banks, where $s(t,x)$ is a known function. Therefore we get for our little cell:

$$\text{increase of pollutant from distributed sources:} \quad s(t,x)\Delta x.$$

The modeling of the sources at $x = 0$ will be done later.

Modeling the oxidation: As in the cell model above, we use the assumption that the oxidation only depends on the pollutant concentration, as if there were so much oxygen, that its (relatively small) variation does not matter. Let k_S be the reaction coefficient. In the cell there is the amount $A(x)\Delta x L(t,x)$ pollutant for oxidation, of this amount per seconds oxidates $k_S A(x)\Delta x L(t,x)$. This gives:

$$\begin{aligned}&\text{decrease of pollutant by oxidation:} \quad -k_S A(x)\Delta x L(t,x),\\&\text{decrease of oxygen by oxidation:} \quad -k_S A(x)\Delta x L(t,x).\end{aligned}$$

Modeling the oxygen exchange with air: The effective surface of the interface water/air is $b(x)\Delta x$ square meters. The difference of saturation concentration c_S (defined by the constant partial pressure of oxygen in the air) and the oxygen concentration in the water is $c_S - C(t,x)$. Using the known exchange velocity k_O we get

$$\text{exchange of oxygen with air:} \quad k_O b(x)\Delta x(c_S - C(t,x)).$$

Summary: To get the overall variation of the pollutant and the oxygen in the cell of length Δx, we sum up the contributions of advection, sources, oxidation and absorption and equate the sum, as always, with the derivatives of the quantities with respect to time. As there are now two independent variables - t and x - we write the derivative as a partial derivative:

$$\begin{aligned}\frac{\partial}{\partial t}(A(x)L(t,x)\Delta x) &= A(x)u(x)L(t,x) - A(x+\Delta x)u(x+\Delta x)L(t,x+\Delta x)\\&\quad + s(t,x)\Delta x - k_S A(x)\Delta x L(t,x),\\\frac{\partial}{\partial t}(A(x)C(t,x)\Delta x) &= A(x)u(x)C(t,x) - A(x+\Delta x)u(x+\Delta x)C(t,x+\Delta x)\\&\quad - k_S A(x)\Delta x L(t,x) + k_O b(x)\Delta x(c_S - C(t,x)).\end{aligned}$$

Then we divide both equations by Δx (which is not zero) and get

$$\begin{aligned}\frac{\partial}{\partial t}(A(x)L(t,x)) &= -\frac{A(x+\Delta x)u(x+\Delta x)L(t,x+\Delta x) - A(x)u(x)L(t,x)}{\Delta x}\\ &\quad - k_S A(x)L(t,x) + s(t,x),\\ \frac{\partial}{\partial t}(A(x)C(t,x)) &= -\frac{A(x+\Delta x)u(x+\Delta x)C(t,x+\Delta x) - A(x)u(x)C(t,x)}{\Delta x}\\ &\quad - k_S A(x)L(t,x) + k_O b(x)(c_S - C(t,x)).\end{aligned}$$

For $\Delta x < 0$ we consider the cell between $x + \Delta x$ and x, where now $x + \Delta x$ is upstream of x. Therefore the the advection balance becomes
$A(x + \Delta x)u(x + \Delta x)L(t, x + \Delta x) - A(x)u(x)L(t, x)$ and similar for the oxygen. All other terms have the length $-\Delta x$ instead of Δx as a factor. Dividing the sum by $-\Delta x$ then yields exactly the same overall balances.

Finally, we let Δx go to zero. Here we use the fact, that the limit $\Delta x \downarrow 0$ from the right, or the limit $\Delta x \uparrow 0$ from the left, or even an oscillating limit is applied to the same right hand side in each of the above two equations. We need this, because in the definition of $\lim_{\Delta x \to 0}$ the approach of Δx to zero is not restricted to one-sided approaches. Furthermore, the left hand sides of the above equations do not depend on Δx and so $\lim_{\Delta x \to 0}$ there can just be omitted. Applying Definition 1.2 of partial derivatives (with $h = \Delta x$ and
$w(t, x) = A(x)u(x)L(t, x)$ or $A(x)u(x)C(t, x)$) we get:

$$\begin{aligned}A(x)\frac{\partial}{\partial t}L(t,x) &= -\frac{\partial}{\partial x}(A(x)u(x)L(t,x)) + s(t,x) - k_S A(x)L(t,x),\\ A(x)\frac{\partial}{\partial t}C(t,x) &= -\frac{\partial}{\partial x}(A(x)u(x)C(t,x)) - k_S A(x)L(t,x) + k_O b(x)(c_S - C(t,x)).\end{aligned}$$

The modeling thus has led to a system of two partial differential equations (PDEs) that contain derivatives of L and C with respect to time as well as with respect to space. For any instant t the state of the model is a vector of two "distributed" functions on $[0, l]$, namely $(L(t, \cdot), C(t, \cdot))$.

Modeling systems that vary in time and space, one considers a dynamic balance for a small region of space. For the rate of change in time t one uses the partial derivative with respect to t and writes the model for the variations as difference quotients in space (where appropriate). Then one lets the size (volume, area, length) of the region go to zero, which renders partial derivatives with respect to space.

Remark. An alternative modeling method is to consider the integral of a state component over a region of space and equate its derivative with respect to time with the surface integral of the flow across the surface of the region. Using Gauß' integral theorem this gives partial differential equations for the integrands and the same models as with the difference quotients above.

Modeling the inflow and the point source at $x = 0$: As in the cell model we use $C_0(t)$ and $L_0(t)$ for the concentration of oxygen and pollutant in the river upstream of $x = 0$ and $S(t)$ for the rate of injection of pollutant by the factory at $x = 0$. We assume that these are known functions. Thus, for the oxygen concentration at $x = 0$ we simply have

$$C(t, 0) = C_0(t).$$

Immediately at the factory the volume $u(0)A(0)$ m^3 of water flows by per second. Therefore, from upstream the factory come $L_0(t)u(0)A(0)$ kmol pollutant (in oxygen equivalents). In addition, per second $S(t)$ kmol pollutant are injected by the factory. The sum $S(t) + u(0)A(0)L_0(t)$ kmol pollutant is distributed by the flow in the volume $u(0)A(0)$ m^3 of water. At $x = 0$ this gives the concentration

$$L(t, 0) = L_0(t) + \frac{S(t)}{u(0)A(0)} =: L_1(t).$$

that we call $L_1(t)$, for abbrevation. $C_0(t)$ and $L_1(t)$ are given functions that prescribe the values of the states C und L at the boundary-point $x = 0$ of the region $[0, l]$ under consideration. They are *boundary conditions*.

Initial conditions: So far we have only modeled the evolution of the system. To specify one solution of these equations, we need to specify the initial state, at time $t_0 = 0$, say. We prescribe the *initial conditions*

$$L(0, x) = L_a(x),$$
$$C(0, x) = C_a(x).$$

where $L_a(x)$ and $C_a(x)$ are given functions on $[0, l]$.

A partial differential equation (PDE) describes an unknown function of two or more variables by a relation between the function and its derivatives. PDEs are supplemented with initial conditions and boundary conditions. The initial conditions specify the values of the unknown function(s) at the beginning of the time of interest. Boundary conditions characterize the unknown functions at the boundary of the spatial region of interest.

Remark. In the above derivation all processes that we considered (flow, reaction, oxygen enrichment from air, injection of pollutant) are summarized in one model. In order to derive a model for the advection (= flow) of L alone (neglecting all other processes), we look at the right hand side of its balance between x and $x + \Delta x$ and divide by Δx:

$$(A(x)u(x)L(t, x) - A(x + \Delta x)u(x + \Delta x)L(t, x + \Delta x))/\Delta x$$

The incompressibility of the water implies $A(x)u(x) = F$ with a constant F that does not depend on x and t. Therefore, after taking the limit $\Delta x \to 0$, F can be pulled out of the partial derivative wrt x. Also, $A(x)$ can be pulled out of the partial derivative wrt t on the left hand side of the balance. Then dividing the equation by $A(x)$, which is nonzero throughout, one gets

$$\frac{\partial}{\partial t}L(t, x) + u(x)\frac{\partial}{\partial x}L(t, x) = 0, \quad t > 0, \quad x \in (0, l).$$

This is the classical advection equation (or one-sided wave equation) for the flow of an incompressible fluid with the property $L(t, x)$ (e.g. the concentration of a dissolved substance, as for the river). The property L varies in time t and space x. The fluid flows in a channel with width $A(x)$. $u(x)$ is the velocity of the flow at position x and does not depend on t. It is inversely proportional to the width of the channel, namely $u(x) = F/A(x)$. For $u > 0$ boundary conditions at the beginning of the channel, at $x = 0$, are needed. $u < 0$ is possible and requires a boundary condition at the end, at $x = l$, and a prescription at $x = 0$ does not make sense in this case. A velocity distribution that is positive for some x and negative for other x in the same channel is impossible, because of the incompressibility of the fluid as in our model, which is correct for water. For compressible fluids like air, the sign of $u(x)$ need not be constant, and compression and rarefaction are included in the model.

Table 1.2: Reaction-Advection-Equations for Example 1.1

model components

component	units	meaning
t	sec	time
x	m	distance along the river from the factory
$L(t,x)$	kmol/m^3	pollutant concentration (O_2-equivalents)
$C(t,x)$	kmol/m^3	oxygen concentration
$L_0(t)$	kmol/m^3	pollutant concentration upstream of factory
$C_0(t)$	kmol/m^3	oxygen concentration upstream of factory
$S(t)$	kmol/sec	pollutant injection from factory
$s(t,x)$	kmol/(m sec)	pollutant injection from distributed sources per length
$L_a(x)$	kmol/m^3	initial pollutant concentration
$C_a(x)$	kmol/m^3	initial oxygen concentration
k_S	1/sec	reaction rate oxidation
k_O	m/sec	rate of gas exchange air-water
c_S	kmol/m^3	saturation concentration O_2
$A(x)$	m^2	area of river cross section at x
$u(x)$	m/sec	flow velocity
$b(x)$	m	area of air-water interface per length

partial differential equations

$$\begin{aligned} A(x)\frac{\partial}{\partial t}L(t,x) &= -\frac{\partial}{\partial x}(A(x)u(x)L(t,x)) \\ &\quad + s(t,x) - k_S A(x)L(t,x), \\ A(x)\frac{\partial}{\partial t}C(t,x) &= -\frac{\partial}{\partial x}(A(x)u(x)C(t,x)) \\ &\quad - k_S A(x)L(t,x) + k_O b(x)(c_S - C(t,x)). \end{aligned} \tag{1.1}$$

boundary conditions

$$\begin{aligned} L(t,0) = L_1(t) &:= L_0(t) + \frac{S(t)}{A(0)u(0)}, \\ C(t,0) &= C_0(t), \quad t \geq 0. \end{aligned}$$

initial conditions

$$L(0,x) = L_a(x), \quad C(0,x) = C_a(x).$$

1.5 Characteristic curves

Let us demonstrate that in special cases, like that of Table 1.2 (which does not contain diffusion terms), it is possible to find a solution of a PDE. A solution of our model is a pair of functions $L(t,x)$ and $C(t,x)$ that satisfy all equations of Table 1.2 for $t \geq 0$ and $0 \leq x \leq l$.

To make the solution process more tractable, we only consider the case of a constant cross section, $A(x) \equiv A$ which implies constant velocity $u(x) \equiv u$, throughout $[0,l]$; we also assume that the effective interface is everywhere the same, i.e. $b(x) \equiv b$ and that the pollutant enters only at $x = 0$, so that $s(t,x) = 0$. Then, in (1.1) $A(x)u(x)$ can be pulled out of the derivative and both sides can be devided by A. Shifting the space derivative to the left hand side and using the abbrevation $k_1 = k_O b/A$ we get

$$\begin{aligned} \frac{\partial}{\partial t}L(t,x) + u\frac{\partial}{\partial x}L(t,x) &= -k_S L(t,x), \\ \frac{\partial}{\partial t}C(t,x) + u\frac{\partial}{\partial x}C(t,x) &= -k_S L(t,x) + k_1(c_S - C(t,x)). \end{aligned} \tag{1.2}$$

A useful concept for advection equations is the total derivative of a function along a curve.

Let $f : \mathbb{R}^n \to \mathbb{R}$ be a differentiable function and $\big(x_1(t), \cdots, x_n(t)\big), t \in [t_0, t_1]$ be a smooth curve in $\mathbb{R}^n$. Then $f(x_1(t), \cdots, x_n(t))$ is a function of one variable t and

$$\frac{d}{dt}f = \frac{\partial}{\partial x_1}f \cdot \frac{d}{dt}x_1 + \cdots + \frac{\partial}{\partial x_n}f \cdot \frac{d}{dt}x_n.$$

is called the total derivative of f along this curve. The total derivative describes the rate of change of f that is measured by an observer who travels along this curve, at time t passing the position with space coordinates $\big(x_1(t), \cdots, x_n(t)\big)$.

Imagine an observer in a boat that travels with the water in the river, measuring the concentrations continuously just at the boat. From the assumption that u is constant, the boat's curve in the (t,x)-plane is $(t, x_0 + u(t - t_0))$. This curve, for $t \geq t_0$ starts at time t_0 at position x_0. In the above notation, $n = 2, x_1(t) = t, x_2(t) = x_0 + u(t - t_0)$. Therefore $\frac{d}{dt}x_1(t) = 1$ and $\frac{d}{dt}x_2(t) = u$.

Let us discuss the case $x_0 = 0$, which means that the boat starts at $x = 0$.

Along the curve $(t, u(t - t_0))$ the total derivatives of L and C are given by

$$\begin{aligned} \frac{d}{dt}L(t,u(t-t_0)) &= \frac{\partial}{\partial t}L(t,u(t-t_0)) + u\frac{\partial}{\partial x}L(t,u(t-t_0)), \\ \frac{d}{dt}C(t,u(t-t_0)) &= \frac{\partial}{\partial t}C(t,u(t-t_0)) + u\frac{\partial}{\partial x}C(t,u(t-t_0)). \end{aligned} \tag{1.3}$$

The right hand sides in (1.3) are exactly the left hand sides in (1.2) at $(t, u(t-t_0))$. Therefore,

$$\begin{aligned}\frac{d}{dt}L(t,u(t-t_0)) &= -k_S L(t,u(t-t_0)),\\ \frac{d}{dt}C(t,u(t-t_0)) &= -k_S L(t,u(t-t_0)) + k_1(c_S - C(t,u(t-t_0)))\end{aligned} \tag{1.4}$$

The partial derivatives have disappeared, because on the curve $(t, u(t-t_0))$ the observer does not feel the advection and measures only the effects of the reaction and the gas exchange. If there were no reaction nor gas exchange in the model, the concentrations would be constant on each curve of the form $(t, u(t-t_0))$ (see Figure 1.4, upper part). The physical interpretation is, that the "information" (here the concentrations) that enters the region at $x = 0$ (given by the boundary condition) is carried along by the flow with velocity u. Such curves are called *characteristic curves* for the PDE (1.2). Along these curves, the total derivative comprises exactly the partial derivatives of the PDE.

Another family of characteristic curves for (1.2) are those emanating from the vertical line $t = 0$. They have the form $(t, x_0 + ut)$ and also are straight lines with slope u (see Fig. 1.4, lower part). Along these curves the information from the initial conditions is carried along. After a sufficiently long time, namely $t = l/u$, all information that dates back to the initial conditions will have left the region $[0, l]$. Therefore, the bounded triangle above $x = ut$ (between $x = 0$ and $x = l$) is the "domain of influence" of the initial condition. The region below $x = ut$, which is unbounded, is the "domain of influence" of the boundary condition.

For variable flow velocity (caused by variable cross section) the characteristic curves would not be straight lines, but curves with slope $u(x)$ for all t. Therefore, these curves would not cross each other and nowhere have negative slope.
Note that in Figure 1.5 no values of $L(t,x), C(t,x)$ are seen. These would have to be drawn above the paper like a landscape. In socalled 3D graphics, the landscape is indicated by perspective drawing.

Also keep in mind, that the construction of characteristic curves and thereby the transformation of PDEs into ODEs is possible only for hyperbolic PDEs such as (1.1). For models that include effects of random movements (see diffusion below), no characteristic curves exist.

1.6 Analytic solution of the reaction-advection equations

The solution of the ordinary differential equation (1.4) is a standard task, since it is a linear ODE. The unique solution is

$$\begin{aligned}L(t,u(t-t_0)) &= e^{-k_S(t-t_0)}L_1(t_0),\\ C(t,u(t-t_0)) &= e^{-k_1(t-t_0)}C_0(t_0) + c_S[1-e^{-k_1(t-t_0)}]\\ &\quad - \frac{k_S L_1(t_0)}{k_1 - k_S}[e^{-k_S(t-t_0)} - e^{-k_1(t-t_0)}].\end{aligned} \tag{1.5}$$

Figure 1.4: Domains of influence of the boundary and the initial condition

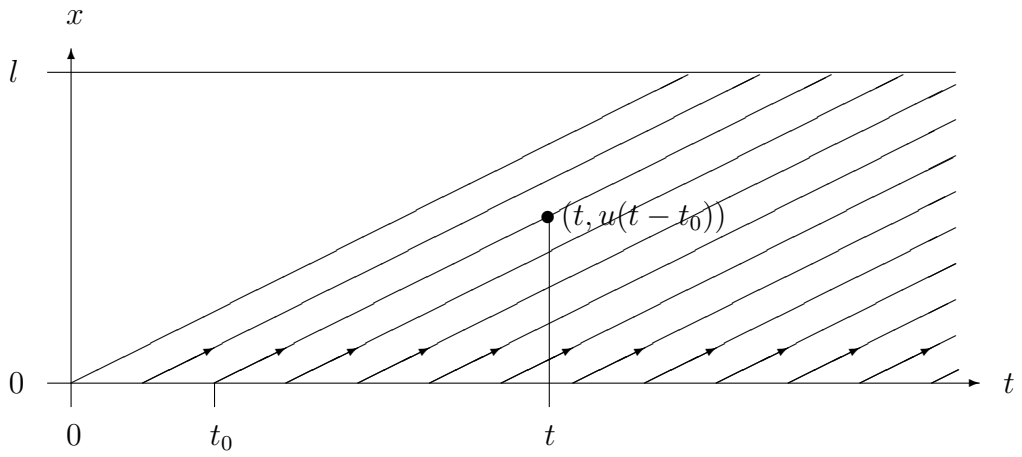

at $x = 0$ the boundary condition L_1, in particular $L_1(t_0)$, is given

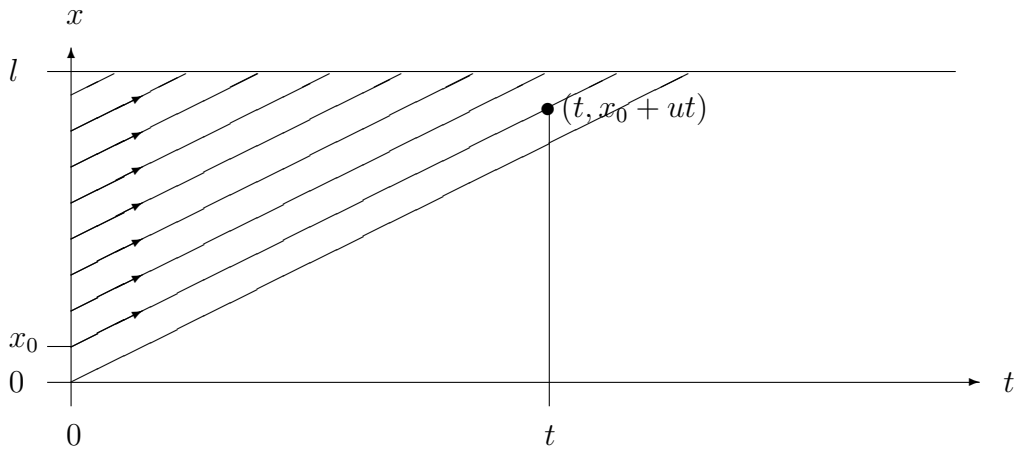

at $t = 0$ the initial condition L_a, in particular $L_a(x_0)$, is given

which can be checked by inserting these functions into the ODEs.

For completeness we describe the procedure of deriving the solutions:
First we can solve the equation for L, since it is independent of C:

$$\frac{d}{dt}L(t, u(t-t_0)) = -k_S L(t, u(t-t_0))$$

This is an homogeneous linear ODE of the form

$$\frac{d}{dt}y(t) = -k_S y(t)$$

with $y(t) = L(t, u(t-t_0))$. Its solution is the exponential function

$$y(t) = e^{-k_S(t-t_0)}y(t_0),$$

that is

$$L(t, u(t-t_0)) = e^{-k_S(t-t_0)}L(t_0, 0) = e^{-k_S(t-t_0)}L_1(t_0).$$

We insert this into the equation for C:

$$\begin{aligned}\frac{d}{dt}C(t,u(t-t_0)) &= -k_S L(t,u(t-t_0)) + \frac{k_O b}{A}(c_S - C(t,u(t-t_0)) \\ &= -k_1 C(t,u(t-t_0)) + k_1 c_S - k_S L_1(t_0) e^{-k_S(t-t_0)}.\end{aligned}$$

This is an inhomogeneous linear ODE of the form

$$\frac{d}{dt}y(t) = -k_1 y(t) + g(t),$$

with $y(t) = C(t,u(t-t_0))$ and $g(t) = k_1 c_S - k_S L_1(t_0) e^{-k_S(t-t_0)}$. Its solution, using the "variation of the constant formula" is

$$y(t) = e^{-k_1(t-t_0)} y(t_0) + \int_{t_0}^{t} e^{-k_1(t-s)} g(s)\, ds,$$

which implies

$$\begin{aligned}C(t,u(t-t_0)) &= e^{-k_1(t-t_0)} C(t_0,0) + \int_{t_0}^{t} e^{-k_1(t-s)}[k_1 c_S - k_S L_1(t_0) e^{-k_S(s-t_0)}]\, ds \\ &= e^{-k_1(t-t_0)} C_0(t_0) + c_S[1 - e^{-k_1(t-t_0)}] \\ &- \frac{k_S L_1(t_0)}{k_1 - k_S}[e^{-k_S(t-t_0)} - e^{-k_1(t-t_0)}].\end{aligned}$$

To determine $L(t,x)$, we must choose t_0 such that $u(t-t_0) = x$ holds, that is

$$t_0 = t - \frac{x}{u}.$$

Then we have

$$\begin{aligned}L(t,x) = L(t,u(t-t_0)) &= e^{-k_S(t-t_0)} L_1(t_0) \\ &= e^{-k_S x/u} L_1(t - \frac{x}{u}).\end{aligned}$$

Similarly,

$$C(t,x) = e^{-k_1 x/u} C_0(t - \frac{x}{u}) + c_S\left[1 - e^{-k_1 x/u}\right] - \frac{k_S L_1(t - \frac{x}{u})}{k_1 - k_S}\left[e^{-k_S x/u} - e^{-k_1 x/u}\right]. \qquad (1.6)$$

These formulas for the solutions $L(t,x)$ and $C(t,x)$ use the given functions of the boundary conditions L_1 and C_0. They are valid only for such (t,x) for which $t - \frac{x}{u} \geq 0$, or $x \leq ut$; otherwise L_1 and C_0 could not be evaluated at their arguments in the formulas; they are functions that are given for arguments greater than 0. Thereby, the formulas reflect the above discussion of the domains of influence. For $x \geq ut$ we must use the initial conditions instead of the boundary conditions. We omit the detailed formulas for this case.

NOTE: In comparison to the cell model the reaction-advection PDE (1.2) is simpler and more elegant and it can be solved analytically, on paper.

As an application of the solution (1.6) we could compute the minimum of C for fixed t by equating the derivative with respect to x with 0. This would give, for any fixed t, the

Figure 1.5: Random movements

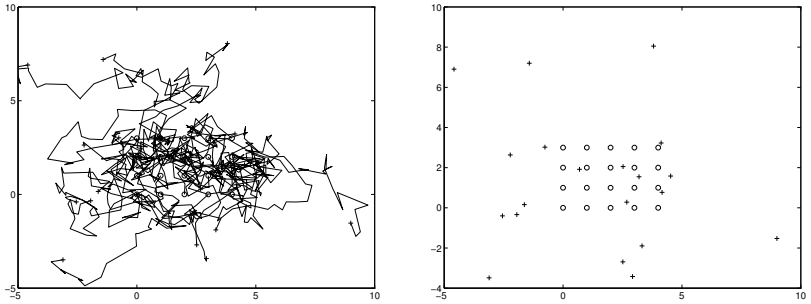

Left: paths of the movements Right: initial and end positions
∘: initial positions, +: end positions

position in the river, where the oxygen concentration is lowest. That answers the question posed in Example 1.1.
The minimum will depend on the input of pollutant in L_1. Turned around, one could compute how large an injection of pollutant is at most allowed, which does not degrade the oxygen concentration below a given lower bound.

A qualitative prediction of the model is the following: when we follow the flow the concentration of pollutant will eventually decrease and the oxygen concentration will recover. In the limit, we have

$$\lim_{t\to\infty} L(t, u(t-t_0)) = 0,$$
$$\lim_{t\to\infty} C(t, u(t-t_0)) = c_S,$$

because for $t \to \infty$ the positive factor $\frac{x}{u} = t - t_0$ in the exponents of the solution formulas tends to $+\infty$; therefore the e-functions tend to 0.
So: far downstream the water regenerates to full oxygen saturation and all pollutant is used up by the oxidation. This may be taken as a plausibility check for the model.

1.7 Modeling diffusion and dispersion

Diffusion and dispersion are random movements. Diffusion is the movement of dissolved molecules, dispersion is the movement of droplets. These are physically different processes, but both result in mixing the solution. In course of time, each dissolved substance is distributed uniformly in the solution. The following modeling of diffusion and dispersion (D&D for short) is the same for both processes, but the values of the parameters are different. Nevertheless, we subsume the effect into one model.

Figure 1.5 is the result of a simulation of random movement. At the beginning 20 particles are in a rectangle in the center of the shown region and start moving randomly. The overal effect is that the particles distribute more or less uniformly in space. From a region with

Figure 1.6: The effect of diffusion

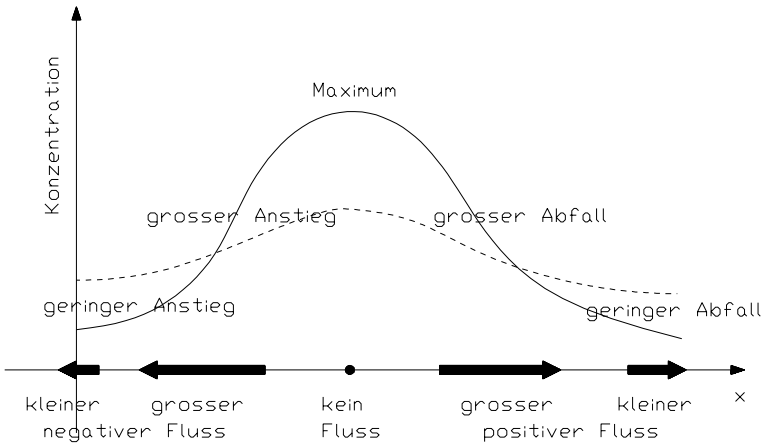

Solid: initial concentration. Dashed: concentration after a while,
The arrows symbolize the strength and the dirction of the flow of particles.

many particles leave more particles into a region with few particles than come in from there.

The modeling of diffusion does not follow the movements of the indiviual molecules, but describes the overall effect of random mixing: from regions with high concentrations of particles there will be a net flow of particles into regions with lower concentrations. We denote by $\Phi(t,x)$ the amount of particles that moves through a given plane at x, per unit of area and per unit of time. We will talk about a "flow" of particles by random movements (in addition to the flow caused by advection). The simplest – yet for many situations appropriate – model is Fick's law. Let us state it for the onedimensional case:

Fick's Law. *Let $L(t,x)$ be the concentration of a diffusing substance and Φ the flow of particles caused by random movement. By convention, positive Φ means flow in the direction of larger x, negative Φ means flow in the other direction. Then*

$$\Phi(t,x) = -D\frac{\partial}{\partial x}L(t,x). \tag{1.7}$$

Here $D \geq 0$ is a constant, the diffusion coefficient. It might depend on the position, then being a function $D(x)$.

Fick's law qualitatively mimics the effects of diffusion: when the concentration grows in positive direction (larger x), then the partial derivative $\frac{\partial}{\partial x}L$ is positive. Then Φ is negative, which leads to a flow in negative direction (smaller x). The larger the slope of the increase of the concentration is, the stronger is the flow in negative direction. Figure 1.7 shows a schematic presentation of the model.
By the way, the same law is valid for the conduction of heat in a solid rod, when $L(t,x)$ stands for the temperature.

Now we complete our model for the river by including diffusion and dispersion. Let $D_S(x)$ and $D_O(x)$ be the diffusion plus dispersion constants for pollutant and oxygen. These two constants can differ due to the different mobility of the molecules. The dispersion constant would be the same, because both substances are in the same droplets. In addition to the flow due to advection, we get the following flow due to diffusion and dispersion (D&D):

$$\Phi_S(t,x) = -D_S(x)\frac{\partial}{\partial x}L(t,x),$$
$$\Phi_O(t,x) = -D_O(x)\frac{\partial}{\partial x}C(t,x).$$

According to our convention, positive Φ points into the direction of larger x. We consider an "infinitesimal small" cell between x and $x+\Delta x$ (we only present the case $\Delta x > 0$; the case $\Delta x < 0$ can be done analogously). At the upstream boundary of the cell at x, the flow $\Phi_S(t,x)$ crosses the cell boundary whose area is $A(x)$. This gives an in- or decrease of $A(x)\Phi_S(x)$ kmol pollutant per second. At the downstream boundary of the cell at $x+\Delta x$, the flow $\Phi_S(x+\Delta x)$ crosses the cell boundary whose area is $A(x+\Delta x)$. This gives an in- or decrease of $A(x+\Delta x)\Phi_S(x+\Delta x)$ kmol per second. Together we have:

rate of increase of pollutant by D&D:
$$A(x)\Phi_S(x) - A(x+\Delta x)\Phi_S(x+\Delta x)$$
$$= -A(x)D_S(x)\frac{\partial}{\partial x}L(t,x) + A(x+\Delta x)D_S(x+\Delta x)\frac{\partial}{\partial x}L(t,x+\Delta x),$$
rate of increase of oxygen by D&D:
$$A(x)\Phi_O(x) - A(x+\Delta x)\Phi_O(x+\Delta x)$$
$$= -A(x)D_O(x)\frac{\partial}{\partial x}C(t,x) + A(x+\Delta x)D_O(x+\Delta x)\frac{\partial}{\partial x}C(t,x+\Delta x).$$

These terms have to be added in the mass balances of the small cell. Before taking the limit $\Delta x \to 0$ we divide by Δx (by $-\Delta x$ if $\Delta x < 0$). The contribution of D&D thus is

$$\lim_{\Delta x\to 0}\frac{A(x+\Delta x)D_S(x+\Delta x)\frac{\partial}{\partial x}L(t,x+\Delta x) - A(x)D_S(x)\frac{\partial}{\partial x}L(t,x)}{\Delta x}$$
$$= \frac{\partial}{\partial x}\left(A(x)D_S(x)\frac{\partial}{\partial x}L(t,x)\right).$$

The diffusion and dispersion for the oxygen is modeled likewise. The new terms are included in the mass balances for L and C.

The river pollution model including diffusion and dispersion hence consists of the two PDEs

$$\begin{aligned} A(x)\frac{\partial}{\partial t}L(t,x) = \quad & \frac{\partial}{\partial x}\left(A(x)D_S(x)\frac{\partial}{\partial x}L(t,x)\right) - \frac{\partial}{\partial x}\big(A(x)u(x)L(t,x)\big) \\ & -k_S A(x)L(t,x) + s(t,x), \\ A(x)\frac{\partial}{\partial t}C(t,x) = \quad & \frac{\partial}{\partial x}\left(A(x)D_O(x)\frac{\partial}{\partial x}C(t,x)\right) - \frac{\partial}{\partial x}\big(A(x)u(x)C(t,x)\big) \\ & -k_S A(x)L(t,x) + k_O b(x)(c_S - C(t,x)). \end{aligned} \tag{1.8}$$

Table 1.3: A reaction-diffusion-advection equation

$\frac{\partial}{\partial t}A(x)L(t,x)$	temporal rate of change partial derivative wrt t
$=$	
$\frac{\partial}{\partial x}\left(D_S(x)A(x)\frac{\partial}{\partial x}L(t,x)\right)$	diffusion second order partial derivative wrt to x
$-\frac{\partial}{\partial x}A(x)u(x)L(t,x)$	advection partial derivative wrt to x of concentration $\times$ cross section $\times$ flow velocity
$+s(t,x)$	contribution of the sources
$-k_S A(x)L(t,x)$	contribution of the chemical reaction form of model depends on the type of the reaction

In the new equations, L and C are differentiated two times with respect to x: diffusion leads to second order partial derivatives in space. To induce uniqueness of solutions, one more boundary condition is needed on each of L and C, for example the concentrations at the downstream end of the region at $x = l$. The physical reason is, that by random movement, particles can enter the region from downstream of $x = l$. For example one could assume that the region is sufficiently long, so that the concentrations at $x = l$ are back to nominal, and set

$$L(t,l) = 0 \text{ and } C(t,l) = c_S. \tag{1.9}$$

Prescribing the function values at a boundary is called Dirichlet boundary conditions. Another common type of boundary conditions are so-called Neumann boundary conditions, which prescribe the spatial derivatives of the solutions. For example one could reasonably require that the spatial derivatives at the downstream boundary are zero,

$$\frac{\partial}{\partial x}L(t,l) = \frac{\partial}{\partial x}C(t,l) = 0, \tag{1.10}$$

which means that the concentration should not vary in space there.

The introduction of diffusion heavily alters the qualitative behavior of solutions. Consider the following scenario: the factory injects at time $t = 0$ a certain amount of pollutant into the river and after a moment shuts off the injection. At a position x_0 an observer is waiting with his sensors. The advection model without diffusion predicts, that the pollutant travels as a sharpely defined packet. This packet will arrive at the observer at time $t = x_0/u$ (distance divided by velocity of the flow). Before that instant, the observer finds no pollutant. At time x_0/u his sensors jump to different values; after a moment they suddenly return to the nominal values and stay there.
Diffusion and dispersion effectuate, that some particles move faster than the flow velocity, and some lag behind. The mathematical model predicts, the the sensors show some

pollutant immediately after $t = 0$ (infinite speed of propagation in the parabolic diffusion equation), the bulk of the pollutant is smeared out over space, its maximum arrives at the observer at time x_0/u. Hereafter, the sensors smoothly return to nominal values.

The method of characteristic curves fails for the diffusion model, because even when the boat swims with the flow, the random movements are still there. There is no total derivative that comprises the derivatives of order two.

REMARK. When the modeling only takes into account diffusion and dispersion and neglects all other processes, then (for constant cross section A) the result is the classical diffusion equation

$$\frac{\partial}{\partial t}L(t,x) = \frac{\partial}{\partial x}\big(D(x)\frac{\partial}{\partial x}L(t,x)\big), \quad t > 0, \quad x \in (0,l).$$

It describes the temporal and spatial evolution of a property L that is solely due to random movements. This is the case for heat conduction in a solid rod; there $L(t,x)$ is the temperature at time t at the position x in the rod. Again, a unique solution is determined by an initial temperature distribution (say $L(t,x) = c$, constant throughout) and boundary conditions at $x = 0$ (say $L(t,0) = c+1$) and at $x = l$ (say $L(t,l) = c-1$).

1.8 Numerical solutions

The phrase "numerical solution" of a mathematical model is used for quantitatively computing a particular example of an approximate solution of the model on a computer. The development and investigation of algorithms that yield numerical solutions of PDEs has grown into its own field within mathematics and scientific computing: Numerical Analysis including proofs of error estimates and convergence rates. Every such algorithm discretizes the PDE in time and space. The most popular approaches are

FD Finite difference methods replace derivatives by difference-quotients; the number and geometry of local grid-points ('stencil') can and should be adjusted appropriately.

FEM Finite element methods replace the space by cells to get ODEs; the functions need not be constant on the cells (as in our cell model above).

SPEC Spectral methods use non-local basis functions (eg. eigenfunctions or Legendre polynomials) that are adjusted to the boundary conditions.

BEM Boundary element methods use finite elements on the (discretized) boundary and yield approximate solutions in the interior by application of the integral theorems of vector analysis.

There are many software packages that promise ease of use of such algorithms by menu driven user interfaces. I think the more convenient the package seems to be, the more likely it is that the user does not realize the mistakes he himself or the package makes.

In the Figure we see simulation results for (1.8) with the same parameters as in Fig 1.2. We have chosen an appropriate input of pollutant $s(t,x)$ on $x \in [0,100]$ and $t \in [0,360]$ and

Figure 1.7: Simulation results with the reaction-advection-diffusion model in Femlab

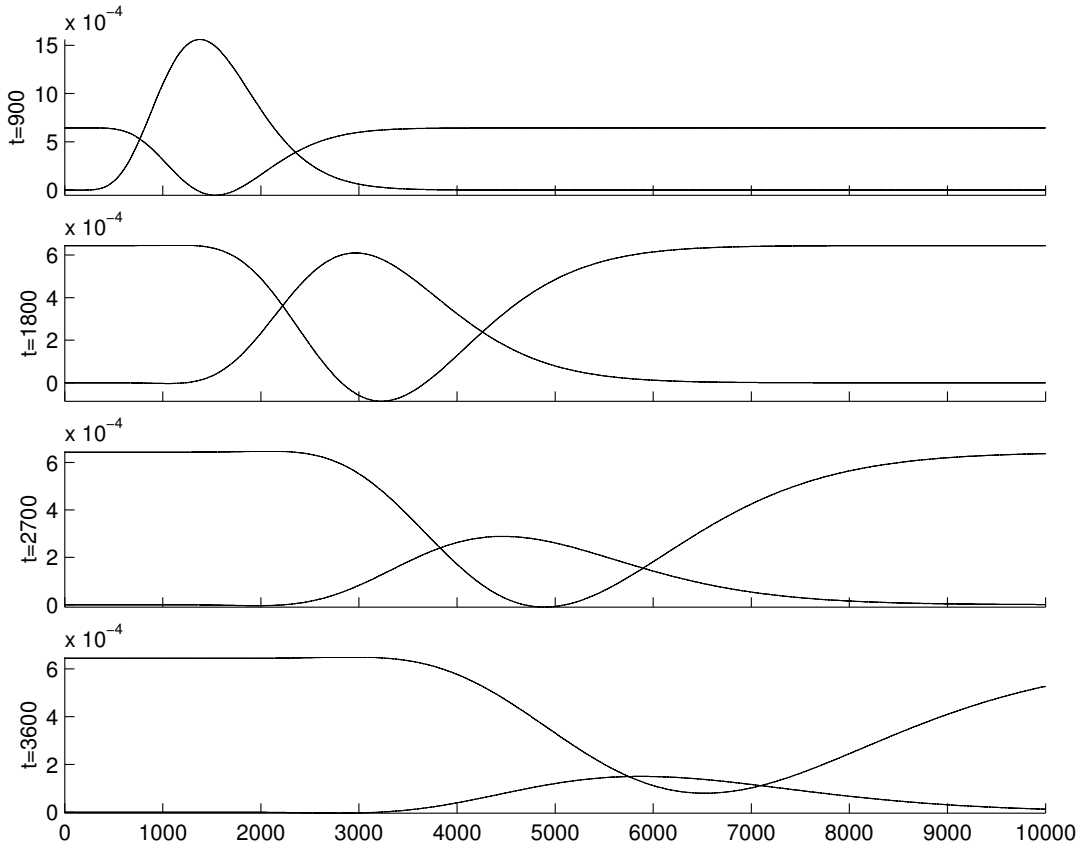

zero else; furthermore, we set $D_S = 60$ and $D_O = 20$. Unfortunately, we again observe meaningless negative concentrations at $t = 900$ and $t = 1800$. This - most likely - is due to the linear reaction submodel which is not realistic for small concentrations of oxygen. To repair this one would try to replace the simple model in "Modeling the Oxidation" (see 1.2) by a more realistic, nonlinear one.

1.9 Conclusion

When modeling spatially distributed dynamical systems, for some purposes it might be appropriate to *first* discretize in space (and time), and then to set up a discrete model like the cell model in 1.2, or merely a simulation executable. Yet, there are many distributed dynamical phenomena, that are better understood by continuous models, namely by PDEs. These reflect and explain the underlying principles in a compact and elegant way, and are amenable to qualitative analysis (such as asymptotics, stability of equilibria, speed of propagation, etc.). Thus, in addition to the possibility of simulating particular examples, the derivation and analysis of PDE models can induce structural understanding of the modeled systems.

13.6 Reaction-Diffusion Systems

Finally, I would like to introduce *reaction-diffusion systems,* a particular class of continuous field models that have been studied extensively. They are continuous field models whose equations are made of only *reaction terms* and *diffusion terms*, as shown below:

$$\frac{\partial f_1}{\partial t} = R_1(f_1, f_2, \ldots, f_n) + D_1 \nabla^2 f_1 \tag{13.53}$$

$$\frac{\partial f_2}{\partial t} = R_2(f_1, f_2, \ldots, f_n) + D_2 \nabla^2 f_2 \tag{13.54}$$

$$\vdots$$

$$\frac{\partial f_n}{\partial t} = R_n(f_1, f_2, \ldots, f_n) + D_n \nabla^2 f_n \tag{13.55}$$

Reaction terms ($R_i(\ldots)$) describe only local dynamics, without any spatial derivatives involved. Diffusion terms ($D_i \nabla^2 f_i$) are strictly limited to the Laplacian of the state variable itself. Therefore, any equations that involve non-diffusive spatial movement (e.g., chemotaxis) are not reaction-diffusion systems.

There are several reasons why reaction-diffusion systems have been a popular choice among mathematical modelers of spatio-temporal phenomena. First, their clear separation between non-spatial and spatial dynamics makes the modeling and simulation tasks really easy. Second, limiting the spatial movement to only diffusion makes it quite straightforward to expand any existing non-spatial dynamical models into spatially distributed ones. Third, the particular structure of reaction-diffusion equations provides an easy shortcut in the stability analysis (to be discussed in the next chapter). And finally, despite the simplicity of their mathematical form, reaction-diffusion systems can show strikingly rich, complex spatio-temporal dynamics. Because of these properties, reaction-diffusion systems have been used extensively for modeling self-organization of spatial patterns. There are even specialized software applications available exactly to simulate reaction-diffusion systems[3].

Exercise 13.16 Extend the following non-spatial models into spatially distributed ones as reaction-diffusion systems by adding diffusion terms. Then simulate their behaviors in Python.

- Motion of a pendulum (Eq. 6.3): This creates a spatial model of locally coupled nonlinear oscillators.

[3] For example, check out Ready (`https://code.google.com/p/reaction-diffusion/`).

- Susceptible-Infected-Recovered (SIR) model (Exercise 7.3): This creates a spatial model of epidemiological dynamics.

In what follows, we will review a few well-known reaction-diffusion systems to get a glimpse of the rich, diverse world of their dynamics.

Turing pattern formation As mentioned at the very beginning of this chapter, Alan Turing's PDE models were among the first reaction-diffusion systems developed in the early 1950s [44]. A simple linear version of Turing's equations is as follows:

$$\frac{\partial u}{\partial t} = a(u-h) + b(v-k) + D_u \nabla^2 u \tag{13.56}$$

$$\frac{\partial v}{\partial t} = c(u-h) + d(v-k) + D_v \nabla^2 v \tag{13.57}$$

The state variables u and v represent concentrations of two chemical species. a, b, c, and d are parameters that determine the behavior of the reaction terms, while h and k are constants. Finally, D_u and D_v are diffusion constants.

If the diffusion terms are ignored, it is easy to show that this system has only one equilibrium point, $(u_{\mathrm{eq}}, v_{\mathrm{eq}}) = (h, k)$. This equilibrium point can be stable for many parameter values for a, b, c, and d. What was most surprising in Turing's findings is that, even for such stable equilibrium points, introducing spatial dimensions and diffusion terms to the equations may destabilize the equilibrium, and thus the system may spontaneously self-organize into a non-homogeneous pattern. This is called *diffusion-induced instability* or *Turing instability*. A sample simulation result is shown in Fig. 13.17.

The idea of diffusion-induced instability is quite counter-intuitive. Diffusion is usually considered a random force that destroys any structure into a homogenized mess, yet in this particular model, diffusion *is* the key to self-organization! What is going on? The trick is that this system has two different diffusion coefficients, D_u and D_v, and their difference plays a key role in determining the stability of the system's state. This will be discussed in more detail in the next chapter.

There is one thing that needs particular attention when you are about to simulate Turing's reaction-diffusion equations. The Turing pattern formation requires small random perturbations (noise) to be present in the initial configuration of the system; otherwise there would be no way for the dynamics to break spatial symmetry to create non-homogeneous patterns. In the meantime, such initial perturbations should be small enough so that they won't immediately cause numerical instabilities in the simulation. Here is a sample code for simulating Turing pattern formation with a suggested level of initial perturbations, using the parameter settings shown in Fig. 13.17:

Figure 13.17: Simulation of the Turing pattern formation model with $(a, b, c, d) = (1, -1, 2, -1.5)$ and $(D_u, D_v) = (10^{-4}, 6 \times 10^{-4})$. Densities of u are plotted in grayscale (darker = greater). Time flows from left to right.

Code 13.8: turing-pattern-PDE.py

```
import matplotlib
matplotlib.use('TkAgg')
from pylab import *

n = 100 # size of grid: n * n
Dh = 1. / n # spatial resolution, assuming space is [0,1] * [0,1]
Dt = 0.02 # temporal resolution

a, b, c, d, h, k = 1., -1., 2., -1.5, 1., 1. # parameter values

Du = 0.0001 # diffusion constant of u
Dv = 0.0006 # diffusion constant of v

def initialize():
    global u, v, nextu, nextv
    u = zeros([n, n])
    v = zeros([n, n])
    for x in xrange(n):
        for y in xrange(n):
            u[x, y] = 1. + uniform(-0.03, 0.03) # small noise is added
            v[x, y] = 1. + uniform(-0.03, 0.03) # small noise is added
    nextu = zeros([n, n])
```

```
    nextv = zeros([n, n])

def observe():
    global u, v, nextu, nextv
    subplot(1, 2, 1)
    cla()
    imshow(u, vmin = 0, vmax = 2, cmap = cm.binary)
    title('u')
    subplot(1, 2, 2)
    cla()
    imshow(v, vmin = 0, vmax = 2, cmap = cm.binary)
    title('v')

def update():
    global u, v, nextu, nextv
    for x in xrange(n):
        for y in xrange(n):
            # state-transition function
            uC, uR, uL, uU, uD = u[x,y], u[(x+1)%n,y], u[(x-1)%n,y], \
                                 u[x,(y+1)%n], u[x,(y-1)%n]
            vC, vR, vL, vU, vD = v[x,y], v[(x+1)%n,y], v[(x-1)%n,y], \
                                 v[x,(y+1)%n], v[x,(y-1)%n]
            uLap = (uR + uL + uU + uD - 4 * uC) / (Dh**2)
            vLap = (vR + vL + vU + vD - 4 * vC) / (Dh**2)
            nextu[x,y] = uC + (a*(uC-h) + b*(vC-k) + Du * uLap) * Dt
            nextv[x,y] = vC + (c*(uC-h) + d*(vC-k) + Dv * vLap) * Dt

    u, nextu = nextu, u
    v, nextv = nextv, v

import pycxsimulator
pycxsimulator.GUI(stepSize = 50).start(func=[initialize, observe, update])
```

This simulation starts from an initial configuration $(u(x,y), v(x,y)) \approx (1,1) = (h,k)$, which is the system's homogeneous equilibrium state that would be stable without diffusion terms. Run the simulation to see how patterns spontaneously self-organize!

Exercise 13.17 Conduct simulations of the Turing pattern formation with several different parameter settings, and discuss how the parameter variations (especially for the diffusion constants) affect the resulting dynamics.

Exercise 13.18 Discretize the Keller-Segel slime mold aggregation model (Eqs. (13.27) and (13.28)) (although this model is not a reaction-diffusion system, this is the perfect time for you to work on this exercise because you can utilize Code 13.8). Implement its simulation code in Python, and conduct simulations with $\mu = 10^{-4}$, $D = 10^{-4}$, $f = 1$, and $k = 1$, while varying χ as a control parameter ranging from 0 to 10^{-3}. Use $a = 1$ and $c = 0$ as initial conditions everywhere, with small random perturbations added to them.

Belousov-Zhabotinsky reaction The *Belousov-Zhabotinsky reaction*, or *BZ reaction* for short, is a family of oscillatory chemical reactions first discovered by Russian chemist Boris Belousov in the 1950s and then later analyzed by Russian-American chemist Anatol Zhabotinsky in the 1960s. One of the common variations of this reaction is essentially an oxidation of malonic acid ($\mathrm{CH_2(COOH)_2}$) by an acidified bromate solution, yet this process shows nonlinear oscillatory behavior for a substantial length of time before eventually reaching chemical equilibrium. The actual chemical mechanism is quite complex, involving about 30 different chemicals. Moreover, if this chemical solution is put into a shallow petri dish, the chemical oscillation starts in different phases at different locations. Interplay between the reaction and the diffusion of the chemicals over the space will result in the self-organization of dynamic traveling waves (Fig. 13.18), just like those seen in the excitable media CA model in Section 11.5.

A simplified mathematical model called the *"Oregonator"* was among the first to describe the dynamics of the BZ reaction in a simple form [50]. It was originally proposed as a non-spatial model with three state variables, but the model was later simplified to have just two variables and then extended to spatial domains [51]. Here are the simplified "Oregonator" equations:

$$\epsilon \frac{\partial u}{\partial t} = u(1-u) - \frac{u-q}{u+q} f v + D_u \nabla^2 u \tag{13.58}$$

$$\frac{\partial v}{\partial t} = u - v + D_v \nabla^2 v \tag{13.59}$$

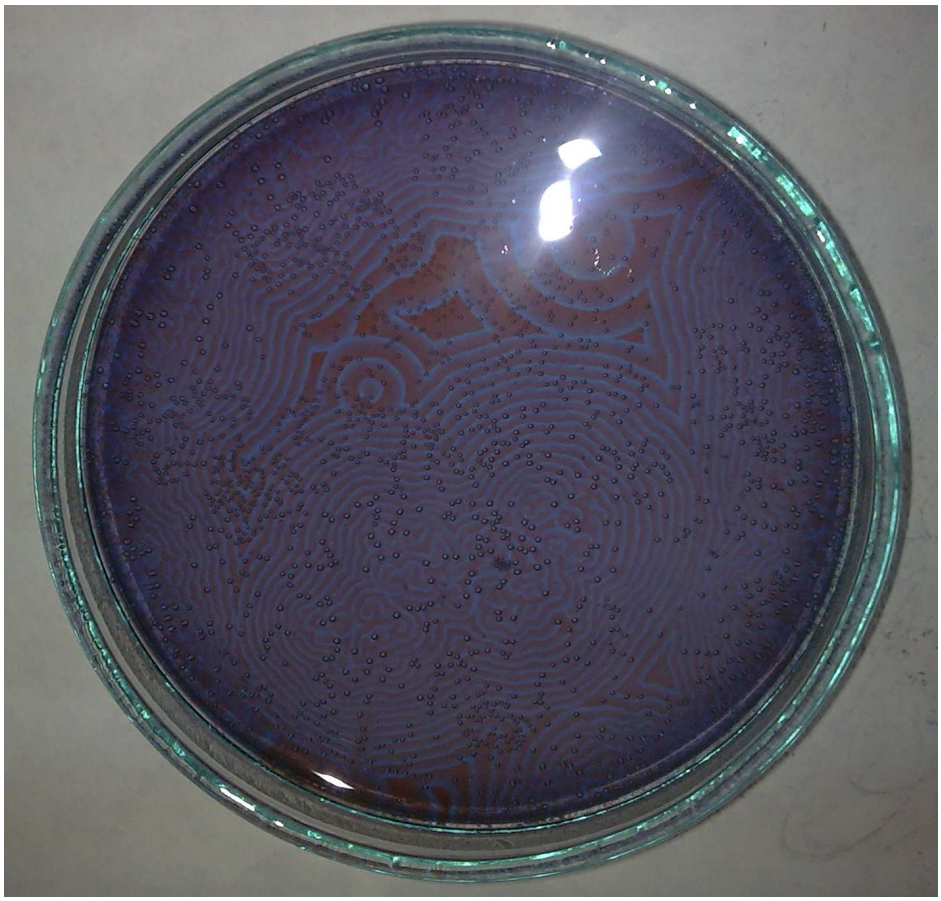

Figure 13.18: Belousov-Zhabotinsky reaction taking place in a petri dish. Image from Wikimedia Commons ("Reakcja Biełousowa-Żabotyńskiego zachodzaca w szalce Petriego" by Ms 1001 – Own work. Trimmed to fit. Licensed under Public domain via Wikimedia Commons – `http://commons.wikimedia.org/wiki/File:Zdj%C4%99cie012.jpg`)

Here, u and v represent the concentrations of two chemical species. If you carefully examine the reaction terms of these equations, you will notice that the presence of chemical u has a positive effect on both u and v, while the presence of chemical v has a negative effect on both. Therefore, these chemicals are called the "activator" and the "inhibitor," respectively. Similar interactions between the activator and the inhibitor were also seen in the Turing pattern formation, but the BZ reaction system shows nonlinear chemical oscillation. This causes the formation of traveling waves. Sometimes those waves can form spirals if spatial symmetry is broken by stochastic factors. A sample simulation result is shown in Fig. 13.19.

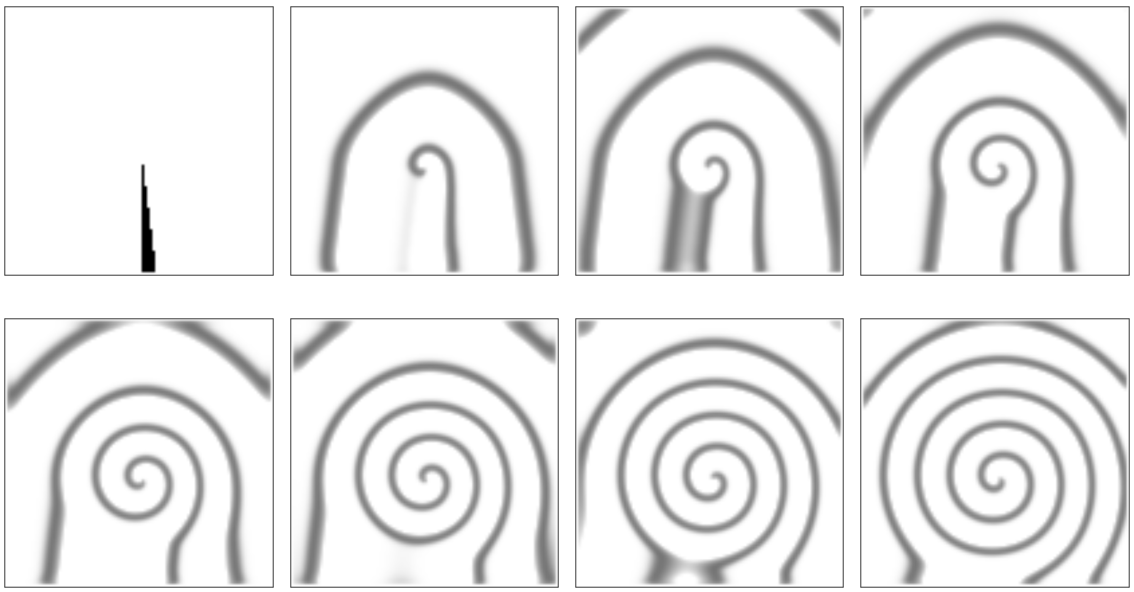

Figure 13.19: Simulation of the "Oregonator" model of the BZ reaction with $(\epsilon, q, f) = (0.2, 10^{-3}, 1.0)$ and $D_u = D_v = 10^{-5}$, starting with a tongue-like initial configuration. The concentration of chemical u is plotted in grayscale (darker = greater). Time flows from left to right (the first row followed by the second row).

Exercise 13.19 Implement a simulator code of the "Oregonator" model of the BZ reaction in Python. Then conduct simulations with several different parameter settings, and discuss what kind of conditions would be needed to produce traveling waves.

Gray-Scott pattern formation The final example is the *Gray-Scott model*, another very well-known reaction-diffusion system studied and popularized by John Pearson in the 1990s [52], based on a chemical reaction model developed by Peter Gray and Steve Scott in the 1980s [53, 54, 55]. The model equations are as follows:

$$\frac{\partial u}{\partial t} = F(1-u) - uv^2 + D_u \nabla^2 u \tag{13.60}$$

$$\frac{\partial v}{\partial t} = -(F+k)v + uv^2 + D_v \nabla^2 v \tag{13.61}$$

The reaction terms of this model assumes the following *autocatalytic reaction* (i.e., chemical reaction for which the reactant itself serves as a catalyst):

$$u + 2v \rightarrow 3v \tag{13.62}$$

This reaction takes one molecule of u and turns it into one molecule of v, with help of two other molecules of v (hence, autocatalysis). This is represented by the second term in each equation. In the meantime, u is continuously replenished from the external source up to 1 (the first term of the first equation) at feed rate F, while v is continuously removed from the system at a rate slightly faster than u's replenishment ($F+k$ seen in the first term of the second equation). F and k are the key parameters of this model.

It is easy to show that, if the diffusion terms are ignored, this system always has an equilibrium point at $(u_{\mathrm{eq}}, v_{\mathrm{eq}}) = (1, 0)$ (which is stable for any positive F and k). Surprisingly, however, this model may show very exotic, biological-looking dynamics if certain spatial patterns are placed into the above equilibrium. Its behaviors are astonishingly rich, even including growth, division, and death of "cells" if the parameter values and initial conditions are appropriately chosen. See Fig. 13.20 to see only a few samples of its wondrous dynamics!

> *Exercise 13.20* Implement a simulator code of the Gray-Scott model in Python. Then conduct simulations with several different parameter settings and discuss how the parameters affect the resulting patterns.

Figure 13.20: (Next page) Samples of patterns generated by the Gray-Scott model with $D_u = 2 \times 10^{-5}$ and $D_v = 10^{-5}$. The concentration of chemical u is plotted in grayscale (brighter = greater, only in this figure). Time flows from left to right. The parameter values of F and k are shown above each simulation result. The initial conditions are the homogeneous equilibrium $(u, v) = (1, 0)$ everywhere in the space, except at the center where the local state is reversed such that $(u, v) = (0, 1)$.

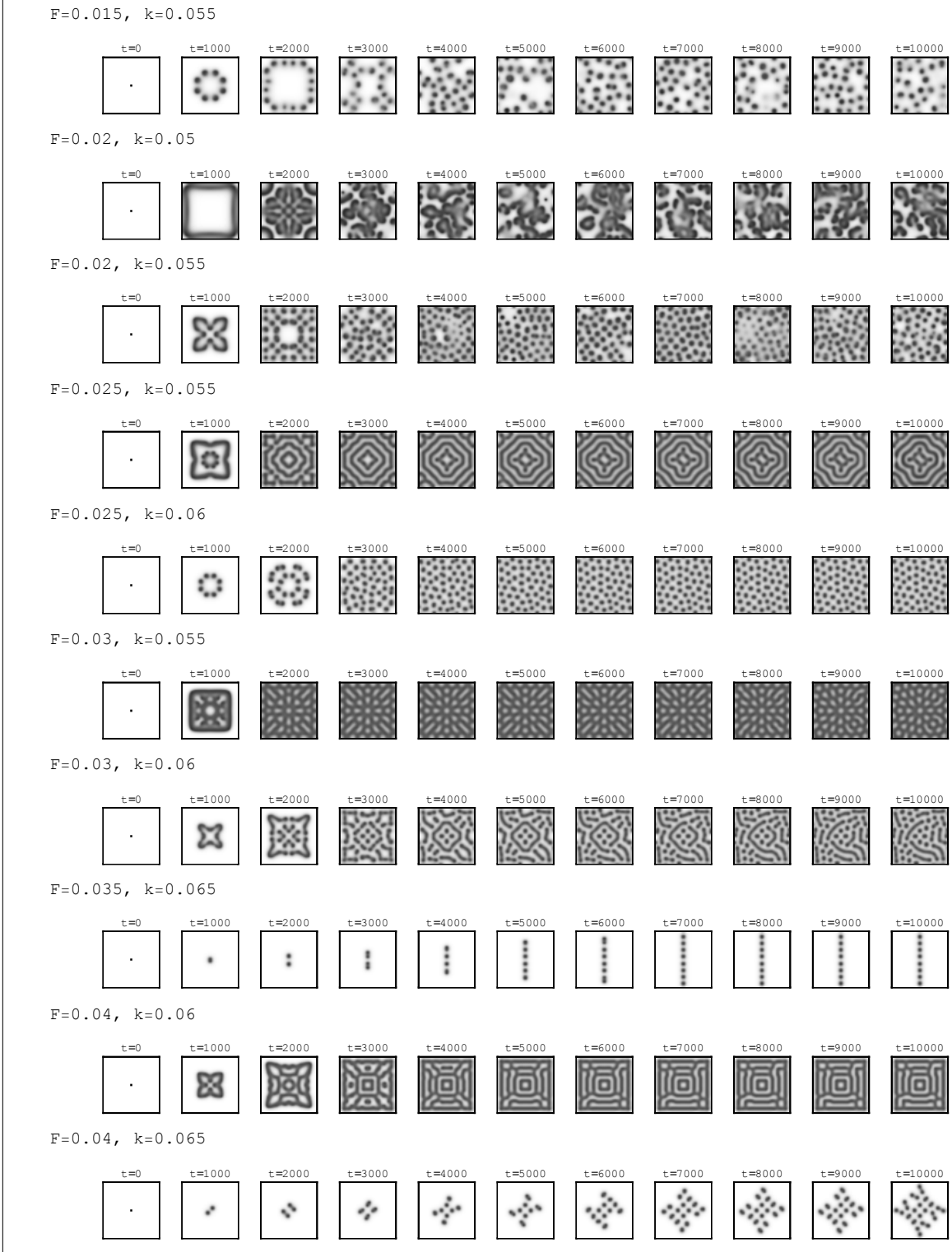
F=0.015, k=0.055
t=0 t=1000 t=2000 t=3000 t=4000 t=5000 t=6000 t=7000 t=8000 t=9000 t=10000
F=0.02, k=0.05
t=0 t=1000 t=2000 t=3000 t=4000 t=5000 t=6000 t=7000 t=8000 t=9000 t=10000
F=0.02, k=0.055
t=0 t=1000 t=2000 t=3000 t=4000 t=5000 t=6000 t=7000 t=8000 t=9000 t=10000
F=0.025, k=0.055
t=0 t=1000 t=2000 t=3000 t=4000 t=5000 t=6000 t=7000 t=8000 t=9000 t=10000
F=0.025, k=0.06
t=0 t=1000 t=2000 t=3000 t=4000 t=5000 t=6000 t=7000 t=8000 t=9000 t=10000
F=0.03, k=0.055
t=0 t=1000 t=2000 t=3000 t=4000 t=5000 t=6000 t=7000 t=8000 t=9000 t=10000
F=0.03, k=0.06
t=0 t=1000 t=2000 t=3000 t=4000 t=5000 t=6000 t=7000 t=8000 t=9000 t=10000
F=0.035, k=0.065
t=0 t=1000 t=2000 t=3000 t=4000 t=5000 t=6000 t=7000 t=8000 t=9000 t=10000
F=0.04, k=0.06
t=0 t=1000 t=2000 t=3000 t=4000 t=5000 t=6000 t=7000 t=8000 t=9000 t=10000
F=0.04, k=0.065
t=0 t=1000 t=2000 t=3000 t=4000 t=5000 t=6000 t=7000 t=8000 t=9000 t=10000